

## CHAPTER 5

# Chelating agents embedded in 80PVAc-borax based HVPDs for the cleaning of metallic surfaces

### 5.1 Introduction

In this chapter the rheological and structural properties of HVPDs prepared from 80PVAc or 87PVAc containing selected chelating agents have been explored. As already discussed in the Chapter 2, chelating species such as the disodium salt of ethylenediamine tetraacetic acid (EDTA), citrate salts, benzotriazole, ammonium carbonate and Rochelle salt are some of the most commonly used by conservators for the removal of salts or corrosion/oxidation patinas from paper, metal objects, and paintings [1-5].

We hypothesized that loading the chelators into xPVAc-borax HVPDs would help to confine the cleaning agents to the desired area of an artifact (allowing for a slow, well-controlled cleaning action), while avoiding the removal of materials integral to the natural protective patina, either the original metallic surface or pigments.

Here, we focus on the effects of adding three chelating agents — disodium EDTA, trisodium citrate (TSC) and triammonium citrate (TAC) — to the HVPDs in terms of their intrinsic mechanical-structural properties and their abilities to act as cleaning agents on some metallic surfaces.

The mechanical properties of these HVPDs have been studied as a function of the concentration of the chelators by means of oscillatory rheological tests. The trends in the magnitudes of the storage modulus  $G'$  and the loss modulus  $G''$  are used to assess the effects of the chelators on the viscoelasticity of the systems and, thus, on their ease of removal in one step minimizing the potential residues.

The rheological changes are correlated with those of structure as assessed by  $^{11}\text{B}$  NMR spectroscopy. Although many  $^{11}\text{B}$  NMR spectroscopic studies have investigated the interconversion [6] and kinetics of interchange [7] of boric acid and tetrahydroxyborate (borate) anions in aqueous solution, our studies investigate the

degree of borate crosslinking to the polymer [8,9], the formation of chelator-borate species, and the effect of adding different metallic salts to the HVPDs with chelators.

In addition, some cleaning tests on laboratory specimens (copper plates artificially degraded to simulate the “bronze disease”) were performed to evaluate the efficacy of these HVPDs in the thinning of the oxidation patinas from well-described metallic surfaces.

The amount of altered copper removed from the copper plates was determined by Inductively Coupled Plasma Optical Emission Spectroscopy (ICP-EOS) analyses thanks to the set-up of an analytical protocol *ad hoc* for the HVPDs systems. The tests demonstrated the utility of these HVPDs to clean corroded copper surfaces.

### 5.2 Preparation of the polymeric dispersions

The chelating species selected to be embedded in the HVPDs were: disodium EDTA, tribasic ammonium citrate (TAC), trisodium citrate (TSC), and sodium/potassium tartrate (Rochelle salt). They are, in fact, the most commonly used by restorers for the conservation of corroded or oxidized artistic surfaces.

Being the use of monophasic systems an essential condition for the control of the cleaning action of the HVPDs, the maximum amount of EDTA, citrate salts and Rochelle salt loadable in these polymeric complex systems was determined by individuating the concentration limits above which phase separation occurs. The preparation procedure was the following.

The 80PVAc/87PVAc was dissolved in a water solution of the chelating agent; then a solution of borax was added and the system was stirred with a VORTEX apparatus until it became rigid in few minutes. The polymer/borax weight ratio was maintained at 4:1 (3 wt% polymer and 0.75 wt% borax). In the EDTA-containing samples, the pH was adjusted to  $9.6 \pm 0.2$  (as indicated by Whatman Indicator Paper, pH 8.0-10.0 narrow range) through the dropwise addition of an aqueous solution of ammonium hydroxide (the amount of ammonia solution varied from 30 to 70  $\mu\text{L}$ , depending on the EDTA concentration).

The maximum loading of EDTA, TAC or TSC in the 80PVAc-borax systems before observing phase separation was found to be 0.5 wt%, 0.3 wt% or 0.5 wt%,

respectively (Table 5.2.1). Substituting the 80PVAc with the 87PVAc (containing ~3% of carboxylate groups) but keeping constant the weight ratio polymer/borax to 4:1 (3 wt% polymer, 0.75 wt% borax) it was possible to incorporate sensibly higher amounts of each chelator: up to 1.5 wt% of EDTA, 0.7 wt% of TAC and 1 wt% of TSC (Table 5.2.1).

**Table 5.2.1.** Maximum amounts (wt%) of the selected chelators that can be loaded in the HVPDs prepared with 80PVAc or 87PVAc respectively.

	Maximum loadable amount (wt%)		
	EDTA	TAC	TSC
80PVAc	0.5	0.3	0.5
87PVAc	1.5	0.7	1

We attribute the slightly enhanced capability of loading chelator to the higher hydrolysis degree of the polymer and to the increased local polarity of the environment surrounding the 87PVAc polymer chains, induced by the presence of the carboxylic groups.

This achievement in the maximum loadable amounts of chelator obtained by substituting the 80PVAc with the 87PVAc is a very important result in the perspective of an application of these systems for the cleaning of artistic surfaces - especially if we consider that traditional methods use 1-5 wt% (or even more concentrated) chelator solutions - because it implies an increase of the cleaning efficacy of them.

### 5.3 Rheological characterization

As observed in previous studies [9], in order to warrant an adequate performance of the HVPDs in terms of ease of application, efficacy and complete removal through a simple peeling action, the systems should preserve adequate elastic properties even upon addition of additives active in the removal of foreign patinas from the works of art surfaces. In particular their intrinsic elastic modulus  $G_0$  values should be always higher than 400 Pa.

To verify if these features were preserved after the addition of chelating agents, mechanical properties of the stable and homogeneous HVPDs set up were explored by means of oscillatory tests (frequency sweeps) carried out in the linear viscoelastic region. The trend of the elastic shear modulus  $G'$  (Pa) and the viscous shear modulus  $G''$  (Pa) were recorded as a function of the frequency (Hz) of the applied shear deformation (whose amplitude was kept constant to 1%, value determined previously through amplitude sweep tests in order to be in the linear viscoelastic region).

As shown in Figure 5.3.1, the 80PVA-borax systems embedded with chelators show the typical viscoelastic behavior of these polymeric dispersions, characterized by two different regimes: for  $\omega > \omega_c$  ( $\omega_c$  is the crossover frequency between the  $G'$  and  $G''$  curves)  $G' > G''$ , indicating a predominantly elastic behavior; for  $\omega < \omega_c$  the viscous character prevails ( $G' < G''$ ).

The frequency sweeps of the 80PVAc-borax HVPDs containing different amounts of the three chelators normalized to the crossover point between the  $G'$  and the  $G''$  curves are reported in Figure 5.3.2. Regardless of the chelator added, the normalized curves, in the investigated frequency range, overlapped indicating that, even if structural changes occur when the concentration of the chelator is increased and even if the global time scale of the relaxation phenomena slightly changes, the mechanism associated with the relaxation is almost the same at all concentrations.

The intrinsic elastic moduli ( $G_0$ ), were calculated as the average of the last five  $G'$  points in the *plateau* regions of the flow curves. As shown in Figure 5.3.3 the  $G_0$  values resulted influenced by the addition of the chelator whose presence, up to a certain concentration, have a “structuring role” as it determines a progressive increase of the intrinsic elasticity represented by the  $G_0$ . In the case of EDTA and TSC,  $G_0$  values increased up to 0.3 wt% of additive (Figures 5.3.3, A and B). As regard TAC-containing HVPDs, the elasticity was enhanced by adding 0.1 wt% of salt but then decreased at higher concentrations of it (0.2 wt% and 0.3 wt%; see Figure 5.3.3 C). Above those concentrations, the  $G_0$  values, although still higher than those of a standard formulation without any chelator, decrease; we ascribe this behavior to the emergence of a metastable regime due the proximity to the maximum limit concentration above which phase separation was observed.

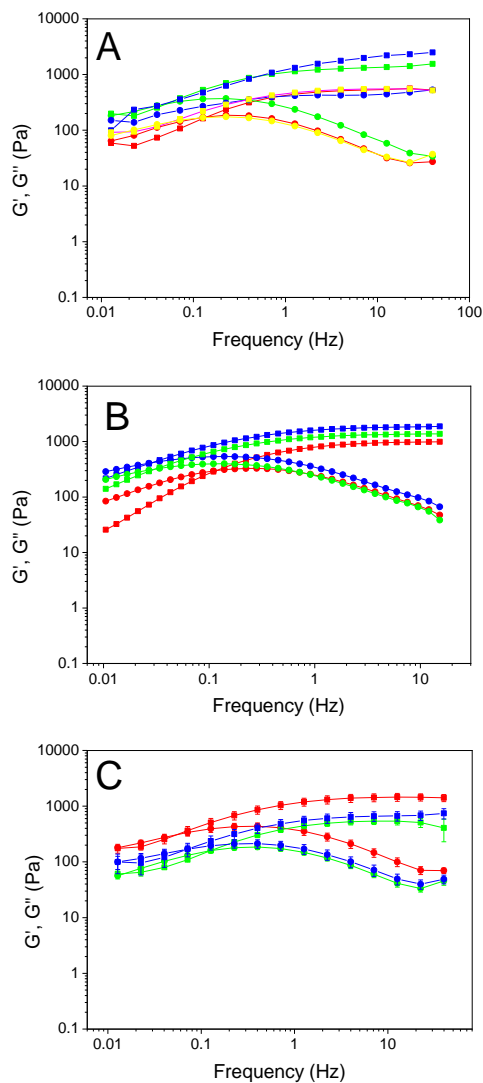


**Figure 5.3.1.** Frequency sweep curves at 1% strain of the  $G'$  modulus (squared symbols) and the  $G''$  modulus (circle symbols) as a function of the frequency (Hz) for the 80PVAc-borax HVPDs with:

(A) 0.1 wt% (red symbols), 0.2 wt% (green symbols), 0.3 wt% (blue symbols), and 0.5 wt% (yellow symbols) of disodium EDTA.

(B) 0.1 wt% (red symbols), 0.3 wt% (blue symbols) and 0.5 wt% (green symbols) of TSC.

(C) 0.1 wt% (red symbols), 0.2 wt% (green symbols) and 0.3 wt% (blue symbols) of TAC.

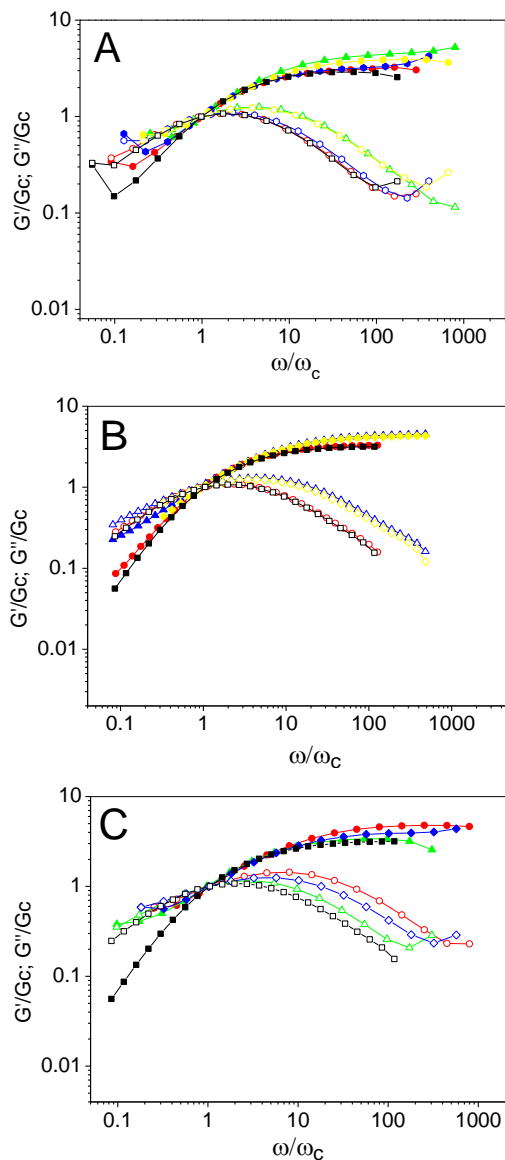


**Figure 5.3.2.** Normalized mechanical spectra for the 80PVAc-borax HVPDs with:  
 (A) 0 wt% (black symbols), 0.1 wt% (red symbols), 0.2 wt% (green symbols), 0.3 wt% (blue symbols) and 0.5 wt% (yellow symbols) of disodium EDTA.  
 (B) 0 wt% (black symbols), 0.1 wt% (red symbols), 0.3 wt% (blue symbols), 0.5 wt% (yellow symbols) of TSC.  
 (C) 0 wt% (black symbols), 0.1 wt% (red symbols), 0.2 wt% (green symbols), 0.3 wt% (blue symbols) of TAC.  
 Closed symbols indicate the  $G'/G_c$  ratio, open symbols indicate the  $G''/G_c$  ratio.  $G_c$  and  $\omega_c$  are the crossover modulus and the crossover frequency respectively.

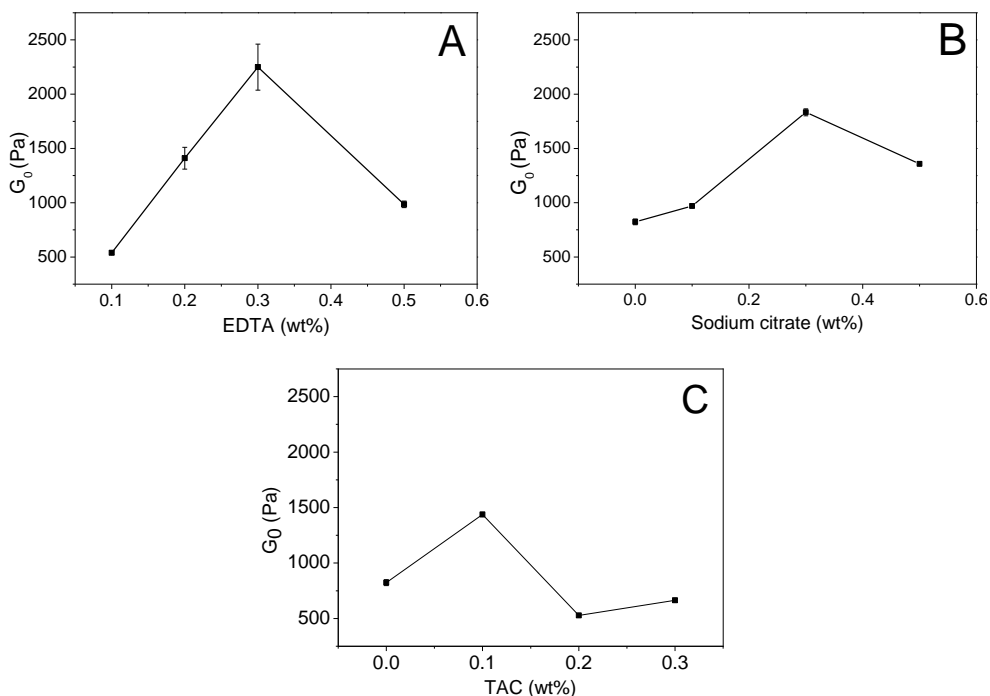


**Figure 5.3.3.** Intrinsic elastic modulus  $G_0$  for the 80PVAc-borax HVPDs as a function of the concentration (wt%) of EDTA (A), TSC (B) and TAC (C).

In particular, considering that in the EDTA-containing systems the mechanical properties could be influenced also by the presence of the ammonia (added to increase the pH to around 10), a further study of the mechanical properties revealed that the elasticity of the HVPDs varied considerably only when both EDTA and ammonium hydroxide were present (red curve in Figure 5.3.4).

The  $G_0$  values showed a very small dependence on the concentration of EDTA (blue curve in Figure 5.3.4) in absence of added ammonium hydroxide.

Also the systems containing only ammonium hydroxide and no EDTA resulted to be characterized by a constant trend of  $G_0$ .

We hypothesized that the observed behavior is due to the combination of salt and pH effects: the minor EDTA tetra-anionic species  $Y^{4-}$  (~10 - 20% fraction), present in the samples with ammonia (pH ~ 9-10), may be involved in crosslinks with the hydroxyl groups on polymer chains, causing the observed increase of elasticity that

is not evidenced when only the EDTA tri-anionic species,  $\text{HY}^{3-}$ , is present (pH ~ 8 - 8.5) [10].

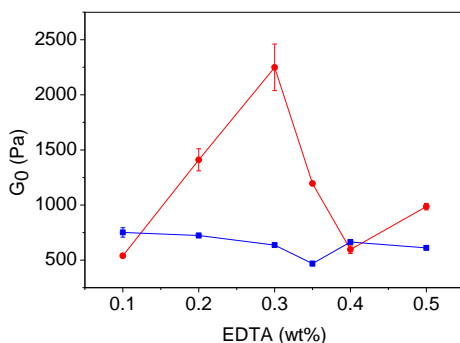


**Figure 5.3.4.** Intrinsic elastic modulus  $G_0$  as a function of the concentration of EDTA for 80PVAc-borax HVPDs with EDTA only (blue squares; pH ~ 8.5) and with EDTA and ammonium hydroxide (red circles; quantities of ammonia selected to maintain pH ~ 9.6).

Furthermore, the elastic properties of the 80PVAc-borax samples containing 0.2 wt% EDTA and four times the molar concentration of sodium acetate (to approximate the same salt effect) were compared (for simplicity, we assumed that the EDTA was 100% deprotonated at pH 10 as we verified that, assuming this, the error committed in calculating the proper amount of sodium acetate to add, in order to have the same ionic strength, was small and negligible for the rheological analyses). The two systems have similar ionic concentrations but differ in their entropies: whereas anions from each EDTA molecule are restricted to the same small region of a solution, those from sodium acetate can be dispersed freely. As expected, the elastic behavior of these HVPDs was influenced by the entropic contribution. Because the  $G_0$  values for the 0.2 wt% EDTA sample was  $1410 \pm 100$  Pa, that containing 0.16 wt% sodium acetate was  $952 \pm 38$  Pa, and that of the HVPD containing neither salt was  $723 \pm 21$  Pa, we conclude that the entropy of the system does play a role in the elasticity. EDTA, with its four space-restricted carboxylate groups, probably forms crosslinks that cause greater levels of interaction among polymer chains and increased stiffness.

Finally, considering the appreciable increment in the maximum loadable amount of chelator achieved with the 87PVAc, also the mechanical properties of the 87PVAc-borax HVPDs containing the chelators were characterized by means of rheological measurements. The frequency sweep curves for all the series of samples are



reported in Figure 5.3.5 and confirmed the behavior typical of viscoelastic dispersions (described previously) also for these systems obtained from 87PVAc.

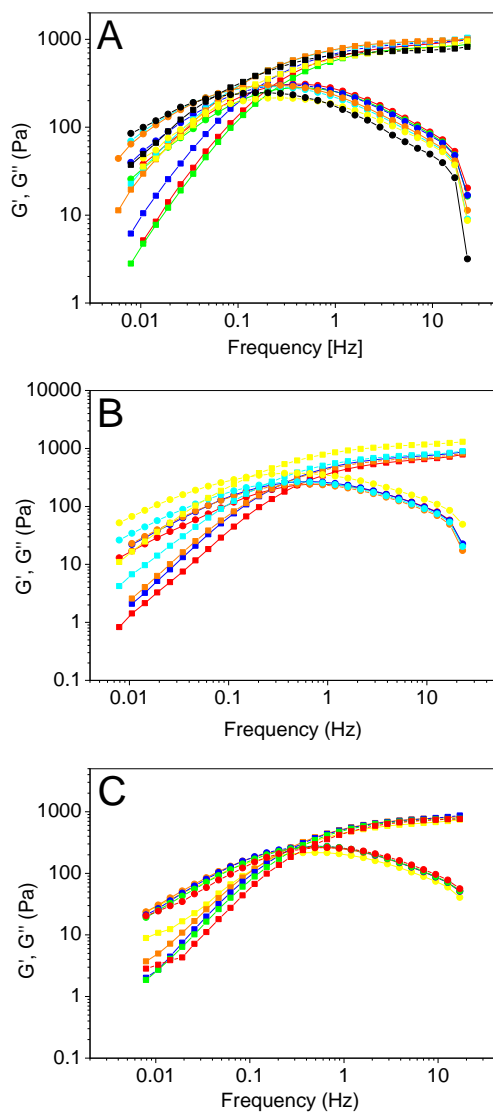


**Figure 5.3.5.** Frequency sweep curves at 1% strain of the  $G'$  modulus (squared symbols) and the  $G''$  modulus (circle symbols) as a function of the frequency (Hz) for the 87PVAc-borax HVPDs with: **(A)** 0.1 wt% (red symbols), 0.2 wt% (green symbols), 0.3 wt% (blue symbols), 0.4 wt% (cyan symbols) and 0.5 wt% (orange symbols), 0.7 wt% (yellow symbols) and 1.5 wt% (black symbols) of disodium EDTA; **(B)** 0.1 wt% (red symbols), 0.3 wt% (blue symbols), 0.5 wt% (orange symbols), 0.7 wt% (cyan symbols) and 1 wt% (yellow symbols) of TSC; **(C)** 0.1 wt% (red symbols), 0.2 wt% (green symbols), 0.3 wt% (blue symbols), 0.5 wt% (orange symbols) and 0.7 wt% (yellow symbols) of TAC.

As concern the normalized mechanical histograms for the 87PVAc-borax HVPDs reported in Figure 5.3.6, again we observed an overlapping of the curves in the investigated frequency range, indicating that, regardless of the chelator added, the mechanism associated with the relaxation is almost the same at all concentrations also for the HVPDs prepared with the 87PVAc.

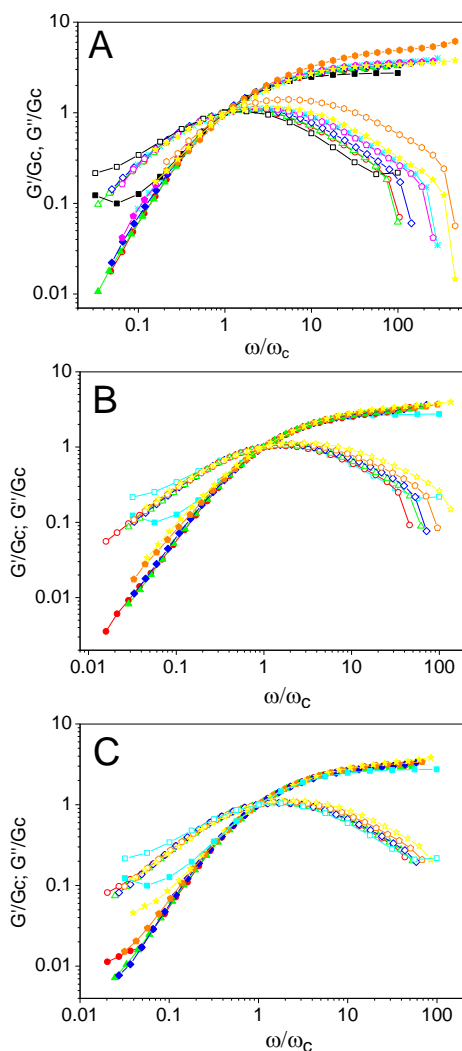


**Figure 5.3.6.** Normalized mechanical histograms for the 87PVAc-borax HVPDs containing: **(A)** 0 wt% (black), 0.1 wt% (red), 0.2 wt% (green), 0.3 wt% (blue), 0.4 wt% (cyan), 0.5 wt% (magenta), 0.7 wt% (orange) and 1.5 wt% (yellow) of disodium EDTA; **(B)** 0 wt% (cyan), 0.1 wt% (red), 0.3 wt% (green), 0.5 wt% (blue), 0.7 wt% (orange) and 1 wt% (yellow) of TSC; **(C)** 0 wt% (cyan), 0.1 wt% (red), 0.2 wt% (green), 0.3 wt% (blue), 0.5 wt% (orange) and 0.7 wt% (yellow) of TAC. Closed symbols indicate the  $G'/G_c$  ratios; open symbols indicate the  $G''/G_c$  ratios.  $G_c$  and  $\omega_c$  are the coordinates of the crossover point.

To complete the rheological characterization of the 87PVAc-based HVPD embedded with chelators, the intrinsic elastic modulus  $G_0$  was determined from the last five values of the  $G'$  in the *plateau* region of the flow curves. Differently from the values obtained for the systems prepared with the 80PVAc, these  $G_0$  moduli, regardless of the type of chelating agent, don't change significantly with respect to the salt concentration, thus the "structuring role" of the chelator recorded for the 80PVAc HVPDs is not evidenced here (Figure 5.3.7).

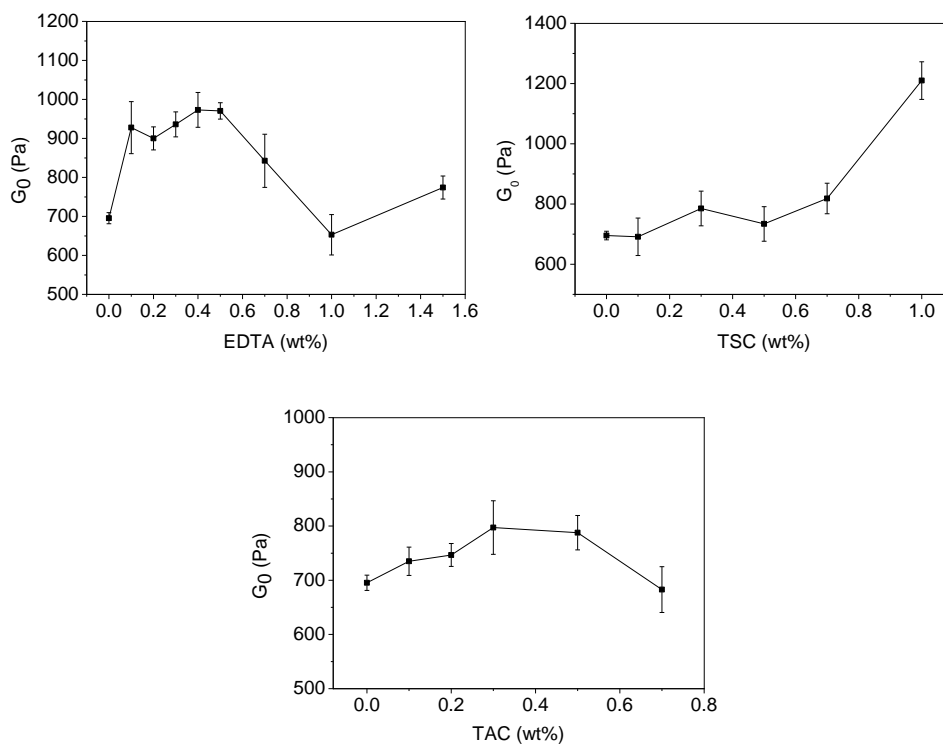


**Figure 5.3.7.** Intrinsic elastic moduli  $G_0$  of 87PVAc-borax HVPDs as a function of the concentration (wt%) of EDTA, sodium citrate (TSC) and triammonium citrate (TAC).

On the contrary, also for the 87PVAc-based viscous dispersions we observed a decrease of the intrinsic modulus at the highest salt concentrations, phenomenon that we ascribed to the proximity of the samples to the maximum limit concentration of the chelator above which the system becomes unstable and undergoes phase

separation. The exception is represented by the sample containing the highest amount of TSC (1 wt%) at which, unexpectedly, a considerable increment of the  $G_0$  is experienced.

To conclude, it's important to underline that these are preliminary results and that the rheological measurements were carried on only once and, thus, they need to be repeated at least two more times in order to verify the reproducibility of the values obtained.

### 5.4 Structural characterization: $^{11}\text{B}$ NMR analyses

The structures of the HVPDs obtained from 80PVAc and containing citrate or EDTA salts had been already examined by  $^{11}\text{B}$  NMR spectroscopy in a previous PhD thesis, to identify the boron-containing species and their relative concentrations [11]. Generally two peaks were detectable: a signal near 1.5 ppm corresponding to boron ions involved in crosslinking through di-diol esterification with vicinal hydroxyl groups along the polymer chains [12] and a signal further downfield (between 16 and 18 ppm) due to exchanging boric acid and borate ions (in the pH range where most PVAc-borax gels form, the interchange between boric acid and borate ions is fast on the NMR time scale, and a single broad peak appears [12,13]) [11].

By integrating the areas of the peaks from crosslinked and 'free' boron species in the NMR spectra it resulted that only a small amount (<15%) of the total boron-containing species is involved in crosslinking with the polymers.

As concern the HVPDs prepared with different amounts of TSC, a new peak at 6.5 ppm was recorded and it was attributed to borate coordinated by citrate (the peak is not detected when the citrate is absent). The peak appeared to be from a 1:1 five-membered mono-diol complex with borate ion [11,14].

In the perspective of an application of these systems for the removal of copper-based oxidation patinas from metallic artistic surfaces, the involvement of a fraction of citrate molecules in the chelation of borate ions could potentially reduce the extracting power of the chelator species and, thus, the effectiveness of the cleaning action performed by the systems in the treatment of salt efflorescences or oxidation patinas from carbonatic or metallic surface of objects of art.

For that reason, a further  $^{11}\text{B}$  NMR study was done on TSC-containing samples added with a small amount of metal ions as  $\text{Cu}^{2+}$ ,  $\text{Mn}^{2+}$ ,  $\text{Al}^{3+}$ ,  $\text{Co}^{2+}$ ,  $\text{Fe}^{3+}$ ,  $\text{Ca}^{2+}$ , introduced into the system to monitor whether they were able to displace the borate ion from the citrate complex [11]. The relative intensity of the peak at 6.5 ppm was monitored and it was found out that all caused a reduction in the citric acid-borate complex peak at 6.5 ppm. The smallest intensity reduction was found upon addition of  $\text{Ca}^{2+}$ , an ion for which citrate is known to have poor affinity [2].

Although the borate ion alone can chelate some metal ions, the stability constants for these complexes are much smaller than those between citrate and metal ions [15]. For that reason, the chelation of metal ions by borate is not expected to hinder the ability of citrate or EDTA to do so, and it was not found to affect to a significant degree the stabilities of the HVPDs, at least at the low ion concentrations investigated. If borate were chelating any of the metal ions added to a significant extent, a new peak in the boron NMR spectra should have been observed; none was seen in the samples investigated [11].

As concern the present work,  $^{11}\text{B}$  NMR spectra of the TAC-embedded HVPDs were acquired to verify if the triammonium citrate, as the sodium citrate, could chelate the borate ions. Considering the substantial increase in the maximum loadable amount of TAC achieved with 87PVAc, only the TAC-containing HVPDs obtained from 87PVAc were analyzed, while those prepared with 80PVAc were excluded.

As expected, the triammonium citrate resulted to form complexes with borate ions, showing the peak at ca. 6.5 ppm which increased in intensity with the concentration of the chelator (Figure 5.4.1).

In the perspective of applying the TAC-containing systems for the thinning of copper-based corrosion patinas from copper/bronze artifacts, the displacement of boron from citrate after the addition of a small amount of  $\text{CuCl}_2$  (3 mM) was then examined. A decrease in the intensity of the coordinated boron signal was observed (Figure 5.4.2). The amount of boron ions coordinated by TAC was reduced from ca. 13% to ca. 6% when the copper salt was added.

Furthermore, as for the 80PVAc-based systems containing TSC or EDTA, by integrating the  $^{11}\text{B}$  NMR signals, it was found out that the amount of boron participating in crosslinks is less than 15% also in presence of the 87PVAc.

The verification of the preferential coordination of the citrate salts towards metal ions rather than the borate ones, made us more confident about the viable use of these HVPDs as cleaning agents for copper/bronze surfaces.

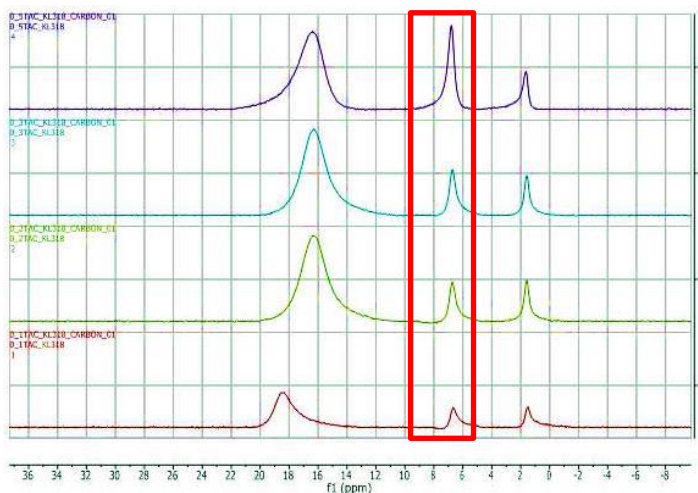


**Figure 5.4.1.**  $^{11}\text{B}$  NMR spectra of the 87PVAc-borax HVPDs containing 0.1 wt% (red), 0.2 wt% (green), 0.3 wt% (cyan) and 0.5 wt% (purple) of TAC. The red box highlights the signal ascribed to boron ions coordinated by TAC.

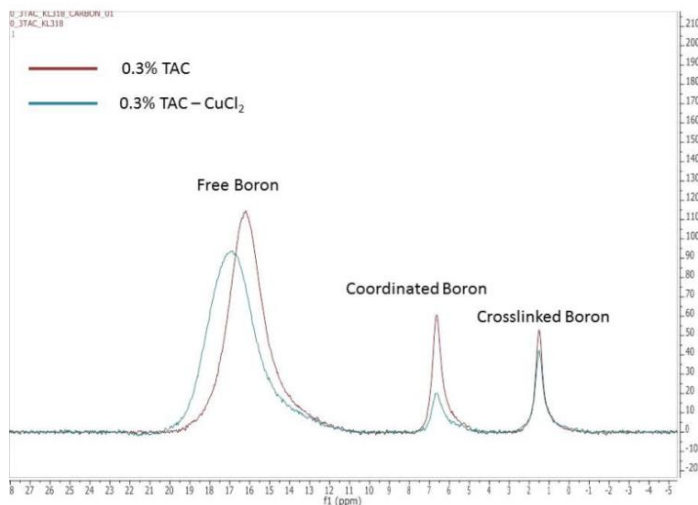


**Figure 5.4.2.**  $^{11}\text{B}$  NMR spectra of 87PVAc-borax HVPDs with 0.3 wt% TAC only (red) and 0.3 wt% TAC and 0.1 wt%  $\text{CuCl}_2$  (green).

## 5.5 Cleaning tests onto laboratory specimens

The effectiveness of the HVPDs containing chelators in the thinning of the corrosion patina from metallic surfaces was tested through preliminary applications on artificially oxidized [16] copper plates (for the artificial oxidation procedure see the Experimental section on paragraph 5.6).

The system selected for the cleaning tests was the 80PVAc-borax HVPD containing the highest achievable amount of EDTA (0.5 wt%). To favor the selective chelation of the copper ions by the EDTA [17], the pH was raised to about 10 through the dropwise addition of an aqueous solution of ammonium hydroxide.

Aliquots (~ 1 g) of the HVPDs were applied onto the copper plate for 10, 20, 30 and 40 min over 2.28 cm<sup>2</sup> areas of contact maintained by placing plastic rings on the plate surfaces (Figure 5.5.1).

The gradualness and effectiveness of the cleaning action performed by these systems was first evaluated qualitatively and macroscopically at naked eye.

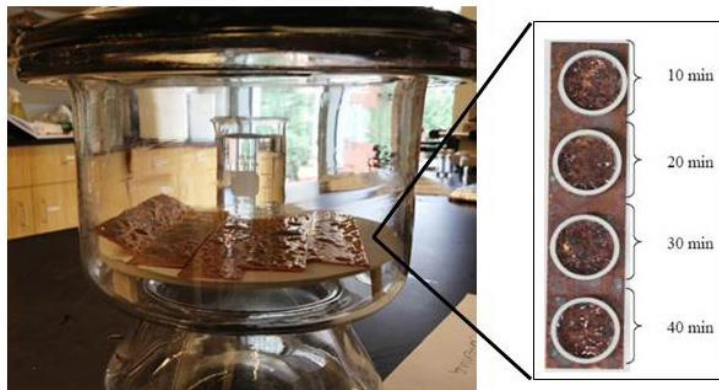


**Figure 5.5.1.** Conditioning of the copper plates at room temperature and high relative humidity, after spraying them with a 0.5 M NaCl solution and a 0.1 M CuCl<sub>2</sub> solution to simulate the “bronze disease” [18]. The picture on the right displays how the four applications of a 0.5 wt% EDTA-containing HVPD were performed.

Then, for a semi-quantitative evaluation of the efficacy in the thinning of the corrosion layer, the HVPD samples collected after each treatment were analyzed by Inductively-Coupled Plasma Optical Emission Spectrometry (ICP-OES).

In fact, thanks to the set-up of an analytical protocol specific for these HVPD systems (for the detailed description of the entire procedure see the subparagraph 5.6.6 of the Experimental section), it was possible to determine the absolute amounts of copper ions removed.

The results revealed that the amount of copper extracted by the HVPD increased upon increasing the contact time, confirming the gentle, progressive cleaning action.

The saturation of the system occurred after 30 min, application time corresponding to the maximum efficiency (Figure 5.5.2).

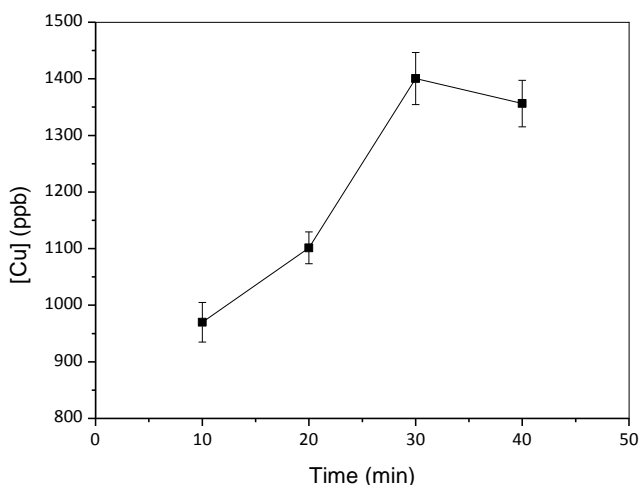


**Figure 5.5.2.** Histogram displaying ICP-OES results on the quantification of copper extracted by the HVPD containing 0.5 wt% EDTA from artificially oxidized copper plates: the amount of copper (ppb) is reported as a function of the duration (min) of the cleaning test.

## 5.6 Experimental section

### 5.6.1 Materials

The partially hydrolyzed poly(vinyl acetate)s were supplied by Kuraray Co., Ltd. as random copolymers: PVA-424H ( $M_w = 47300$ , 80% hydrolyzed) and KL318 (87% hydrolyzed, 3% of carboxylate groups). The 80PVAc was washed copiously with ice-cold water and dried under vacuum in order to eliminate by-products and



residual free acetate; the 87PVAc was used as received. Sodium tetraborate decahydrate (Fluka, > 99.5%), disodium ethylenediamine tetraacetic acid dihydrate (Baker analyzed, 99.0-101.0%), aqueous ammonium hydroxide (Sigma, 28-30% NH<sub>3</sub> content), sodium citrate (Sigma, ≥ 99.0%), ammonium citrate tribasic (Sigma, ≥ 97%), sodium acetate (J.T. Baker, anhydrous powder, assay 99.3%), cupric chloride dihydrate (the SCIENCE Company, Lab Grade Crystal, 99.0% minimum), aluminium chloride (Acros, 98.5% anhydrous), manganese (II) chloride (Aldrich, 99+%), cobalt chloride (II) hexahydrate (Sigma-Aldrich, 98%), calcium chloride (Baker Analyzed, 96%), iron (III) chloride hydrate (Baker Analyzed), hydrochloric acid (MACRON, 36.5-38.0%), and deuterium oxide (Cambridge Isotope Laboratories, Inc., 99.9% D) were used as received. Water was deionized by a Millipore Elix3 apparatus (R ≥ 15 MΩ cm).

#### *5.6.2 Preparation of the polymeric dispersions*

Measured amounts of polymer and chelating agent were stirred in water at room temperature until they dissolved. An aliquot of a 3 wt% aqueous borax solution was added dropwise to the polymer solution and the system was stirred with a VORTEX apparatus. The mixture became rigid and viscoelastic in a few minutes. The polymer/borax weight ratio was maintained at 4:1 in all formulations (3 wt% polymer and 0.75 wt% borax). In the EDTA-containing samples, the pH was adjusted to  $9.6 \pm 0.2$  (as indicated by Whatman Indicator Paper, pH 8.0-10.0 narrow range) through the dropwise addition of an aqueous solution of ammonium hydroxide (the amount of ammonia solution varied from 30 to 70 μL, depending on the EDTA concentration).

All measurements with the HVPDs were performed at least 48 h after the samples were prepared in order to minimize effects from non-equilibration.

#### *5.6.3 Rheological measurements*

Oscillatory shear measurements and extensional rheology tests were carried out at 25 °C on an Anton Paar Physica MCR 301 rheometer using a cone and plate geometry (25 mm diameter and 1° cone angle) for frequency sweeps and a parallel-plate geometry (25 mm diameter) for extensional rheology. Frequency sweep measurements were performed in the linear viscoelastic region (1% strain) based

on an amplitude sweep test. The storage modulus ( $G'$ ) and the loss modulus ( $G''$ ) were measured over a 0.01 - 40 Hz angular frequency range. For the extensional rheology measurements, the initial gap between the plates was 0.5 mm. Once loaded between the plates, samples were allowed to equilibrate until the force applied on the top plate was close to 0 Newtons. The top plate was lifted at a constant velocity of 1  $\mu\text{m/s}$  and the normal force was measured; the maximum force is reported. The data were collected using RheoPlus/32 Service V3.10 software.

### 5.6.4 NMR spectroscopy

$^{11}\text{B}$  NMR studies were performed on a Varian 400 MHz spectrometer and data were collected at 128.3 MHz with 320 FIDs in quartz NMR tubes (5 mm diameter, Wilmad Glass). Chemical shifts were referenced in some spectra to a borontrifluoride etherate (external) standard that was sealed in a glass capillary and placed inside the NMR tube. Because no noticeable change was observed in the highest field peak of spectra from a variety of the HVPD samples (*vide infra*), the standard was not used in all measurements. The relaxation delay was 0.01 s and the optimal observation pulse was determined empirically to be 48  $\mu\text{s}$ . Samples were prepared using deuterium oxide as the solvent: the polymer solution containing the chelating agent was added to the quartz NMR tube, followed by the borax solution, and the mixture was homogenized by stirring with a long stainless steel needle. In some cases, gentle heating was necessary to remove air bubbles from the samples. MestReNova software was used to process the FIDs and obtain the spectra.

### 5.6.5 Artificial oxidation of copper plates

Copper plates (2 x 10 x 0.1 cm) were artificially oxidized by spraying them with a 0.5 M NaCl solution and a 0.1 M  $\text{CuCl}_2$  solution and then placing them in a desiccator for 20 days at room temperature under high relative humidity. This process leads to the “bronze disease”, a common pathology that affects bronze and copper artifacts, resulting in the formation of an oxidized layer composed of copper chlorides and hydroxychlorides (atacamite and paratacamite). (Scott, D.A. Copper and bronze in art: corrosion, colorants, conservation. *Getty Publications* **2002**, Los Angeles)

### 5.6.6 Inductively-Coupled Plasma Optical Emission Spectrometry (ICP-OES) measurements

ICP-OES analyses were performed using a Varian 720-ES ICP-OES spectrometer with an optical detector. The external, auxiliary, and nebulizer flows were 16.5, 1.50, and 0.75 L/min, respectively. A solution of 50 ppm of germanium was used as the internal standard to quantify the analyte of interest (copper). Before being analyzed, the HVPD samples (~ 1 g) were solubilized with 50 µL of conc hydrochloric acid (37%) and diluted 1:100 using MilliQ ultrapure water. A 1 wt % HNO<sub>3</sub> solution with 1000 ppm of Cu was used to prepare standards with different copper concentrations. To each solution was added 100 µL of the internal standard Ge solution. For each sample, three measurements were acquired. The copper concentrations (ppb) were determined as the average recorded at 213.598, 224.700, 324.754, and 327.395 nm detection wavelengths.

The effective concentration  $C_e$  (ppm) of copper removed by the HVPD in the unknown samples was determined from the ratio between the signals from copper and germanium using the formula:

$$C_e = \frac{C_d \cdot P_i}{P_e} \cdot 100$$

where  $P_i$  is the initial amount of HVPD sample used for the cleaning test (mg),  $C_d$  is the amount of copper (ppm) measured in the diluted HVPD sample, and  $P_e$  is the effective amount (mg) of the HVPD sample collected after the application onto the copper plate and actually used for the ICP analysis.

## 5.7 Bibliography

- [1] H. BURGESS, *The Paper Conservator*, 1991, 15, 36.
- [2] A. PHENIX, A. BURNSTOCK, *The Conservator*, 1992, 16, 28.
- [3] J. HEUMAN, *The Conservator*, 1992, 16, 12.
- [4] I.D. MACLEOD, *Studies in conservation*, 1987, 32, 25.

- [5] L. CARLYLE, J.H. TOWNSEND, S. HACKNEY, *Triammonium citrate: An investigation into its applications for surface cleaning*, in *Dirt and Pictures Separated: papers given at a conference held jointly by UKIC and the Tate Gallery*, January 1990, United Kingdom Institute for Conservation: London, 1990, 44-48.
- [6] W.G. HENDERSON, M.J. HOW, G.R. KENNEDY, E.F. MOONEY, *Carbohydrate Research*, 1973, 28, 1.
- [7] K. ISHIHARA, A. NAGASAWA, K. UMEMOTO, H. ITO, K. SAITO, *Inorganic Chemistry*, 1994, 33, 3811.
- [8] L.V. ANGELOVA, P. TERECH, I. NATALI, L. DEI, E. CARRETTI, R.G. WEISS, *Langmuir*, 2011, 27, 11671.
- [9] I. NATALI, E. CARRETTI, L.V. ANGELOVA, P. BAGLIONI, R.G. WEISS, L. DEI, *Langmuir*, 2011, 27, 13226.
- [10] M. CHEN, R. STEPHEN REID, *Can. J. of Chem.*, 1993, 71, 763.
- [11] L.V. ANGELOVA, *Gels from borate-crosslinked partially hydrolyzed poly(vinyl acetate)s: characterization of physical and chemical properties and applications in art conservation*, PhD thesis in Chemistry, Georgetown University, Washington D.C., 2013, 131-138.
- [12] S.W. SINTON, *Macromolecules*, 1987, 20, 2430.
- [13] W.G. HENDERSON, M.J. HOW, G.R. KENNEDY, E.F. MOONEY, *Carbohydrate Research*, 1973, 28, 1.
- [14] M. BISHOP, N. SHAHID, J.Z. YANG, A.R. BARRON, *Dalton Trans.*, 2004, 17, 2621.
- [15] A. BOUSHER, *J. Coord. Chem.*, 1995, 34, 1.
- [16] M.P. CASALETTO, T. DE CARO, G. INGO, C. RICCUCCI, *Applied Physics A*, 2006, 83, 617.
- [17] P. CREMONESI, *L'uso di tensioattivi e chelanti per la pulitura di opere policrome*, Collana I Talenti, Il prato, 2002.
- [18] D.A. SCOTT, *Copper and bronze in art: corrosion, colorants, conservation.*, Getty Conservation Institute, Los Angeles, 2002.

## CHAPTER 6

# Chelating agents embedded in 80PVAc-borax based HVPDs for the removal of gypsum degradation layers

### 6.1 Introduction

As discussed in Chapter 1, a common degradation that affects artifacts made of natural or artificial carbonatic materials is the sulphatisation, the transformation of calcium carbonate in calcium sulfate bihydrate (gypsum) due mainly to the interaction with the atmospheric sulfur dioxide in the presence of humidity and oxidation catalysts [1]. The elementary cell of gypsum occupies almost a double volume compared to that of calcium carbonate. In the case of carbonatic supports, when this reaction takes place and new crystals of gypsum form inside the porous structure, the consequent volume expansion determine mechanical stresses that cause cracking, fissuring and pulverization of the carbonatic matrix [2]. In particular, for frescoes, when the phenomenon is particularly severe, we observe lifting and detachment of the paint layer, with loss of decoration and pigments [3].

One of the most effective traditional treatments for the gypsum removal from carbonatic supports is the Ferroni-Dini method [4], developed in 1966 by Enzo Ferroni, chemistry professor at the University of Florence, and Dino Dini, headmaster in the restoration of frescoes. It's a two-phases treatment consisting in the solubilization of gypsum with a water solution of ammonium carbonate followed by the application of barium hydroxide that ensures the consolidation of the degraded matrix and at the same time makes the sulfate unreactive and insoluble [5-7].

An alternative, widely used technique for the removal of soluble salts and, in particular, of calcium sulfate from frescoes, mural paintings and plasters consists in the use of ion-exchanger resins [8,9]. Generally they are synthetic resins that swell when in contact with water and are completely insoluble in it [10]. Due to this feature, when ion-exchangers are in contact with an artwork contaminated by salts,

their action is limited to the surface up to a depth of about 70-100  $\mu\text{m}$ , without penetrating into the porosity of the object, thus avoiding the interaction with the original materials to preserve [11].

Other substances used by restorers to treat the efflorescences are chelators. The most diffused are disodium EDTA, Rochelle salt (especially for the cleaning of gilded bronzes because of its mild action that preserve the original gilded foil [12]), citrate salts and benzotriazole [13-17]. Usually they are applied in aqueous solution (1-5% of additive) [18]. The solution pH has a fundamental role for the dissociation equilibria of the chelator and its selectivity towards different ions.

A potential risk in the use of these substances is that calcium ions coming from the carbonate matrix could be solubilized as well. To limit the penetration of the cleaning agent into the inner layers and to avoid the solubilization of the original material constituting the plaster and the paint layer, chelators aqueous solutions are usually adsorbed into poultices of carboxymethylcellulose or gelled with a thickener as Klucel G [19,20] or Carbopol [6].

The main drawback of these applicative methods is the “residue question” [21], as the thickened systems release residues onto the treated surface. The necessity of a clearance step with a neat liquid (generally water) and/or extra mechanical action can be critical in presence of fragile or hydrophilic surfaces/materials.

Considering the great versatility of the xPVAc-borax HVPDs, their interesting viscoelastic properties thank to which they can be removed from a surface in one step by a simple peeling action minimizing the residues and on the basis of the good preliminary cleaning results achieved in the treatment of corroded metal surfaces (see Chapter 5), HVPDs embedding chelators potentially active in the removal of gypsum degradation layers were formulated and studied.

Three chelating species were selected: disodium EDTA, ammonium carbonate and sodium/potassium tartrate. The maximum loadable amount of each, before observing phase separation, was determined. The viscoelastic properties of HVPDs containing different amounts of chelator were investigated to study how the additive influence their elastic response.

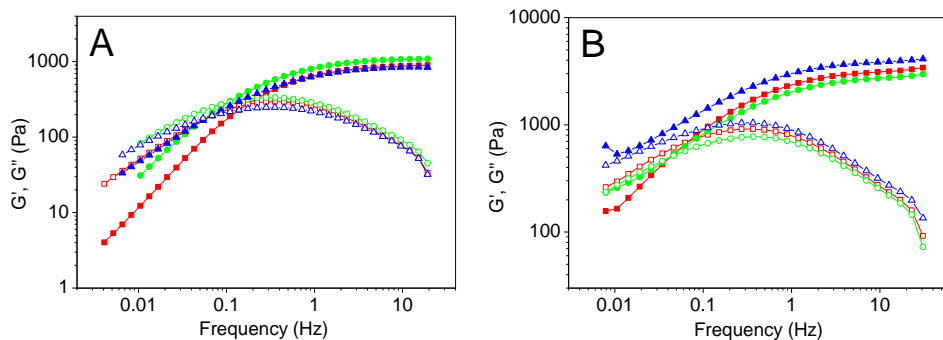
To evaluate the efficacy in the removal of calcium sulfate, these HVPDs embedded with chelators were tested onto artificially sulfated travertine tiles. HVPD samples collected after the cleaning tests were analyzed through Ion Chromatography and Inductively Coupled Plasma techniques. The quantification of the gypsum extracted

was possible thank to the set-up of an analytical protocol for the pre-treatment and the analysis of samples that was suitable for IC/ICP.

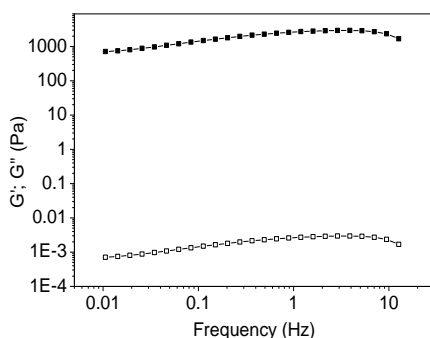
## 6.2 Rheological characterization

Being the use of monophasic systems an essential condition to control the cleaning action of the HVPDs, the maximum amount of EDTA, Rochelle salt and ammonium carbonate loadable in the 80PVAc-borax systems before observing phase separation was determined. The obtained values were 0.5 wt%, 1 wt% and 0.5 wt% respectively.

In a previous paper it was observed that to warrantee an adequate performance in terms of ease of application and complete removal through a peeling action [22], the HVPDs should preserve adequate elastic properties even upon addition of additives active against the foreign patinas of the artifacts. In particular their intrinsic elastic modulus  $G_0$  values should be always higher than 400 Pa. To verify if these features were preserved after the addition of chelators, the mechanical properties of the HVPDs set up were explored. Figure 6.2.1 shows that upon the addition of ammonium carbonate (A) or Rochelle salt (B), the mechanical behavior of the HVPDs is invariant for chelator concentrations respectively up to 0.5 and 0.9 wt%. Figure 6.2.2 displays that a further increase of Rochelle salt concentration up to 1 wt% determines the formation of a gel (the shear elastic modulus  $G'$  is higher than the shear viscous modulus  $G''$  over the entire range of frequencies explored) [23]. The frequency sweeps of the HVPDs containing different amounts of ammonium carbonate or Rochelle salt normalized to the crossover point between the  $G'$  and the  $G''$  curves (Figure 6.2.3) indicate that even if changes occur in the timescale of the relaxation process when the concentration of the chelator is increased, the mechanism associated with the relaxation remains almost the same.



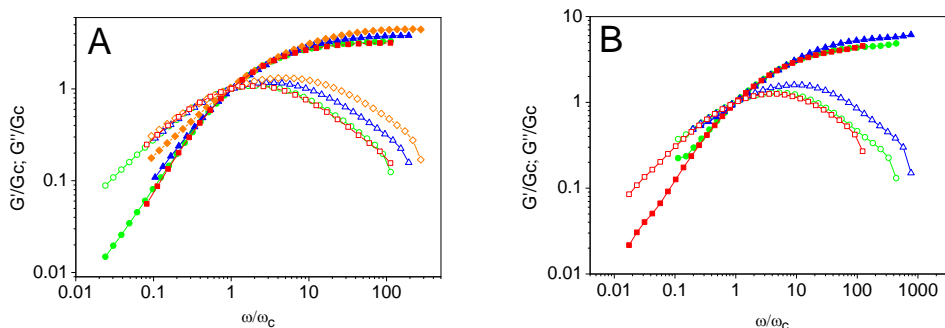
**Figure 6.2.1.** Flow curves of the  $G'$  (closed symbols) and  $G''$  moduli (open symbols) for the HVPDs containing: (A) 0.1 wt% (squares), 0.3 wt% (circles), 0.5 wt% (triangles) of ammonium carbonate; (B) 0.5 wt% (squares), 0.7 wt% (circles), 0.9 wt% (triangles) of Rochelle salt.



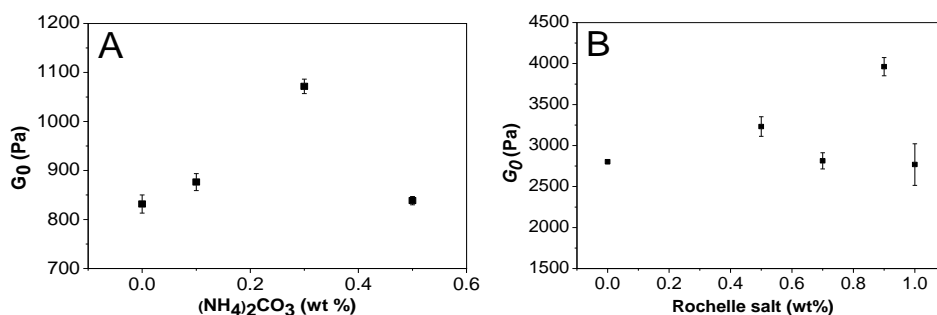
**Figure 6.2.2.** Flow curves of the  $G'$  (closed symbols) and  $G''$  moduli (open symbols) for the HVPD sample with 1 wt% Rochelle salt, showing the rheological behavior typical of a gel ( $G' \gg G''$ ).

Figure 6.2.4 shows the trends of the  $G_0$  values as a function of  $(\text{NH}_4)_2\text{CO}_3$  (A) and Rochelle salt (B) content; for concentrations around 0.3 wt% and 0.9 wt% respectively, the salts addition has a structuring effect on the systems as indicated by the increase of their elasticity. In presence of a higher amount of additive, the lowering of  $G_0$  indicates a reduction of the entanglements density of the PVA network.





**Figure 6.2.3.** Normalized mechanical histograms for the 80PVAc-borax with: (A) 0 wt% (red squares), 0.1 wt% (green circles), 0.3 wt% (blue triangles) and 0.5 wt% (orange diamonds) of ammonium carbonate; (B) 0 wt% (red squares), 0.5 wt% (green circles) and 0.7 wt% (blue triangles) of Rochelle salt. Closed symbols indicate the  $G'/G_c$  ratios; open symbols indicate the  $G''/G_c$  ratios.  $G_c$  (Pa) and  $\omega_c$  (Hz) are the coordinates of the crossover point.



**Figure 6.2.4.** Intrinsic elastic modulus  $G_0$  of 80PVAc-borax HVPDs as a function of ammonium carbonate (A) and Rochelle salt (B) concentrations (wt%).

Finally, as already shown in the paragraph 5.3 of the Chapter 5 (Figure 5.3.1), the addition of EDTA determines a significant increase in the intrinsic elasticity ( $G_0$ ) due to a structuring role of the salt. This behavior was ascribed to a combination of salt and pH effect, assuming that the EDTA tetra-anionic species [24]  $Y^{4-}$  (~50% at pH ~11 as that of our EDTA-containing systems), mediates some cross-links between the hydroxyl groups of 80PVAc chains (Matarrese et al., paper in preparation).

### 6.3 Application of HVPDs embedded with chelators onto the sulfated travertine tiles

Even if traditional gel systems obtained with KluGel G or Carbopol contain higher concentrations of chelators (1-5 wt%), the ones achievable with the 80PVAc-borax HVPDs, although significantly lower, were expected to be still adequate for cleaning purposes. An auxiliary benefit of the lower chelator concentrations is that the cleaning action is more gradual and controllable, favoring the preservation of the original layers of the artifacts.

The HVPDs selected for the application tests on sulfated travertine tiles, contained 0.25 wt% EDTA (pH = 11), 0.5 wt% ammonium carbonate and 1 wt% Rochelle salt, respectively (Table 6.3.1).

**Table 6.3.1**

Composition of the HVPDs used for the cleaning tests on sulfated travertine tiles.

HVPD	PVAc (wt%)	Borax (wt%)	Additive (wt%)		H <sub>2</sub> O (wt%)
System A	3%	0.75%	Disodium EDTA	0.25%	95.55%
			NH <sub>3</sub>	0.45%	
System B	3%	0.75%	Ammonium carbonate	0.5%	95.75%
System C	4%	1%	Rochelle salt	1%	94%

The aim was to evaluate their efficacy in the gypsum patina removal as a function of both the additive type and the application time.

The procedure for the cleaning tests was the following. A weighed amount (1 g) of an HVPD containing the chelator was applied onto a confined area (2.28 cm<sup>2</sup>) of a sulfated travertine tile using a plastic ring in order to better confine the cleaning action and to ensure also a quick and easy removal step (Figure 6.3.1). Different contact times were selected: 5, 10, 20, 30, 60 min. Each test was repeated four times.

For samples containing ammonium carbonate or Rochelle salt, additional applications lasting 1080 and 1380 min were performed.

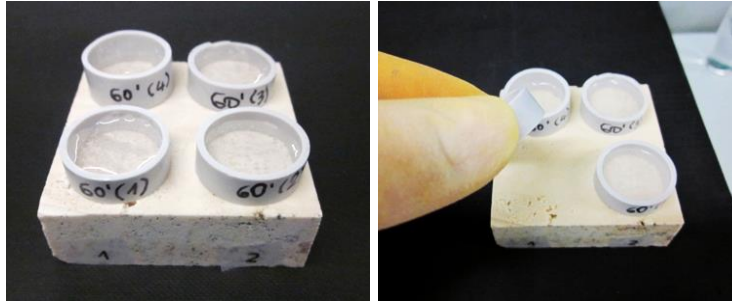


**Figure 6.3.1.** Exemplifying images showing the four “60 min-long” applications of the HVPD containing EDTA onto the sulfated travertine tile (left) and the ease removal step (right) achieved by confining the HVPD into a plastic ring.

#### 6.4 Absorption Index and optical microscopy

To verify the retentive capability of the HVPDs towards the liquid fraction confined into them once in contact with the porous matrixes, the HVPDs weight was monitored before and after each test. To eliminate the contribution due to the water evaporation, a “blank” adsorption was recorded by weighing a HVPD kept close to the samples on which the cleaning tests were carried out without being in contact with the porous matrix. The weight loss of the blank was subtracted to the one registered for the HVPDs applied onto the tiles [25]. The ratio between the water content before and after the test gives the Absorption Index (A.I.%):

$$A.I.\% = \frac{W_{Abs} - W_{Ref}}{W_i - W_{Ref}} \times 100 \quad \text{Eq. (2)}$$

where  $W_{Abs}$  is the weight of the absorbed water,  $W_{Ref}$  is the weight of the evaporated water,  $W_i$  is the initial weight of the water in the HVPDs in contact with the travertine surface. Figure 6.4.1 shows the A.I.% as a function of the application times of the HVPDs containing the different chelators.

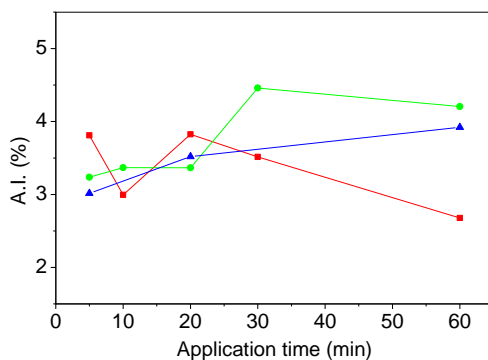


**Figure 6.4.1.** Absorption Index (%) as a function of the application time for the system containing 0.25 wt% EDTA (squares), 0.5 wt% ammonium carbonate (circles) and 1 wt% Rochelle salt (triangles).

The weight loss undergone by the system due to the migration of the liquid fraction (water solution) into the porous structure of the stone resulted very low: around 4% after 60 min of application for samples containing ammonium carbonate and Rochelle salt and around 3% for those with EDTA. These data confirmed the very good retentive properties of the HVPDs, even when embedded with chelators.

Optical micrographs (Figure 6.4.2) of the sulfated travertine surfaces before (B) and after (C) the application of the HVPDs loaded with  $(\text{NH}_4)_2\text{CO}_3$  0.5 wt% (contact time 60') indicate that the system is effective in the superficial removal of the gypsum patina.

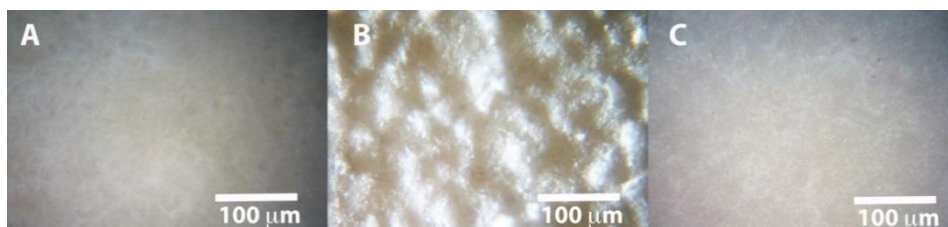


**Figure 6.4.2.** Optical micrographs (20x magnification) of the travertine surface before the sulfation treatment (A), the sulfated surface before (B) and after (C) the cleaning test with the HVPD containing 0.5 wt% ammonium carbonate.

## 6.5 IC and ICP analyses

To quantitatively evaluate the amount of sulfates removed, IC analyses were performed and a measuring protocol for the preparation and the analyses of the samples was developed as follow.

Standard solutions for calibrations were freshly prepared in precleaned polyethylene vials by diluting a stock standard solution ( $1000 \text{ mg L}^{-1}$ ) purchased from Merck (Darmstadt, Germany). To take into account the matrix effect, a “blank” HVPD sample without the analyte of interest (the sulfate ion) was dissolved with HCl (37% mol), diluted 1:100 in MilliQ ultrapure water and added in each standard solution. The sample had previously been applied for 5 min onto a no-sulfated travertine tile, so that the standard solutions contained all the components present in the unknown samples except for the analyte of interest. Before being analyzed, the HVPD samples containing the extracted calcium sulfate dihydrate ( $\sim 1 \text{ g}$ ) were solubilized with  $50 \mu\text{L}$  of HCl 37% and diluted 1:100 using MilliQ ultrapure water. The sulfate concentration was determined from the calibration curve based on the signal intensity ( $\mu\text{S}$ ) of the analyte (Figure 6.5.1). Considering that the retention time of the sulfate ion and, thus, the instrument sensitivity can slightly change due to measurement conditions or to the matrix complexity, the calibration curve was constructed for each measuring session.

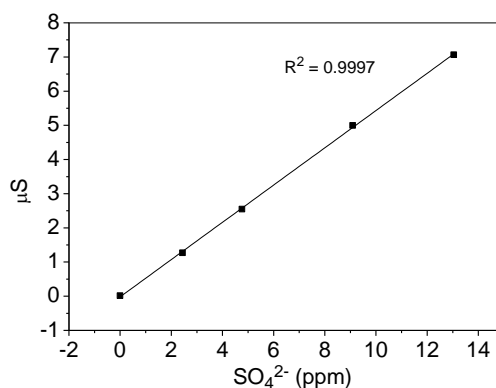


**Figure 6.5.1.** Example of an IC calibration curve for the sulfates obtained from standard solutions.

Figure 6.5.2 shows the IC chromatograms of the HVPD samples embedded with EDTA after the different cleaning tests.

Sulfate shows a retention time of 4,30 min while the ionic species responsible for the peak at 4,70 min could not be identified but did not represent a drawback for the reliable measurement of sulfate peak.

The sulfate peak increased with the contact time between the sulfated surface and the HVPD, whatever was the chelator supported by the system (Table 6.5.1).

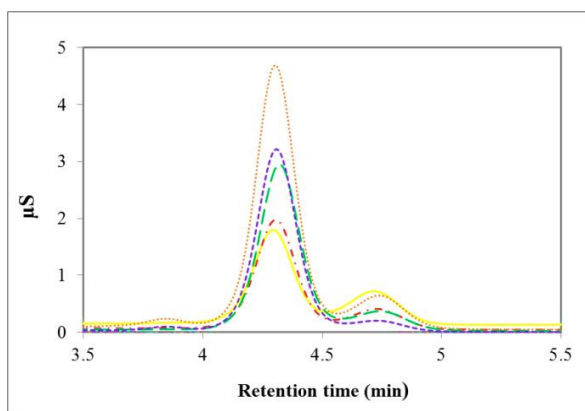


**Figure 6.5.2.** IC chromatograms for the EDTA-containing samples after being applied onto the travertine tile for 5' (yellow solid), 10' (red dash-dot), 20' (green dashed), 30' (purple short dashed) and 60' (orange dotted). The peak coming from the sulfate ions is at ~ 4,30 min.

**Table 6.5.1**

IC results displaying the amount of sulfates extracted (ppm) at different contact times for the HVPD containing 0.25 wt% EDTA, 0.5 wt% ammonium carbonate and 1 wt% Rochelle salt.

Contact time	EDTA		Ammonium carbonate		Rochelle salt	
	ppm	St. dev.	ppm	St. dev.	ppm	St. dev.*
5'	2.76	0.21	4.30	0.26	1.96	/
10'	3.51	0.15	5.13	0.35	/	/
20'	5.19	0.16	8.52	1.14	2.69	/
30'	6.03	0.30	9.55	1.30	/	/
60'	8.92	0.30	25.11	3.62	27.97	/

\* the experimental error is not reported because tests were carried on only once.

As regard samples containing Rochelle salt, IC technique wasn't suitable for the sulfates detection. The peak at 4,35 min due to the tartrate ions significantly

overlapped with the sulfate peak at around 4,15 min (Figure 6.5.3); thus, the quantification of the sulfates extracted was affected by a big error.

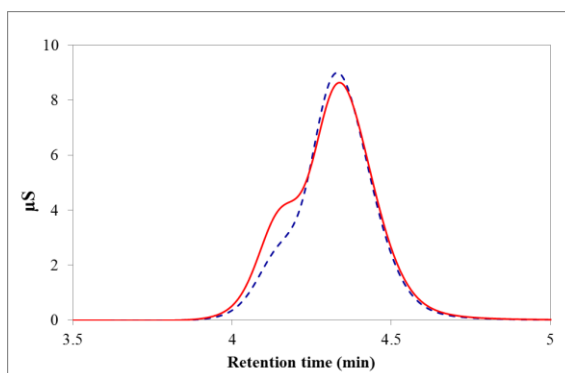


**Figure 6.5.3.** IC chromatograms for the Rochelle salt-containing samples after being applied onto the travertine tile for 5' (blue dashed) and 60' (red solid). The peak coming from the sulfate ions is at ~ 4,15 min while the peak at 4,35 min comes from the tartrate ions.

Taking into account the experimental uncertainty on Rochelle salt-containing samples, the percent of sulfates removed by each additive was determined and compared (Table 6.5.2). Ammonium carbonate resulted more effective for the thinning of the gypsum patina (the values relative to the systems functionalized with Rochelle salt were considered affected by a 50% error).

**Table 6.5.2**

Sulfates extracted per unit area (%) at different contact times for the HVPDs containing 0.25 wt% EDTA, 0.5 wt% ammonium carbonate and 1 wt% Rochelle salt.

Contact time	% of sulfates removed per unit area (2.28 cm <sup>2</sup> )		
	EDTA	Ammonium Carbonate	Rochelle salt
5'	1.91	3.04	1.36
10'	2.45	3.68	/
20'	3.81	6.04	2
30'	4.45	6.81	/
60'	6.67	18.43	21.29

A more accurate quantification of the sulfates extracted by the HVPDs containing 1 wt% Rochelle salt was achieved via ICP analyses by measuring the sulfur contained in samples collected after being applied for 60', 1080' and 1380'. To make a comparison, cleaning tests of the same duration were carried out using the HVPD with 0.5 wt% ammonium carbonate (that had resulted the most performing according to the previous tests) and the samples were analyzed through ICP technique as well. Also for ICP analyses a measuring protocol was developed. Before being analyzed, the HVPD samples (~1 g) were solubilized with 50  $\mu\text{L}$  of HCl (37%) and diluted 1:100 using MilliQ ultrapure water. A standard solution with 1000 ppm of  $\text{SO}_4^{2-}$  was used to obtain standard solutions with different  $\text{SO}_4^{2-}$  concentrations in which 100  $\mu\text{L}$  of a solution containing Ge as internal standard was then added. For each sample, a triplicate measurement was carried on. The sulfur concentrations (ppb) were determined as the average in ppb recorded at two different detection wavelengths (180.669 nm and 181.972 nm). The concentration of sulfate anions  $\text{SO}_4^{2-}$  present in the diluted HVPD samples was determined from the sulfur concentration given by the instrument, based on stoichiometric calculations (assuming that the detected sulfur came exclusively from the sulfates extracted by HVPD). Considering the 1:100 dilution, the effective concentration  $C_e$  (ppm) of sulfur removed resulted from Eq. (3):

$$C_e = \frac{C_d \cdot P_i}{P_e} \cdot 100 \quad \text{Eq. (3)}$$

where  $P_i$  is the initial amount of HVPD sample used for the cleaning test (mg),  $C_d$  is the amount of sulfate anion (ppm) measured in the diluted HVPD sample,  $P_e$  is the effective amount (mg) of the HVPD sample collected after the cleaning test and actually used for the ICP analysis.

ICP results led to believe that, as expected, IC data regarding Rochelle salt-containing HVPDs were affected by a significant error and the values were overestimated. In fact, according to ICP analyses, only 6.58% of sulfates were extracted after a 60 minutes-long treatment against the 21.29% calculated on the basis of IC analyses.

Comparing both IC and ICP analyses, the most performing additive for the extraction of gypsum still resulted ammonium carbonate, removing 37% of sulfates



after an application of 1380' (Figure 6.5.4). Regardless of the additive, the extraction power increased with the contact time. Systems containing ammonium carbonate and Rochelle salt gave significantly better performances when applied for 60' or more.

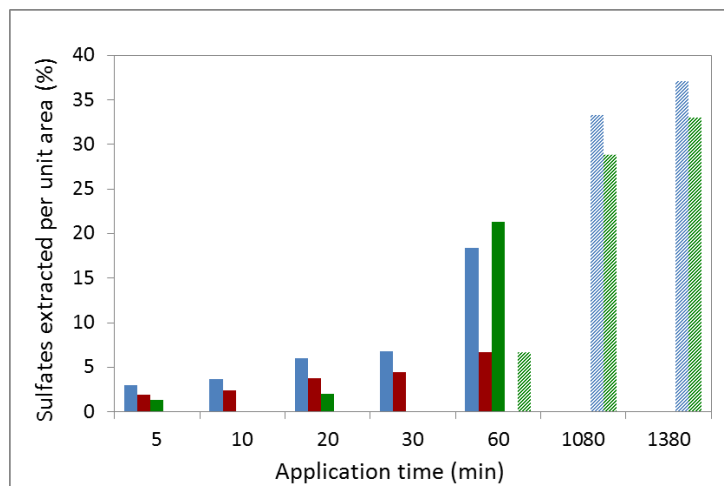


**Figure 6.5.4.** Sulfates extracted per unit area (%) at different contact times based on IC (filled histograms) and ICP (striped histograms) results for the HVPD containing 0.5 wt% ammonium carbonate (light blue), 0.25 wt% EDTA (dark red) and 1 wt% Rochelle salt (green).

## 6.6 Experimental section

### 6.6.1 Materials

80% hydrolyzed poly(vinyl acetate) was supplied by Kuraray Co., Ltd. as random copolymer ( $M_w = 47300$ ) and was used as received. Sodium tetraborate decahydrate (99,5-100%, Sigma-Aldrich), ammonium carbonate (Sigma-Aldrich), disodium EDTA dihydrate (99-100%, ACS reagent, Sigma-Aldrich), potassium sodium tartrate tetrahydrate (99%, ACS reagent, Sigma-Aldrich), ammonium hydroxide (Sigma,  $NH_3$  content 28-30%), hydrochloric acid 37% (CARLO ERBA, min. assay 36.5%) and sulphuric acid 96% ( $96\pm 1\%$ , CARLO ERBA) were used as received. Water was purified by a Millipore Elix3 apparatus ( $R \geq 15 M\Omega\text{ cm}$ ).

### 6.6.2 Preparation of the polymeric dispersions

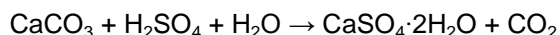
The PVAc was dissolved in a water solution of the chelating agent; then a solution of borax was added and the system was stirred with a VORTEX apparatus until it became rigid in few minutes. The polymer/borax weight ratio was kept to 4:1. The pH of all the systems was adjusted in order to warrantee the maximum complexation ability. All the measurements and cleaning tests were carried out one week after the samples preparation to ensure their equilibration.

### 6.6.3 Travertine samples sulfation

The sulfation of the travertine tiles was inducted by soaking one of their surface (4.8 x 4.8 cm) into a 5M H<sub>2</sub>SO<sub>4</sub> solution for 1h. Then they were let dry until a constant weight was reached.

### 6.6.4 Gravimetric determination of the calcium sulfate dihydrate formed onto the travertine samples

The average amount (g) of gypsum formed ( $W_{\text{CaSO}_4 \cdot 2\text{H}_2\text{O}}$ ) onto the travertine tiles was determined gravimetrically, according to the stoichiometric equilibrium of the sulfation reaction, using the formula in Eq. (1):



$$W_{\text{CaSO}_4 \cdot 2\text{H}_2\text{O}} = \frac{\Delta W \cdot MW_{\text{CaSO}_4 \cdot 2\text{H}_2\text{O}}}{MW_{\text{CaSO}_4 \cdot 2\text{H}_2\text{O}} - MW_{\text{CaCO}_3}} \quad \text{Eq. (1)}$$

where  $\Delta W$  (g) is the difference between the final weight  $W_f$  (g) and the initial weight  $W_i$  (g) of the travertine tile after the sulfation,  $MW_{\text{CaSO}_4 \cdot 2\text{H}_2\text{O}}$  and  $MW_{\text{CaCO}_3}$  are the molecular weights of CaSO<sub>4</sub>·2H<sub>2</sub>O and CaCO<sub>3</sub> respectively. The total average amount of CaSO<sub>4</sub>·2H<sub>2</sub>O formed onto the travertine surface was 6.7 mg/cm<sup>2</sup>.

### 6.6.5 Rheological measurements

Oscillatory shear measurements were performed with a Paar Physica UDS200 rheometer working at 25 ± 0.1°C (Peltier temperature control system) using cone-plate geometry (25 mm diameter and 1° cone angle). The gap between the plates was 0.5 mm. After being loaded, samples were equilibrated for 30 min at 25°C prior

to start the experiments. Frequency sweep measurements were done in the linear viscoelastic region (2-3% strain) based on an amplitude sweep test. The storage modulus  $G'$  (Pa) and the loss modulus  $G''$  (Pa) were measured over the frequency range 0.001-100 Hz. The intrinsic elastic modulus  $G_0$  (Pa), represented by the asymptotic value of the elastic shear modulus  $G'$  was calculated as the average value of the last five  $G'$  points in the *plateau* region of the flow curves.

#### 6.6.6 Ion Chromatography (IC)

IC analyses were performed with a Dionex ICS-90 Ion Chromatography System, using a Dionex AG4A guard-column (4 mm diameter, 5 cm length) and a Dionex AS4A column (4 mm diameter, 20 cm length). The eluent was a buffer solution with  $\text{Na}_2\text{CO}_3$  (1.8 mM) and  $\text{NaHCO}_3$  (1.8 mM) in MilliQ water (1.65 mL/min flow). A 10 mM  $\text{H}_2\text{SO}_4$  solution was used as the regeneration fluid for the conductivity suppressor (3.36 mL/min flow). The injection loop was 25  $\mu\text{L}$ .

#### 6.6.7 Inductively Coupled Plasma Optical Emission Spectrometry (ICP-OES)

ICP analyses were performed using a Varian 720-ES ICP-OES spectrometer with an optical detector. The external, auxiliary, and nebulizer flows were 16.5, 1.50, and 0.75 L/min, respectively. A 50 ppm solution of Germanium was used as the internal standard to quantify the analyte of interest.

### 6.7 Bibliography

- [1] R. STEUDEL, *Angew. Chem.*, 1995, 34, 1313.
- [2] L. BORGIOLO, *Polimeri di sintesi per la conservazione della pietra*, Collana I Talenti, Il Prato, 2002.
- [3] E. FERRONI, P. BAGLIONI, *Proceedings of the Symposium on Scientific Methodologies Applied to Works of Art*, Firenze, 1984, Montedison Progetto Cultura, Milano, 1986, 108.
- [4] M. CIATTI, *Appunti per un manuale di storia e di teoria del restauro*. Dispense per gli studenti, Edifir, 2009.
- [5] M. MATTEINI, S. SCUTO, *Consolidamento di manufatti lapidei con idrossido di bario*, Arkos 1, 2001.

- [6] L. CAMPANELLA ET AL., *Chimica per l'arte*, Zanichelli Editore, 2007.
- [7] P. BAGLIONI, E. CARRETTI, L. DEI, R. GIORGI, *Self-Assembly* (Ed.: B.H. Robinson), IOS, Amsterdam, 2003, 32-41.
- [8] A. GIOVAGNOLI, C. MEUCCI, M. TABASSO LAURENZI, *Ion-exchange resins employed in the cleaning of stone and plasters: research of optimal employment conditions and control of their effects*, in: *Deterioration and preservation of stones*, Proceedings of the 3rd International Congress, Venezia, October 24-27, 1979, Università degli studi—istituto di chimica industriale, Padova, 1982, 499-510.
- [9] M. MATTEINI, A. MOLES, M. OETER, I. TOSINI, *Ion exchange resins in the cleaning of stone materials and of mural paintings: experimental tests and applications*, in: *The cleaning of architectural surfaces*, Proceedings of a symposium, Bressanone, July 3-6, 1995, Libreria Progetto, Padova, 1995, 283-292.
- [10] P. FIORENTINO, M. MARABELLI, M. MATTEINI, A. MOLES, *Studies in Conservation*, 1982, 27, 145.
- [11] N. BERLUCCHI, R.G. CORRADINI, R. BONOMI, E. BEMPORAD, M. TISATO, *“La Fenice” theatre-foyer and Apollinee rooms – consolidation of fire-damaged stucco and marmorino decorations by means of combined applications of ion-exchange resins and barium hydroxide*, in: *Proceedings of the 9th International Congress on Deterioration and conservation of stone*, Venezia, 2000, 23-31.
- [12] G. CARBONARA, *Trattato di Restauro Architettonico*, Torino, 1996.
- [13] H. BURGESS, *The Paper Conservator*, 1991, 15, 36.
- [14] A. PHENIX, A. BURNSTOCK, *The Conservator*, 1992, 16, 28.
- [15] J. HEUMAN, *The Conservator*, 1992, 16, 12.
- [16] I.D. MACLEOD, *Studies in conservation*, 1987, 32, 25.
- [17] L. CARLYLE, J.H. TOWNSEND, S. HACKNEY, *Triammonium citrate: an investigation into its applications for surface cleaning*, in: *Dirt and Pictures Separated*, United Kingdom Institute for Conservation, London, 1990, 44-48.
- [18] R. WOLBERS, *Cleaning painted surfaces: aqueous methods*, Archetype Publications, London, 2000.
- [19] *Materiali tradizionali ed innovativi nella pulitura dei dipinti e delle opere policrome mobili*, in: *Proceedings of Primo Congresso Internazionale - Colore e conservazione: materiali e metodi nel restauro delle opere policrome mobili*, Piazzola sul Brenta, October 25-26, 2002, Il prato, 2003.
- [20] A. ONESTI, *CAB newsletter*, 1993, 2, 10-13.

- [21] D. STULIK, V. DORGE, *Solvent gels for the cleaning of works of art: the residue question*, Getty Publications, Los Angeles, 2004.
- [22] E. CARRETTI, C. MATARRESE, E. FRATINI, P. BAGLIONI, L. DEI, *Soft Matter*, 2014, 10, 4443.
- [23] L. PICULELL, M. EGERMAYER, J. SJOSTROM, *Langmuir*, 2003, 19, 3643.
- [24] M. CHEN, R. STEPHEN REID, *Can. J. of Chem.*, 1993, 71, 763.
- [25] S. GRASSI, E. CARRETTI, P. PECORELLI, F. IACOPINI, P. BAGLIONI, L. DEI, *Journal of Cultural Heritage*, 2007, 8, 119.

## CHAPTER 7

## Study of the HVPDs residues through fluorescence spectroscopy

## 7.1 Introduction

As already discussed in the Chapter 3, one of the main drawbacks of thickened or gelled systems (*Solvent gels*; poultices obtained from cellulose ethers as *Klucel G* or from polyacrylic acid as *Carbopol...*) traditionally used in conservation for the cleaning of artworks is the release of residues potentially dangerous for the piece of art. Thus, the necessity of a clearance step with a neat solvent or an extra mechanical action nullifies the advantage of entrapping the cleaning liquid into a highly retentive structure.

Our xPVAc-borax HVPDs, due to their viscoelastic properties, can be removed with a single peeling action, potentially without leaving any residue onto the treated surface.

It's also true that the transparency of these systems, although favorable for the visual control of the cleaning operation, could hinder the detection of eventual residues.



**Figure 7.1.1.** Exemplifying image showing the transparency of the HVPD systems (Carretti et al., *J. Cult. Heritage*, 2010, 11, 373).

For this reason, part of the work I did during my study period at the Georgetown University of Washington DC, under the supervision of the professor Richard G. Weiss, was focused on the covalent attachment of a fluorescent probe to the PVAc in order to make the polymer fluorescent and to study the presence and the spatial distribution of its residues through of UV-vis spectroscopic investigations (both absorption and fluorescence), and confocal microscopy.

A steady-state fluorescence study tailored to the construction of a calibration curve usable for the quantitative evaluation of PVA residues was also carried out.

## 7.2 Covalent attachment of the fluorescent probe to the polymer

Considering the promising application perspectives of the HVPDs obtained from the 87PVAc due to the significant increment in the maximum loadable amount of chelating agents achieved, the 87PVAc was the polymer selected to be functionalized with a fluorescence marker, for the fluorescence spectroscopy studies of the residues left by these viscous polymeric dispersions.

The chromophore chosen was the fluorescein (Figure 7.2.1).

This dye, in fact, is widely used for various fluorescence probes and labels because of its high quantum efficiency in aqueous media, its stability, because both its excitation and emission wavelength are in the range of the visible region which is beneficial for its detection [1].

Another reason that led us to use the fluorescein is that there are, in literature, several studies on the fluorescein in PVA solutions or films, which we could refer to [1-4].

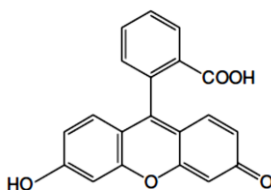


**Figure 7.2.1.** Chemical structure of the fluorescein [1].

For the labeling of the polymer with fluorescein I repeated the synthesis procedure used by the Dr. L.V. Angelova [5] for the functionalization of many poly(vinyl acetates) with different hydrolysis degree and molecular weight that was in turn adapted from Guan et al. [1] (Figure 7.2.2) and predicted the use of the 3-epoxypropoxy fluorescein (EPF) as intermediate. The epoxy group, in fact, provides a convenient site to react with many nucleophilic groups, such as  $\text{OH}^-$ ,  $\text{NH}_2^-$ ,  $\text{COO}^-$ , and  $\text{CN}^-$ , through which the fluorescein could be attached to macromolecules.<sup>1</sup> Moreover, the EPF largely preserved the well-known pH dependence of the fluorescence of fluorescein [1,6,7].

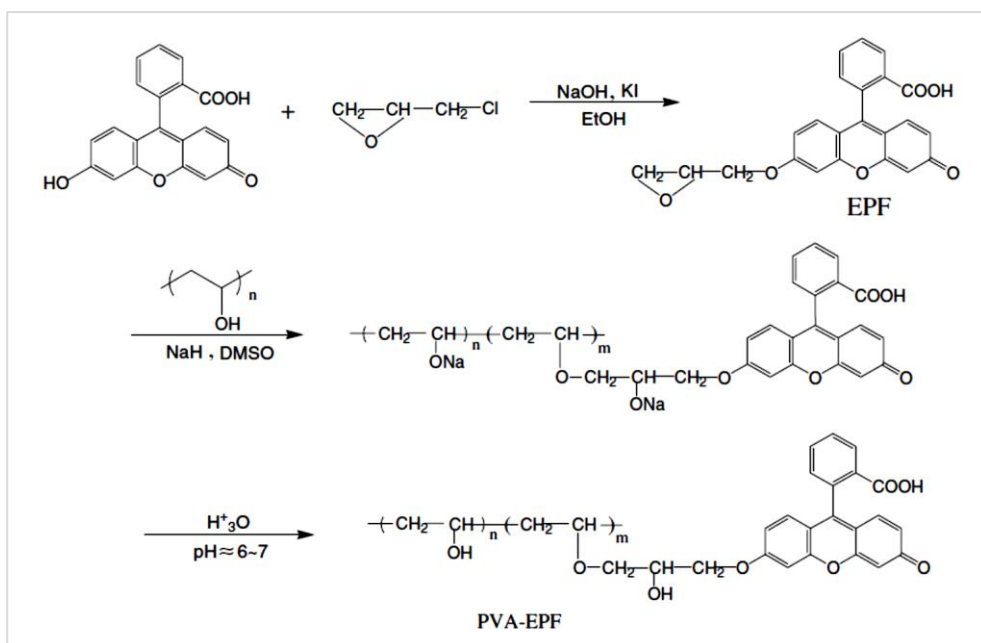


**Figure 7.2.2.** The synthesis of PVA-EPF performed by Guan et al. [1].

The 3-epoxypropoxy fluorescein (Figure 7.2.3) was synthesized by reacting the fluorescein with the epichlorohydrin in anhydrous ethanol and nitrogen atmosphere, at 50-60°C for 8 hours in the presence of  $\text{KI}$  (the detailed description of the procedure is reported in the subparagraph 7.6.2 of the Experimental section).  $\text{K}_2\text{CO}_3$  was added (in place of  $\text{NaOH}$ ) to obtain a basic pH.



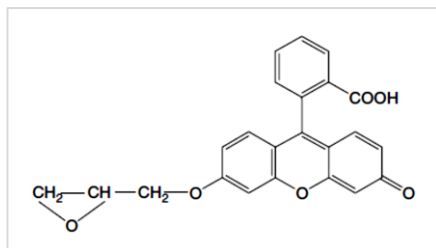


**Figure 7.2.3.** Chemical structure of the EPF [1].

In the second phase of the synthesis, the 87PVAc (previously washed with ice-cold water and dried so as to eliminate any waste byproducts present in the commercial product) was reacted with the EPF in pure dimethyl sulfoxide (DMSO), under nitrogen atmosphere, in presence of NaH as catalyst reaction, under magnetic stirring for 2 hours at room temperature (the detailed description of the procedure is reported in the subparagraph 7.6.3 of the Experimental section).

Finally, the product (named EPF-87PVAc) was neutralized with HCl (0.5 ml HCl conc. in 10 ml deionized water) to reach pH 7.

In order to verify that unattached EPF wasn't present in the final product, a very small amount of EPF-87PVAc was stirred in acetone for 48 hours (EPF is soluble in acetone, the polymer is not) and then the possible presence of unreacted EPF was detected through UV-Vis absorption and fluorescence emission.

UV-Vis absorption spectra are reported in Figure 7.2.4. Fluorescein and EPF spectra are identical because they have the same shape with three peaks at : 430 nm, 455 nm and 484 nm.

EPF-87PVAc in acetone don't show any of the absorbance peaks of EPF/fluorescein in the investigated wavelengths range (from 400 to 600 nm) and this confirmed to us that no unattached EPF was present in the samples.

Also the fluorescence emission spectra were acquired. The excitation wavelength was 455 nm (fluorescein maximum of absorption is at 455 nm). Figure 7.2.5 shows a comparison between the emission spectra of fluorescein, EPF and the derivatized polymer (all in acetone). EPF and fluorescein showed an emission band between 517 nm and 556 nm while EPF-87PVAc didn't emit and this was considered an additional proof that no free EPF was present in the final product.

To characterize the fluorescein-tagged polymer, it was dissolved in distilled, deionized water at pH 7 and the UV-vis spectrum was recorded in a 1 cm glass cuvette (Figure 7.2.6). The maximum of absorbance resulted at 498 nm.

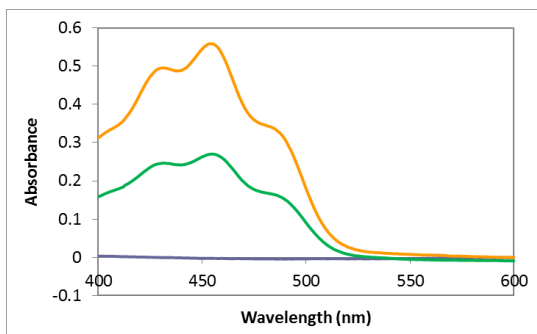


**Figure 7.2.4.** UV-Vis absorbance spectrum of EPF (orange), fluorescein (green) and EPF-87PVAc (purple). The solvent is acetone.

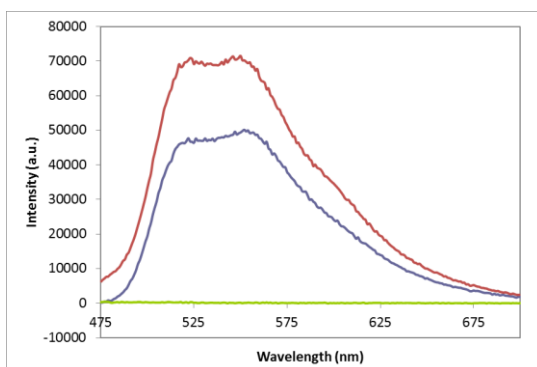


**Figure 7.2.5.** Emission spectra of EPF (purple), EPF-87PVAc (green) and fluorescein (red) in acetone.

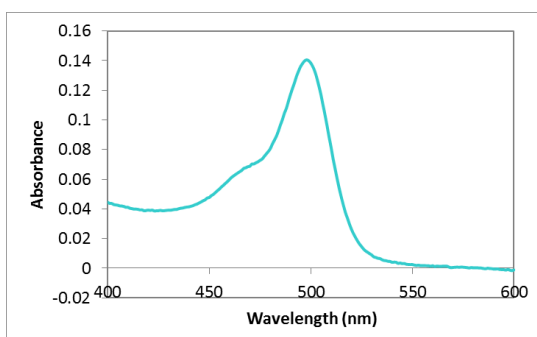


**Figure 7.2.6.** UV-Vis absorbance spectrum of EPF-87PVAc in deionized, distilled water.

Using the extinction coefficient of the 3-O-methylfluorescein,  $26000 \text{ M}^{-1}\text{cm}^{-1}$  at pH 7 [8], to approximate the extinction coefficient of the fluorescein bonded to the 87PVAc chain, the approximate percent molar substitution of the dye was back calculated from the absorption spectrum of the functionalized polymer dissolved in distilled deionized water at pH 7. In fact, the 3-O-methylfluorescein dye, has a methoxy group in place of the hydroxyl group on the fused benzene moiety of fluorescein and the molar extinction coefficient should be similar to that of epoxy-propoxy-fluorescein [5] (for the detailed description of the calculations see the subparagraph 7.6.4 of the Experimental section).

The approximate amount of fluorescein substitution was found to be less than 0.01% of OH monomers (corresponding to an EPF molar concentration of  $\sim 2.6 \times 10^{-6} \text{ M}$ ) which is very small but enough for having a fluorescent polymer which gives a detectable fluorescence signal; furthermore in this way the effect of dye substitution on the properties of the HVPD were limited.

### 7.3 UV-vis absorption/emission studies on free and bound fluorescein

Fluorescein was covalently bonded to the polymer chains for residue analysis.

In a preliminary phase of the work, the dye was also incorporated into the liquid fraction of 87PVAc aqueous solutions and 87PVAc-borax HVPDs in order to elucidate the fluorescence properties of the free dye in the presence of pure polymer or polymer and borax, and of the bound dye in solution or in the HVPD.

Fluorescein is known to have six different forms (Figure 7.3.1) which give different fluorescence absorption/emission spectra (Figure 7.3.2). The one that dominates is dependent on the pH of the aqueous solution or the nature of the solvent in which the dye is dissolved (Figure 7.3.3) [4,7].

Considering that the pH of the 87PVAc-borax HVPD resulted to be 8.97 (due to the borax solution), in order to have comparable measurements, the pH of the solutions containing free or bound fluorescein was brought to 9 by dissolving the dye in aqueous solutions of ammonium hydroxide ( $5.5 \cdot 10^{-5} \text{ M}$ ) at pH 9.

In these pH conditions, only the dianionic species is stable with a main absorption peak is at 490 nm and a shoulder at 475 nm (Figure 7.3.2).

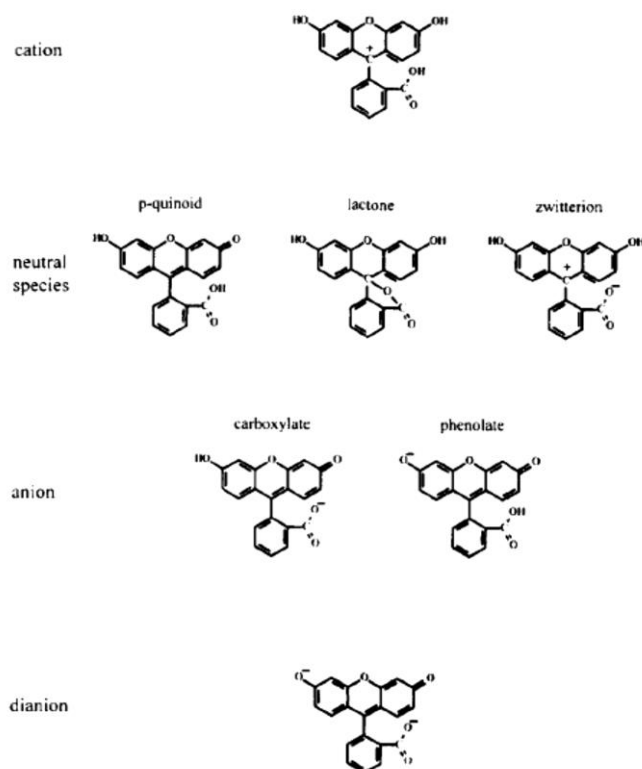


Figure 7.3.1. Chemical structures of fluorescein [7].

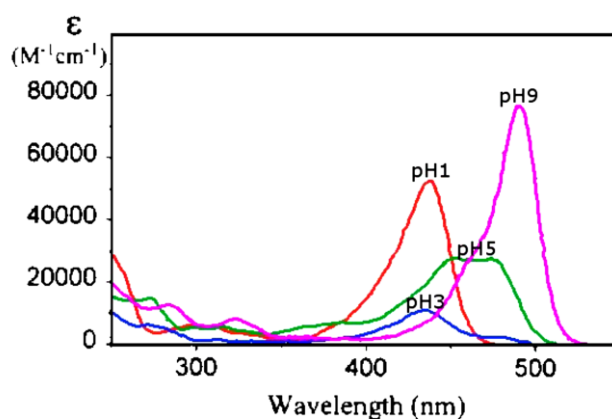
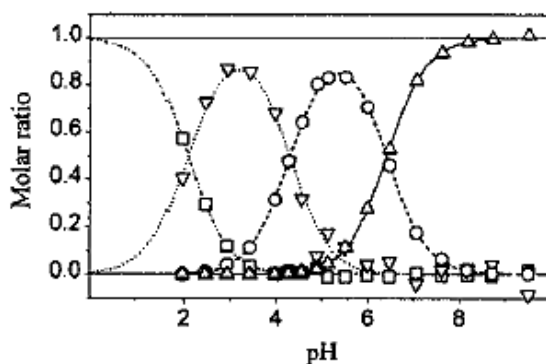


Figure 7.3.2. UV-Vis spectra of the different species of fluorescein: the dianionic one (magenta curve); the anionic one (green curve); the cationic one (red curve); the neutral one (blue curve) [7].



**Figure 7.3.3.** pH dependence of the concentration of the fluorescein protolytic forms: cation (squares), neutral species (triangles pointing down), anion (circles) and dianion (triangles pointing upwards) [7].

Considering that, according to calculations reported in the section 7.6.4 of the Experimental section, the amount of fluorescein attached to the polymer was in the order of  $10^{-6}$  M, the fluorescein aqueous solutions used to obtain the polymer solutions or the HVPDs for the fluorescence studies were prepared so as to have a  $10^{-6}$  M dye concentration. As concern the samples containing the bound fluorescein, the amount of labelled polymer taken in order to have a  $10^{-6}$  M probe concentration was 0.2 wt% (this, in fact, was the 87PVAc-EPF quantity corresponding to the  $2.6 \cdot 10^{-6}$  M fluorescein concentration value derived, through the Lambert-Beer law, from the UV-vis intensity absorbance signal of the functionalized polymer dissolved in deionized water; see the section 7.6.4 of the Experimental section for the details).

In the Table 7.3.1 the compositions of the samples containing the 87PVAc-EPF are reported.

**Table 7.3.1.** Compositions of the samples prepared with the labelled polymer.

Components		Solution (wt%)	HVPD (wt%)
polymer	87PVAc	2.8	2.8
	87PVAc-EPF	0.2	0.2
borax		/	0.75
water		97	96.25

The UV-vis absorption and emission spectra of free and bound fluorescein in solution and in the HVPD are reported in Figure 7.3.4 (A and B respectively). As expected, only the dianion absorbance with a  $\lambda_{\max} \sim 490$  nm and a shoulder at  $\sim 475$  nm is present in the spectrum; a bathochromic shift was observed when the dye was covalently attached to the polymer. This could be due to the decrease in the micro-polarity of the environment immediately surrounding the probe attached to the polymer chain.

By comparing the absorbance/emission spectra of the HVPD containing the fluorescent polymer collected immediately after the preparation of the sample ( $t = 0$ ) and after six days from it ( $t = 6$ ), we didn't observe any change in the intensity or the profile of the signals, indicating that, at least from a spectroscopic viewpoint, the system was equilibrated immediately after its synthesis.

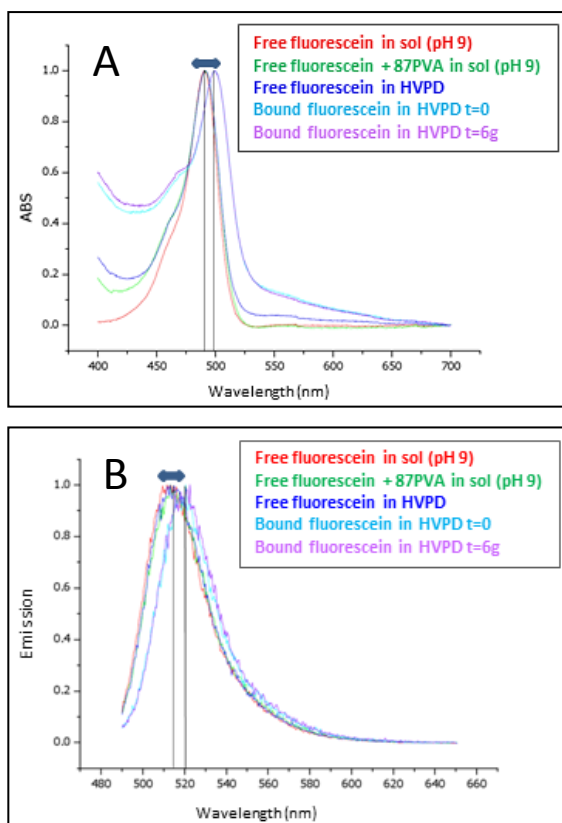


**Figure 7.3.4.** UV-vis absorption (A) and emission (B) spectra of free and bound fluorescein in solution and in the HVPD at pH 9. In both the spectra the bathochromic shift is evidenced.

## 7.4 Residues studies: confocal microscopy imaging and spectrophotometry

After studying the behavior of both free and bound fluorescein by UV-vis fluorescence spectroscopy, the qualitative analysis of the residues released by HVPDs containing a small amount of fluorescent 87PVAc (0.2 wt%), after their application and removal from laboratory glasses, were performed by means of confocal microscope imaging.

Confocal microscopy [9] is a recent technique that overcome some limitations of traditional optical microscopy, due to the phenomenon of light diffusion. What allows to overcome these limitations is the presence of both an input and an output pinhole, i.e. a shutter, which reduces the input beam to a point source and attenuates the output contributions from the layers out of focus, allowing to illuminate only a very limited area of the sample and to collect only the light coming from it. In this way the collimated and polarized light, is focused on a single point of the sample, the *focal point*. The light emitted and/or reflected by the focal point of the sample is focused on a second point, the *confocal point*, where the outlet pinhole is located, and passes through it to reach the detector. For this reason, it can be observed always and only a single point at a time [10]. By moving the beam along the *xy* plane, the sample can be scanned, creating in this way the image to be acquired.

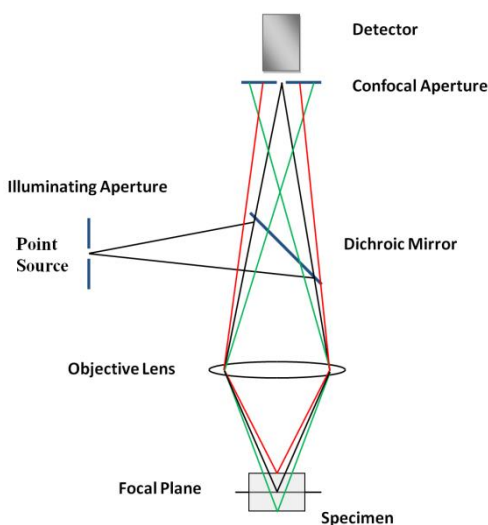


**Figure 7.4.1.** Schematic representation of the confocal microscope.

For carrying out the residues analysis, around 1 g of fluorescent HVPD was applied onto the surface of laboratory glasses for different contact times: 2, 3 and 4 hours. The use of glass as the support was imposed by the technique itself that works in transmission and requires a transparent surface penetrable by the beam. In order to facilitate the application/removal procedure and to confine the test to a well-defined area ( $2.28 \text{ cm}^2$ ), the samples were applied using plastic rings (diameter 1.7 cm) as shown in Figure 7.4.2.

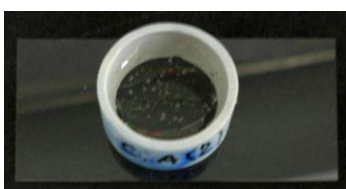


**Figure 7.4.2.** Exemplifying image for the application of the HVPD sample onto the glass surface with the aim of a plastic ring.

During of each test, the HVPD was kept covered with a petri plate, in order to minimize the evaporation of the volatile component (water).

The systems were then removed with the aim of a spatula, without performing the final clearance step (typical of traditional cleaning methods and potentially harmful for porous surfaces).

Once the HVPD was removed, the glass was subjected to the imaging analysis to detect the presence of residual polymer. The scanning wavelength was 488 nm in the range 500-700 nm (for more details about the experimental conditions see the subparagraph 7.6.7 of the Experimental section).

The scan was performed on multiple points of the surface to analyze the spatial distribution of the residues. The images acquired for each of the three applications are reported in Figures 7.4.3, 7.4.4 and 7.4.5.



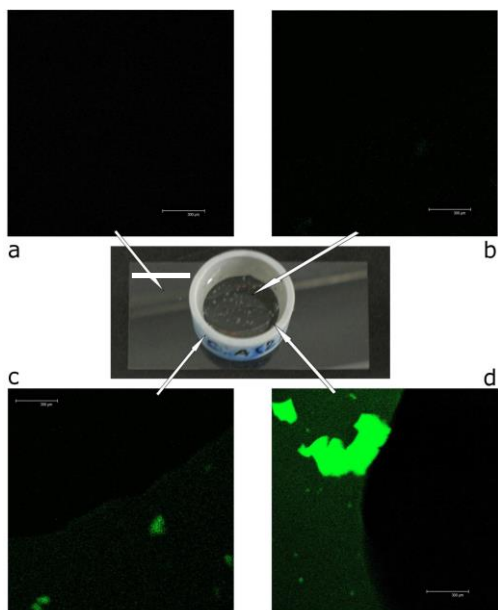


**Figure 7.4.3.** Confocal microscope images of the glass where the fluorescent HVPD had been applied for 2 hours. **a:** untreated area; **b:** central area of the application; **c:** outer edge of the application zone; **d:** inner edge of the application area. The fluorescent areas indicate the presence of residual EPF-labelled polymer. The metric reference is 300  $\mu\text{m}$ .

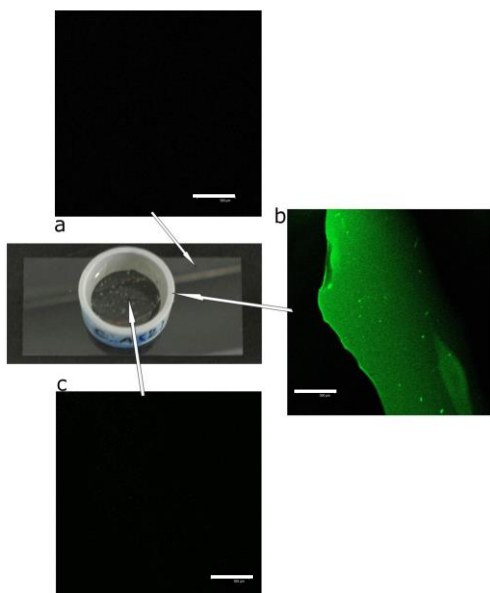


**Figure 7.4.4.** Confocal microscope images of the glass where the fluorescent HVPD had been applied for 3 hours. **a:** untreated area; **b:** inner edge of the application area; **c:** central area of the application. The fluorescent areas indicate the presence of residual EPF-labelled polymer. The metric reference is 300  $\mu\text{m}$ .

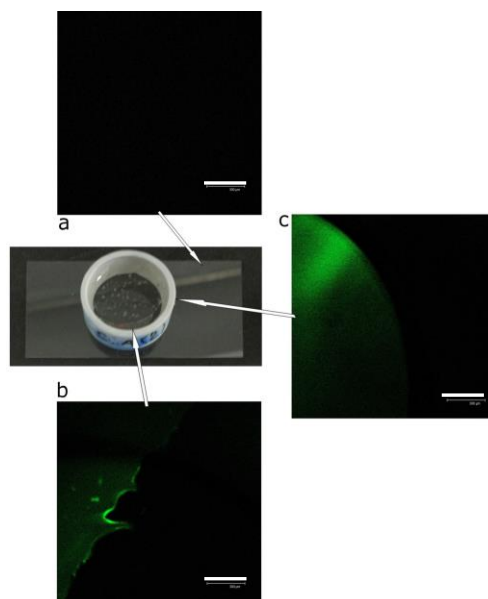


**Figure 7.4.5.** Confocal microscope images of the glass where the fluorescent HVPD had been applied for 4 hours. **a:** untreated area; **b:** outer edge of the application area; **c:** inner edge of the application zone. The fluorescent areas indicate the presence of residual EPF-labelled polymer. The metric reference is 300  $\mu\text{m}$ .

The experimental data deducible from the confocal microscopy was the absence of residual fluorescent polymer in the central area of the application zone. The few detected residues resulted concentrated on the edges of the treated surface. This "edge effect" could likely be due to the greater adhesion forces between the HVPD molecules and the support in the peripheral zone. By contrast, in the internal zone the cohesion forces within the HVPD prevailed on the adhesion, thus allowing a more effective removal.

A confirmation of these imaging results was given by the spectrophotometric analysis performed still with the confocal microscope.

For each glass sample three areas were selected, i.e. the external untreated zone, the internal edge of the application area and the central part of the treated surface, and the spatially resolved fluorescence emission spectra in the range 500-700 nm were acquired (Figure 7.4.6), using an excitation wavelength of 488 nm (for more details about the experimental conditions see the subparagraph 7.6.7 of the Experimental section).

As expected, the fluorescence emission signal due to the fluorescent polymer residues was recorded essentially only in correspondence of the edge of the treated area and it was found out to increase in intensity with the increment of the application time of the HVPD.

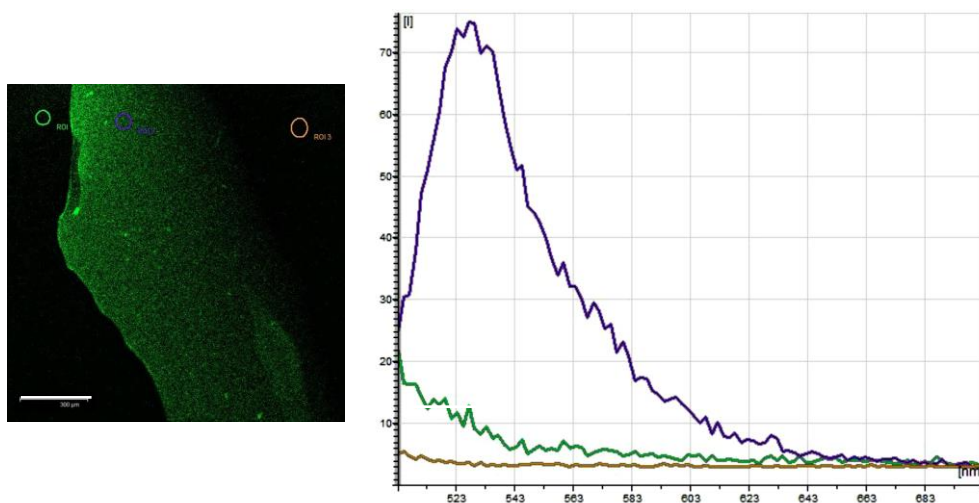


**Figure 7.4.6.** Exemplifying confocal microscope image of the glass subjected to the 3-hours application with the three spots where the emission spectra reported in the graph on the right were acquired: the green color corresponds to the signal emitted by the outer untreated area; the brownish orange spot and signal correspond to the central part of the treated area; the purple color is related to the edge of the application zone. The metric reference is 300 μm.

## 7.5 Quantitative analysis of the polymer residues: construction of a calibration curve

The confocal microscopy analyses permitted only a qualitative study of the presence and the distribution of the HVPD residues.

In the perspective of quantifying them, a calibration curve with the fluorescence emission intensity as a function of the concentration of the fluorescent 87PVAc was created, by recording the spectra of EPF-87PVAc films containing incremental known amounts of polymer.

Five aqueous solutions at different concentration of EPF-87PVAc were prepared; their composition is reported in Table 7.5.1.

**Table 7.5.1.** Composition of the polymer solutions used to create the calibration curve.

Sample	Total polymer (wt%)	Water (wt%)	EPF-87PVAc (wt%)	87PVAc (wt%)
1	5	95	80	20
2	5	95	60	40
3	5	95	40	60
4	5	95	20	80
5	5	95	10	90

The solutions were spread onto the surface ( $4 \text{ cm}^2$ ) of laboratory glasses and let dry to get thin polymeric films. To obtain an homogeneous distribution of them over the entire surface of the support, the application was performed with a spin coater (Automated Spin Coater P-6700 Speciality Coating System Inc). The parameters used are reported in Table 7.5.2.

**Table 7.5.2.** Spin coating parameters.

Solution amount	300 $\mu\text{l}$
Rotation speed	2000 spin/min
Time	30 s

The samples were let dry for 24 hours and then the fluorescence emission spectra were acquired (excitation wavelength = 460 nm; 500-650 nm range).

From the intensity of the emission peak at  $\sim 520 \text{ nm}$  of the samples, knowing the area of the glasses and the amount (mg) of labelled polymer present on them, it was possible to construct the calibration curve (Figure 7.5.1) with the intensity of the fluorescence signal as a function of the quantity of EPF-87PVAc per unit area ( $\text{mg}/\text{cm}^2$ ).

In the perspective of extending the residues studies by means of fluorescence spectrophotometry to laboratory specimens simulating real artistic surfaces, this curve will be useful for the quantification of the residual polymer present onto different type of supports used in art production.

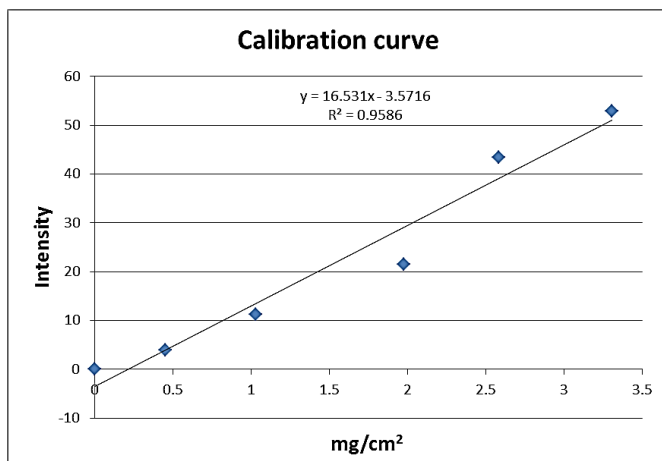


**Figure 7.5.1.** Calibration curve obtained by measuring the fluorescence emission intensity at 520 nm of polymeric films prepared with incremental known amounts of fluorescent 87PVAc.

## 7.6 Experimental section

### 7.6.1 Materials

87% hydrolyzed poly(vinyl acetate) was supplied by Kuraray America Inc. (Kuraray K-POLYMER KL318, 85-90 mol% hydrolysis degree, 1.5% max. ash content) and was washed copiously with ice-cold water and dried under vacuum in order to eliminate by-products and residual free acetate. Sodium tetraborate decahydrate (99.5-100%, Sigma-Aldrich), methanol (Sigma-Aldrich, ACS reagent,  $\geq 99.8\%$ ), fluorescein (free acid, dye content 95%, Sigma-Aldrich), epichlorohydrin (99%, ACROS ORGANICS), potassium iodide (Baker analyzed reagent, purity unknown), anhydrous ethanol (200 proof,  $\geq 99.5\%$ , Sigma-Aldrich), potassium carbonate (Sigma Aldrich, ACS-reagent,  $\geq 99.0\%$ ), methanol-D4 (99.8%, Cambridge Isotope Laboratories), sodium hydride (Alfa Aesar, 57-63% oil dispersion), dimethyl sulfoxide (spectrophotometric grade, 99.9+%, Alfa Aesar), acetone (Sigma Aldrich for HPLC,  $\geq 99.9\%$ ), chloride acid (Macron, ACS-standard, 36.5-38.0%) were used as received. Water was purified by a Millipore Elix3 apparatus ( $R \geq 15 \text{ M}\Omega \text{ cm}$ ).

### 7.6.2 Synthesis of the EPF

The synthesis of 3-epoxypropoxy fluorescein (EPF) was performed through the following procedure, which was adapted from Guan et al. [1]:

- 0.83 g (5mmol) of KI was ground and placed in a dry 3-neck round bottom flask
- 0.39 mL (0.39mmol) of epichlorohydrin and 10 mL anhydrous ethanol were added, reaction mixture was refluxed under N<sub>2</sub> for 30 minutes at 50-60°C with vigorous stirring.

- Ground K<sub>2</sub>CO<sub>3</sub> (0.415 g, 2 mmol) was added to the flask, which was then stirred for 10 additional minutes.

- Fluorescein (0.17 g, 0.5 mmol) was dissolved in 15 mL anhydrous ethanol, and the solution was slowly added with a dropping funnel. The reaction mixture was allowed to stir 8 hours after which, the reaction was cooled and vacuum filtered.

To purify the orange solid, the solid was dissolved in 1:1 ethyl acetate:methanol, and column chromatography was performed.

Percent yield was 24%.

### 7.6.3 EPF attachment on the 87PVAc polymer

EPF attachment on the 87PVAc polymer was performed through a procedure adapted from Guan et al. [1].

The polymer was previously washed with ice-cold water and dried in vacuum oven for a couple of hours and then at open air for a couple of days (spread on a Teflon plate). The amounts of polymer and EPF were calculated in order to have a percent molar substitution of 0.05%.

The procedure was the following:

- 2 g of polymer were weighed and put it in round bottom flask (50 mL volume) to dry under vacuum at 40-45°C (water bath) for 24h

- the polymer was then dissolved in 20 mL of spectrophotometric grade DMSO under reflux at 85-90°C and under stirring

- 0.304 g NaH (60% purity in parafilm) were weighed and put it in 3 neck round bottom flask (100 mL volume) under N<sub>2</sub> flow, in ice-cold water bath

- the polymer solution was added dropwise under stirring and N<sub>2</sub> reflux and it was kept stirring until no more H<sub>2</sub> bubbles were present

- EPF solution (11.7 mg EPF in 5 mL DMSO) was added slowly for 20 mins under stirring, then kept stirring for 1 hour at room temperature.

Acetone was used to precipitate the product, which was then solubilized in deionized water (pH tested ~ 10) and neutralized with an HCl solution (0.5 ml HCl conc. in 10 ml DI water). The fluorescent polymer was precipitated a second time with acetone and ethyl acetate.

Percent yield was 22%.

#### 7.6.4 Calculation of the percent molar substitution of the OH groups of the 87PVAc with the EPF

The approximate mol% substitution of EPF in 87PVAc was back calculated, through the Lambert-Beer law in eq. 7.1, by measuring the absorbance at 470 nm of the functionalized polymer dissolved in distilled deionized water at pH 7, using the extinction coefficient of the 3-O-methylfluorescein ( $26000 \text{ M}^{-1}\text{cm}^{-1}$  at pH 7 and 470 nm) [8] to approximate the extinction coefficient of the fluorescein bonded to the 87PVAc chain:

$$A = \epsilon bc \quad \text{Eq. 7.1}$$

where  $\epsilon = 26000 \text{ M}^{-1}\text{cm}^{-1}$ ,  $b = 1 \text{ cm}$ , and  $A = 0.068$  in the UV-vis spectrum of 0.0102 g of 87PVAc-EPF dissolved in 5 mL of  $\text{H}_2\text{O}$  (0.2 wt% polymer solution).

The calculations were the following:

$$\frac{0.0102 \text{ g PVA}}{44 \frac{\text{g}}{\text{mol OH}} (0.87) + 86 \frac{\text{g}}{\text{mol Ac}} (0.13)} = 2.06 \times 10^{-4} \times (0.87) = 1.79 \times 10^{-4} \text{ mol OH groups}$$

$$\frac{1.79 \times 10^{-4} \text{ mol OH monomer}}{5 \times 10^{-3} \text{ L}} = 0.036 \text{ M OH monomer}$$

$$C = \frac{A}{\epsilon b} = \frac{0.068}{26000 \text{ M}^{-1} \text{ cm}^{-1} \times 1 \text{ cm}} = 2.62 \times 10^{-6} \text{ M EPF}$$

$$\frac{2.62 \times 10^{-6} \text{ M}}{0.036 \text{ M}} \times 100 = 0.0072\% \text{ of OH monomers substituted}$$

### *7.6.5 Preparation of the HVPD samples containing free fluorescein for the fluorescence spectroscopy characterization*

To prepare the HVPD samples containing free fluorescein ( $10^{-6}$  M) the polymer was solubilized in a  $10^{-6}$  M fluorescein solution with the aim of a VORTEX apparatus or, when necessary, under magnetic stirring in hot bath ( $40^{\circ}\text{C}$ ). The solution was decanted into the cuvette for the UV-vis spectroscopic analysis. Then the 3 wt% borax solution (previously prepared dissolving the salt in a  $10^{-6}$  M fluorescein solution) was added into the cuvette and the system was stirred with the VORTEX to obtain the highly viscous polymeric dispersion.

The HVPD formed inevitably presented a high content of bubbles which did not allow for good fluorescence measurements since they cause light-scattering phenomena. To overcome this problem, the samples were centrifuged (ALC Centrifugette 4206 Thermo Electron Corporation) at 4000 rpm for about 15 minutes or until all the bubbles were gone.

### *7.6.6 UV-vis absorption spectroscopy and spectrofluorimetry*

As concern the measurements conducted at the Chemistry Department of the Georgetown University of Washington DC, UV/vis absorption spectroscopy studies were performed on a Varian Cary 300 Bio UV/Visible spectrophotometer.

Fluorescence emission and excitation spectra were collected with a Photon Technology International Fluorimeter (SYS 2459) with the flattened 1 mm cuvette oriented front-face at an angle of  $\sim 45^{\circ}$  with respect to the incident beam and the emission was collected at  $90^{\circ}$  with respect to the excitation source.

The spectra were normalized to the highest intensity and baseline corrected.

As regard the measurements conducted at the Chemistry Department of the University of Florence, UV/vis absorption spectra were acquired with a Varian Cary 100 Bio UV-Vis Spectrophotometer while the fluorescence emission and excitation spectra were collected with a Perkin Elmer Luminescence Spectrometer LS 50 B.

As concern the emission spectra, the excitation wavelength was 460 nm and the acquisition interval was 490-650 nm; for the excitation spectra, the emission wavelength was 530 nm and the acquisition interval was 350-510 nm.



### 7.6.7 Confocal microscopy

*Imaging analyses* on the residues left by the HVPDs prepared with the fluorescent polymer onto the surface of laboratory glasses were acquired with a Leica TCS SP2 Confocal Laser Scanning Microscope equipped with a 10x objective instrument by using the 488 nm Argon laser line and acquiring the fluorescence emission in the range 500-700 nm with a PMT. The spatially resolved fluorescence emission spectra were acquired exciting the samples at the same wavelength (488 nm) and recording the fluorescence emission in the range 500-700 nm with 1 nm step and 5 nm spectral window.

### 7.7 Bibliography

- [1] X.L. GUAN, X.Y. LIU, Z.X. SU, P. LIU, *React. Funct. Polym.*, 2006, 66, 1227.
- [2] M. TALHAVINI, T.D.Z. ATVARIS, *J. Photoch. Photobio. A*, 1998, 114, 73.
- [3] D. DIBBERN-BRUNELLI, T.D.Z. ATVARIS, *J. Appl. Polym. Sci.*, 1995, 55, 889.
- [4] D. DIBBERN-BRUNELLI, T.D.Z. ATVARIS, *J. Appl. Polym. Sci.*, 2000, 75, 815.
- [5] L.V. ANGELOVA, *Gels from borate-crosslinked partially hydrolyzed poly(vinyl acetate)s: characterization of physical and chemical properties and applications in art conservation*, PhD thesis in Chemistry, Georgetown University, Washington D.C., 2013, 131-138.
- [6] M.M. MARTIN, L. LINDQVIST, 1975, 10, 381.
- [7] R. SJÖBACK, J. NYGREN, M. KUBISTA, *Spectrochimica Acta part A*, 1995, 51, L7.
- [8] E. GOTTLIN, X. XU, D. EPSTEIN, S. BURKE, J. ECKSTEIN, D. BALLOU, J. DIXON, *J. Biol. Chem.*, 1996, 271, 27445.
- [9] R. DENEGRI, A. ESPOSITO, G. SALAMI, *Confocal Laser Scanning Microscopy*, 1998 ([http://quantitative-microscopy.org/images/5/55/UG\\_clsm.pdf](http://quantitative-microscopy.org/images/5/55/UG_clsm.pdf), consulted on December 2014).
- [10] D.B. MURPHY, *Fundamentals of light microscopy and electronic imaging*, Wiley-Liss, Inc., 2001.

## CHAPTER 8

## HVPDs: applicative tests on metallic supports of artistic and historical interest

## 8.1 Cleaning tests onto the North Door of the Baptistry of Florence

The Florence Baptistry (*Battistero di San Giovanni*), is one of the oldest buildings in the city, constructed between 1059 and 1128 in the Florentine Romanesque style (Figure 8.1.1). It is renowned for its three sets of artistically important bronze doors with relief sculptures. The south doors were done by Andrea Pisano and the north and east doors by Lorenzo Ghiberti.



**Figure 8.1.1.** The North Door of the Baptistry of Florence by Lorenzo Ghiberti (gilded bronze). The red rectangle indicatively highlights the area where the cleaning tests were carried out.

The experimentation of the HVPDs onto a small portion of the North Door of the Baptistery was performed as a part of the institutional collaboration between the CSGI Consortium and the *Opificio delle Pietre Dure* (OPD) of Florence where the restoration of the door is being carried on.

The zones interested by the cleaning tests (~ 4 cm x 3 cm) were located along the lateral frame on the right side of the door (see the red rectangle in Figure 8.1.1). They were characterized by a thick patina composed of copper corrosion products (oxides, chlorides, sulfates), a crystalline wax applied onto the surface as a protective and dust.

Because of the presence of copper oxidation products, we decided to use the HVPDs containing chelating agents with good chelation properties towards copper ions; on the other hand, considering the hydrophobic nature of the wax and the hydrophilic one of the dust we chose, respectively, also a system embedded with an oil in water (o/w) microemulsion and one containing only water as the liquid fraction. Thus, the 80PVAc-borax HVPDs selected for the experimentations contained: 0.5 wt% EDTA at pH 8; 0.5 wt% EDTA at pH 10; 0.9 wt% Rochelle salt; the microemulsion SDS-PeOH-xylene; no additive (basic formulation).

On the zone 2 (Figure 8.1.2 A) we applied the dispersion without any additive for 10 minutes (Figure 8.1.2 B): the removal was easily performed in one step with the aim of a spatula and after a clearance step with a cotton swab soaked with deionized water or ethanol, no HVPDs residues were naked eye detectable but the system probably removed only some superficial dust, resulting ineffective in the thinning of the degradation layer (Figure 8.1.2 C).

The best result was obtained onto the zone 5 (Figure 8.1.3 A) where we carried on two consecutive applications (around 20 minutes-long) of the HVPDs containing 0.5 wt% EDTA at pH 8 followed by a third one using the system with 0.5 wt% EDTA at pH 10 (5 minutes-long). After each test, the HVPD was removed easily, resulted green-colored and the treatment was effective in the thinning of the patina (Figure 8.1.3 C). No residues were left after the washing step with the cotton swab soaked with deionized water/ethanol.

On the zone 12 (Figure 8.1.4 A) we performed three applications using the HVPD embedded with 0.5 wt% EDTA at pH 10 (Figure 8.1.4 B), increasing progressively the application time (10 minutes, 15 minutes and 20 minutes respectively). The system resulted more elastic than the one with 0.5 wt% EDTA at pH 8 used for the

cleaning tests onto the zone 5 and was removed better (Figure 8.1.4 C). The cleaning action was good but not as effective (Figure 8.1.4 D).

Onto the zone 7 (Figure 8.1.5 A) it was applied the HVPD containing 0.9 wt% of Rochelle salt for 20 minutes (Figure 8.1.5 B). The system was removed very easily with the spatula (Figure 8.1.5 C) but it didn't result active against the corrosion patina and, furthermore, a bleaching effect was observed (Figure 8.1.5 D).

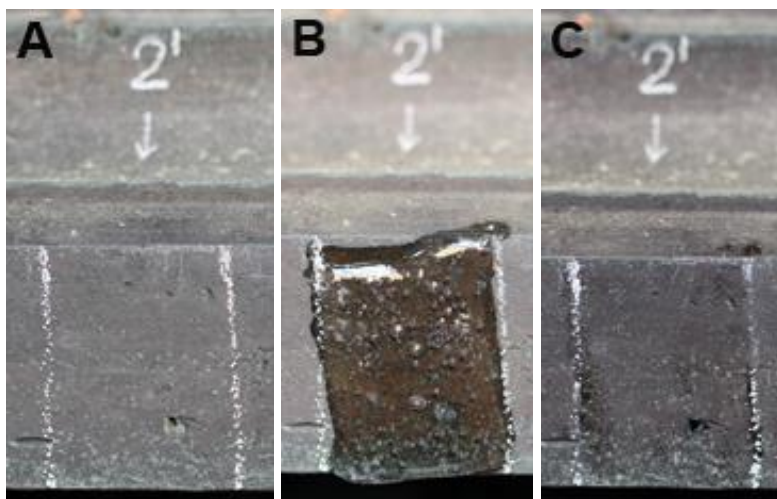


**Figure 8.1.2.** The zone 2 before (A), during (B) and after (C) the application of the HVPD containing no additive.

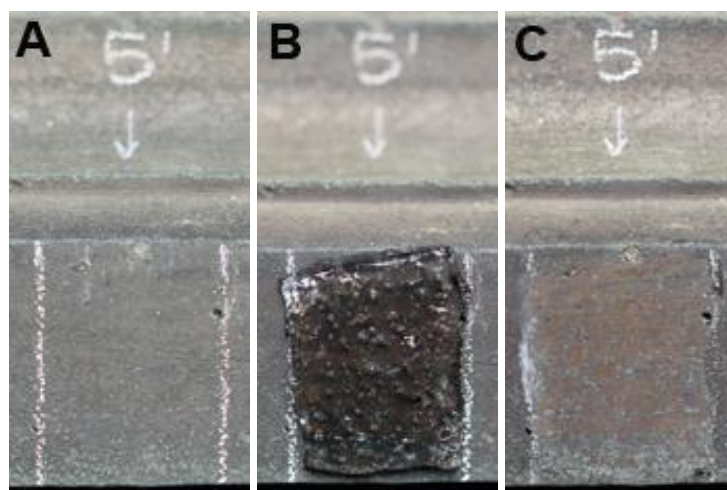


**Figure 8.1.3.** The zone 5 before (A), during (B) and after (C) the application of the HVPD containing 0.5 wt% EDTA at pH 8 and pH 10.

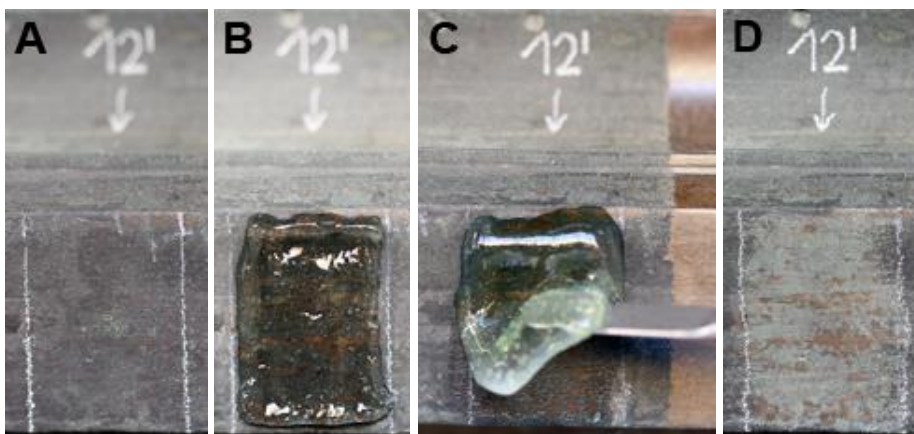


**Figure 8.1.4.** The zone 12 before (A), during (B,C) and after (D) the application of the HVPD containing 0.5 wt% EDTA.

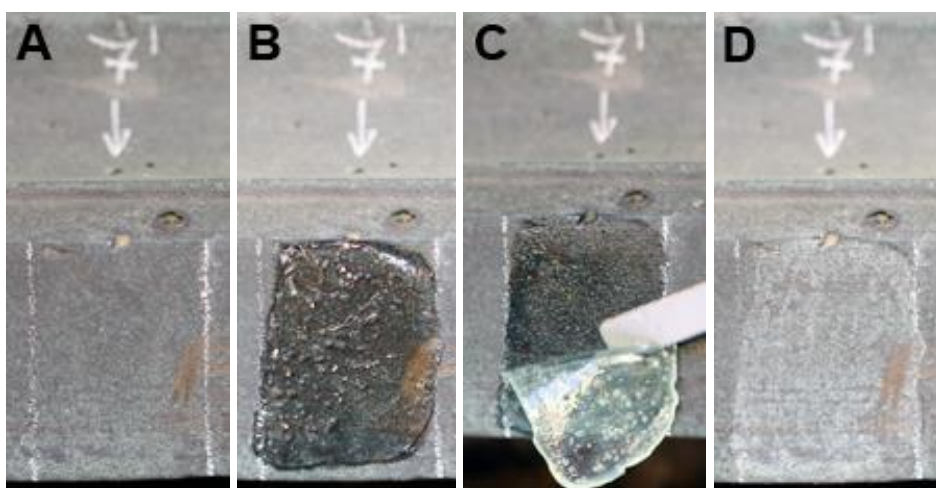


**Figure 8.1.5.** The zone 12 before (A), during (B,C) and after (D) the application of the HVPD containing 0.9 wt% Rochelle salt.

Finally, on the zone 11 (Figure 8.1.6 A) we applied the system containing the microemulsion SDS/penthanol/xylene for 20 minutes (Figure 8.1.6 B); the cleaning action was very mild (Figure 8.1.6 C).

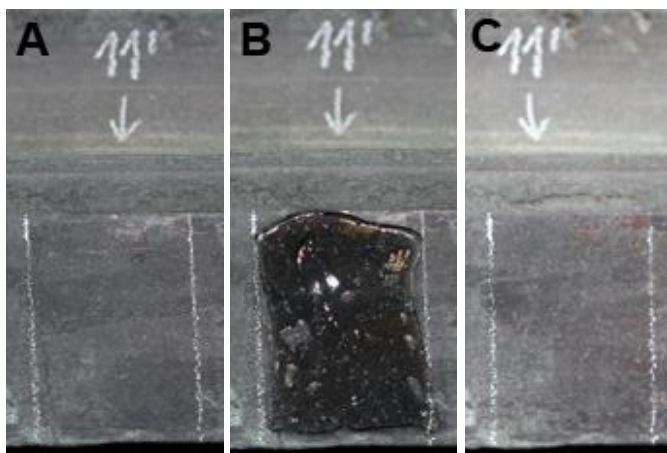


**Figure 8.1.6.** The zone 11 before (A), during (B) and after (C) the application of the HVPD containing the microemulsion SDS/PeOH/xylene.

In correspondence of the lower edge of a molding, the presence of a small gypsum spot, confirmed through the analyses performed with the portable FTIR spectrophotometer by the conservators of the OPD. Its presence probably has to be ascribed to the “lost-wax” technique used for the realization of the door which provided the use of gypsum casts.

Onto the small gypsum spot (Figure 8.1.7 A), we applied the system with 0.5 wt% EDTA at pH 10 (active against the calcium ions) for 20 minutes. The HVPD, interacting with the gypsum, became white and released some liquid (Figure 8.1.7 B). The removal step with the aim of tweezers was good (Figure 8.1.7 C) but the gypsum deposit was just slightly thinned (Figure 8.1.7 D).

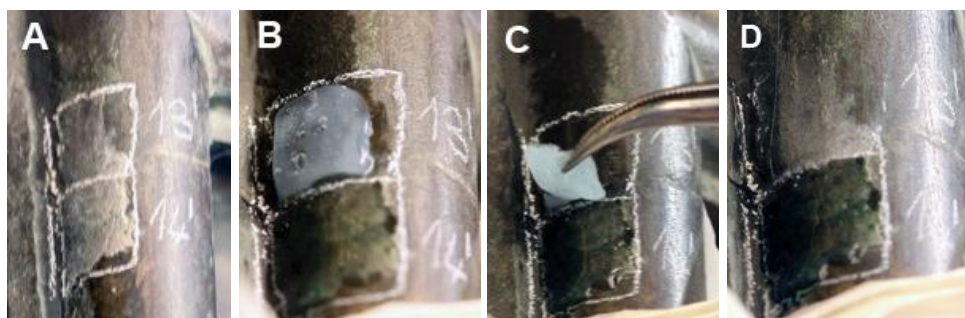


**Figure 8.1.7.** The zone 13 before (A), during (B,C) and after (D) the application of the HVPD containing 0.5 wt% EDTA at pH 10.



The context in which these tests were carried out is the development of a cleaning methodology aimed at the removal of the degradation coatings from those areas of the surface of the door where the gilding has been preserved.

In fact, these zones are particularly sensitive because of the gilding and consequently the use of cleaning tools as the HVPD which demonstrated to be effective against the alteration patina and to have the right consistency and elasticity in order to be removed easily in one piece without a strong mechanical action could potentially be the right choice.

Thus, in the perspective of applying the HVPDs also onto gilded bronze surfaces, we did some “impact tests” on two small gilded bronze dowels (artificially aged and not) in order to verify that the HVPDs wouldn't exercise a tearing action against the gold coating.

The systems selected were the one without any additive and the one with 0.5 wt% EDTA at pH 10.

As shown in Figure 8.1.8 A-B, the gold coating of both the intact dowel (rectangular shaped) and the aged one (square shaped), seemed not to be affected after the removal of both the systems (no gold traces were visible in the HVPD samples once removed from the gilded surface, B).

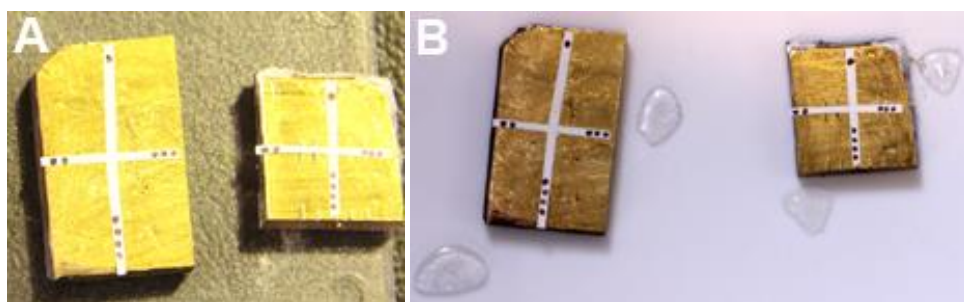


**Figure 8.1.8.** The two small gilded bronze dowels, artificially aged (the squared one) and not (the rectangular one), before (A) and after (B) the application of the HVPD without any additive and the one containing 0.5 wt% EDTA at pH 10.

To conclude, beyond the individual results, the conservators were pretty satisfied of the performance of our HVPDs, first of all because of the gradualness of their action that let to control the level of the cleaning, then for their good adhesion to the

treated surface and their easiness of removal in one piece without requiring a strong mechanical action, feature very appreciated in the perspective of applying them onto the gilded parts of the door because it let to preserve the gilding.

Finally, even when the thinning of the patina onto the bronze surface seemed not so good, the degradation layer resulted anyway enough softened and swollen to be easily and completely removed mechanically using the scalpel.

## 8.2 Cleaning tests onto the “*Cassetta-reliquiario con stemma dell’Arte di Calimala*”, a reliquary box of Florentine manufacture

A second experimentation of the xPVAc-borax HVPDs was conducted, once again in collaboration with the restorers of the *Opificio delle Pietre Dure* (OPD) of Florence, onto the metallic surface of the “*Cassetta-reliquiario con stemma dell’Arte di Calimala*” (Figure 8.2.1), a bronze reliquary box of Florentine manufacture and currently part of the collection of the Ognissanti Museum in Florence.

The box most likely dates back to the thirteenth century, while the door and the crucifix to the sixteenth century. Originally, it was placed in the Baptistery of Florence and it was used to contain the relics of saints. In 1504, upon the arrival in Florence of another important relic, the habit of St. Francis, assigned to the custody of the Franciscans and the patronage of Calimala, it was decided to keep it in the ancient box.<sup>1</sup>

The area interested by the cleaning tests was affected by the “bronze disease” (for the detailed description of this degradation phenomenon see the subparagraph 1.2.3 in the Chapter 1).

The contemporary presence of chloride and copper (and tin) revealed by the preliminary XRF analyses conducted by the conservators of the OPD, in fact, evidenced the presence of *atacamite* that is one of the main alteration products constituting the affections from bronze disease; the FTIR spectra revealed also the presence of wax and oxalates.

---

<sup>1</sup> From the catalog of the exhibition in Bonn, entitled "Florence", written by Dr. Annamaria Giusti.



The objective of the experimentation was to evaluate the performance of the HVPDs in terms of ease of application, removal (peeling) and cleaning efficacy, in comparison with a chemical method traditionally used for the treatment of metal surfaces, in order to evaluate the advantages and disadvantages of the proposed systems.



**Figure 8.2.1.** Left: “Cassetta-reliquiario con stemma dell’Arte di Calimala”; the area affected by bronze disease is highlighted by the red box. Right: magnification of the zone where the 4 cleaning tests were carried out.

Considering the necessity of removing copper salts, we selected the HVPD containing the 0.5 wt% of EDTA at pH 9.5 - 10.5 because of its potential chelation action against copper ions; a purely aqueous HVPD without any additive, at neutral pH or at pH 9.5-10.5, was also chosen as a comparison.

The first test was conducted onto the area 4 and consisted in the application of the aqueous HVPD at neutral pH for about 4 minutes (Figure 8.2.2 a-d).

As evidenced in Figure 8.2.2 d and in the images at the stereomicroscope (Figure 8.2.3), there was a slight reduction of the greenish efflorescences present on the surface. For the complete removal of the HVPD the use of a cotton swab soaked with ethanol was necessary.

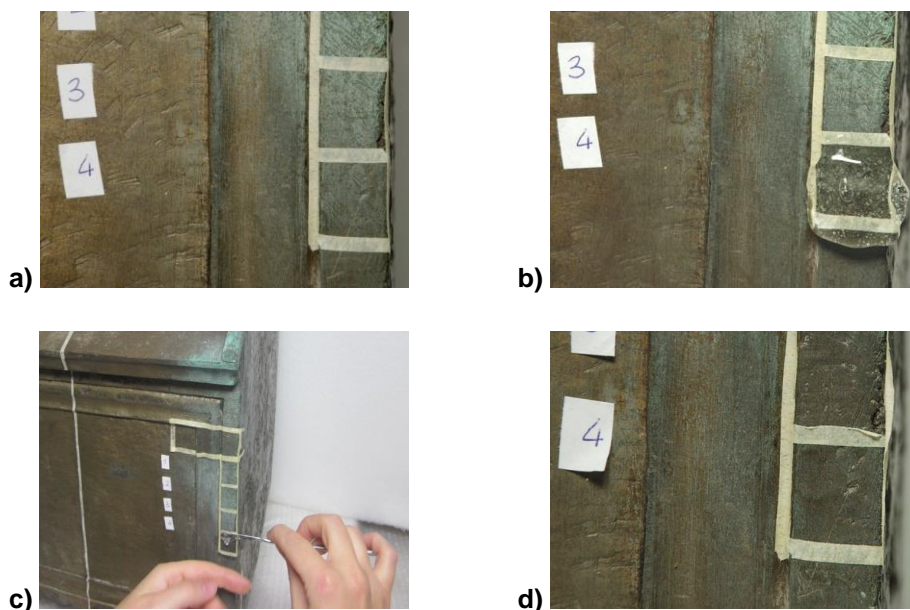


**Figure 8.2.2.** a) Area 4 before applying the HVPD; b) application of the aqueous HVPD for about 4 min; c) Removal of the HVPD; d) Area 4 after the cleaning.

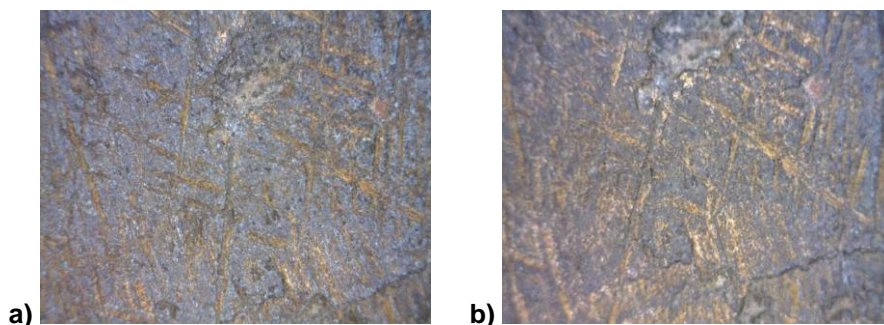


**Figure 8.2.3.** Images of the area 4 obtained with the stereomicroscope: a) before and b) after the cleaning with the pure water-based HVPD.

On the area 2 two consecutive applications (4 minutes and 10 minutes long respectively) of the system embedded with 0.5 wt% EDTA at pH 9.5-10.5 were performed (Figure 8.2.4 a-d). The removal of the dispersion was very easily and no residues were visually detectable. However, we proceeded with a single washing with deionized water to avoid that invisible traces of HVPD could remain on the bronze surface (Figure 8.2.4 c).

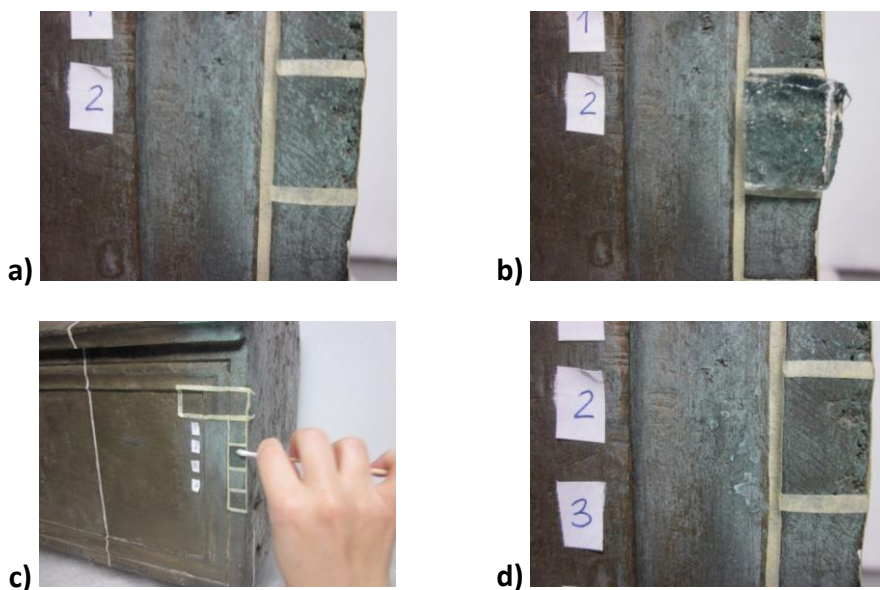


**Figure 8.2.4.** a) Area 2 before the cleaning; b) application of the HVPD; c) washing with deionized water; d) area 2 after the two applications of the HVPD with 0.5 wt% EDTA at pH 9.5 - 10.5.

After performing the second application, the patina resulted appreciably thinned indicating the gradual, controlled but effective cleaning action of the system (Figure 8.2.5).

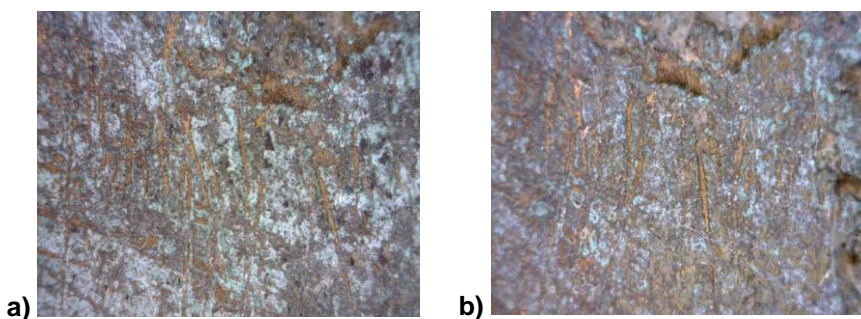


**Figure 8.2.5.** Images of the area 2 obtained with the stereomicroscope: a) before and b) after the cleaning with the HVPD containing 0.5 wt% EDTA at pH 9.5 - 10.5.

During previous restorations, the reliquary box had been subjected to a final protection treatment with a wax, in order to avoid the occurrence of additional

degradation phenomena and to improve the aesthetic appearance of the artwork. Since the presence of any residual wax made the removal of the alteration patina extremely difficult, onto the area 1 it was performed a preliminary cleaning with acetone and ethanol. Moreover, by doing this, it was possible to better compare the application of the system with 0.5 wt% EDTA at pH 9.5 - 10.5 with the traditional cleaning procedure which provide the prior degreasing of the metal surface with the same solvents.

Although the mechanical degreasing with the cotton swab soaked with acetone and ethanol had already removed part of the greenish patina, two consecutive applications (5 minutes each) of the HVPD loaded with EDTA were carried out, completing the treatment with a gentle, gradual cleaning action (Figure 8.2.6).

In order to compare this result with the traditional methodology, onto the area 3 it was applied for 5 minutes a gel made with hydroxypropylcellulose (Klucel G), at neutral pH and containing the 5 wt% of EDTA (Figure 8.2.7).

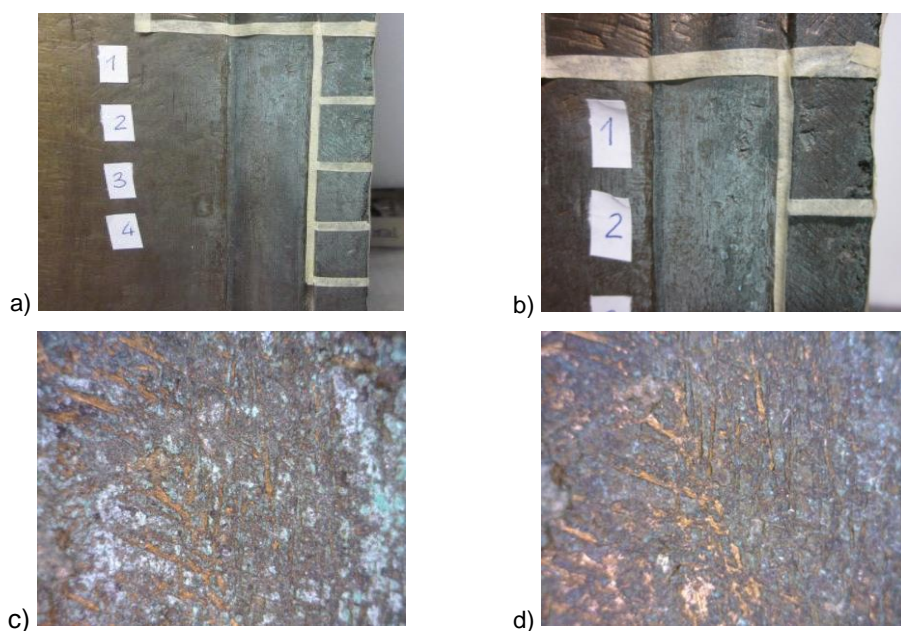


**Figure 8.2.6.** Pictures (a,b) and images at the stereomicroscope (c,d) of the area 1 before (a,c) and after (b,d) the cleaning with the HVPD containing 0.5 wt% EDTA at pH 9.5 - 10.5. A noticeable reduction of the green patina is evidenced.



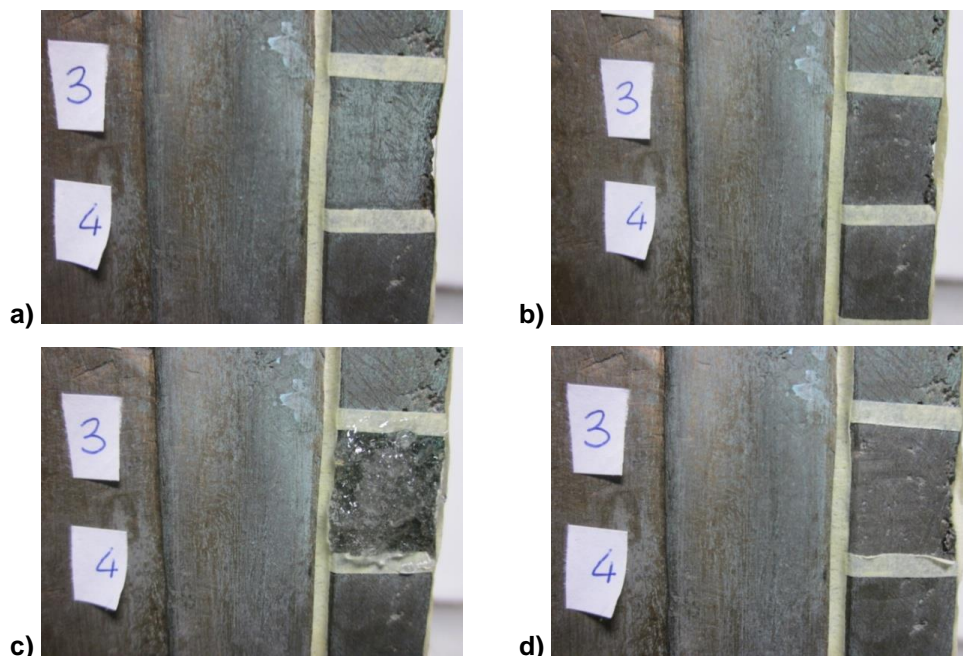


**Figure 8.2.7.** Area 3 a) before the cleaning; b) after the degreasing, c) during the application of the Klucel G gel with 5 wt% EDTA; d) after the cleaning.

Undoubtedly the traditional cleaning method made a better performance in terms of efficacy in the thinning of the degradation layer as confirmed by the portable XRF and FTIR analyses (carried on by the conservators of the OPD) which recorded a drastic decrease of the signals due to the *atacamite*. Also the time required for the treatment was minor compared to the HVPD systems, due to the ten times higher amount of chelator. On the other hand, the Klucel G has the great disadvantage of leaving an excessive quantity of residues, imposing an extra mechanical action with organic solvents that in the case of the HVPD often is not necessary or is very mild because the system has been almost completely removed in one piece with the spatula. XRF and FTIR analyses revealed, in fact, the total absence of HVPD residues onto the treated areas and the presence, on the contrary, of the Klucel G ones.

To conclude about the experimentation onto the “*Cassetta-reliquiario con stemma dell’Arte di Calimela*”, the preliminary visual evaluation at naked eye and with the stereomicroscope and later the XRF and FTIR analyses confirmed that the performance of the HVPD systems embedded with the chelating agent was

effective in the thinning of the alteration patina (a sensibly minor amount of *atacamite* was detected after the tests), performing an appreciably gradual and controllable cleaning action, tunable simply by varying the application time or by performing more than one application onto the same area. Furthermore the systems showed a good adhesion onto the vertical metallic surface and easiness of removal thank to their elastic properties that let to remove them in one piece minimizing the residues, avoiding a strong mechanical action.

## CONCLUSIONS

The aim of the present PhD project was to carry on the study and the characterization of the Highly Viscous Polymeric Dispersions (HVPDs) obtained from PVA/xPVAc and borax developed, within the chemistry department of the University of Florence and CSGI consortium, to overcome the limits of the traditional cleaning technologies used in the conservation of artworks.

According to the preliminary studies onto the first formulations with PVA and 80PVAc, they showed very interesting viscoelastic properties responsible for their well-known characteristic of *peelability* by which they can be removed from the treated surface in one piece minimizing the residues, without requiring any additional mechanical action or clearance step with organic solvent.

Here, the mechanical-structural characteristics of HVPDs obtained from a PVAc with a lower hydrolysis degree (75% hydrolyzed, "75PVAc") and those of new formulations containing chelating agents were analysed and then related to the performance of the systems in the thinning of alteration patinas from metallic and carbonatic supports.

Dynamic rheological measurements confirmed the viscoelastic character also for the 75PVA-borax HVPDs: they behave like elastic solids at short observation times (high frequencies) and like viscous liquids at long observation times (low frequencies). Furthermore, it resulted that higher is the 75PVAc concentration and higher are the chain entanglements and, thus, the elasticity, higher the temperature of loose strength  $T_{ls}$ , higher the amount of bound water. The time-weighted relaxation spectra of these HVPDs revealed the presence of a main relaxation mechanism, defined "sticky reptation", that is unchanged upon increasing 75PVA concentration. The increase of the width of the peak observed by increasing the 75PVA concentration, was related to extra relaxation modes, mainly attributable to the enhancement of the entanglement density.

As anticipated, the possibility of loading chelators into the HVPD was also explored. The rheological measurements confirmed that upon the addition of the selected chelating species (EDTA, ammonium carbonate, Rochelle salt, trisodium citrate or

## CONCLUSIONS

---

TSC, triammonium citrate or TAC) the mechanical properties of the HVPDs resulted still adequate for their removal from the treated surface in one step by a simple peeling action, as the intrinsic elastic modulus  $G_0$  was higher than the threshold value of 400 Pa. Up to a certain concentration, these salts have a structuring effect on the HVPDs as indicated by the increase of their intrinsic elasticity ( $G_0$ ). For higher amounts of additive, a lowering of  $G_0$  was recorded, indicating a reduction of the entanglements density of the network.

As concern the systems embedded with EDTA and ammonia (the latter is added to have pH 9-10), a further rheological study demonstrated that the  $G_0$  changes observed depend on the presence of both EDTA and ammonium hydroxide solution as a consequence of a salt/pH effect.

$^{11}\text{B}$  NMR spectral analyses onto TAC-containing systems confirmed what already found out in previous studies: less than 15% of the borate species are involved in crosslinking with the PVAc chains in the formulations examined; in presence of the citrate salt, the complexation of borate ions by TAC is evidenced. In the perspective of applying the TAC-containing systems for the thinning of copper-based corrosion patinas from copper/bronze artifacts, the potential displacement of boron from citrate after the addition of a small amount of  $\text{CuCl}_2$  was then examined. The preferential coordination by the citrate salt of copper ions rather than the borate ones was confirmed, as well as, consequently, the viable use of these HVPDs as cleaning agents for copper/bronze surfaces.

An enhancement of the maximum loadable amount of chelators in the HVPDs was achieved by substituting the 80PVAc with the 87PVAc due to the higher hydrolysis degree and to the presence of carboxylic groups (~ 3%) that cause a local increase of the polarity of the continuous aqueous phase.

The cleaning efficacy and the easiness of removal of the systems embedded with disodium EDTA (pH 9-10), ammonium carbonate, Rochelle salt were tested through several applications on artificially sulfated travertine tiles: they were removed easily in one step (with the aim of plastic rings) without leaving any visible residue. Optical micrographs of the sulfated surfaces before and after the cleaning tests revealed their effectiveness in the thinning of the gypsum patina. The quantification of the sulfates extracted was achieved through IC and ICP techniques by setting up measuring protocols specifically tailored for the pre-treatment and the analysis of the HVPD samples. Regardless of the additive, the extracting power increased with



the contact time between the surface and the cleaning systems, confirming their gradual, gentle action. The ammonium carbonate resulted the most effective, removing 37% of sulfates.

HVPD systems loaded with disodium EDTA at pH 9-10 were tested also onto chemically oxidized copper plates. The HVPDs showed a gradual but effective cleaning action, removing most of the corrosion patina. ICP analyses performed on HVPD samples collected after the applications revealed that the amount of removed copper ions increase with the application time and that the saturation of the cleaning system occurs after 30 minutes.

The results of the experimentations onto two metallic surfaces of historical-artistic interest, the "*Cassetta-reliquiario con stemma dell'Arte di Calimala*", a reliquary box affected by "bronze disease", and the North Door of the Baptistery of Florence, characterized by a thick patina composed of copper corrosion products, a wax and dust, were satisfying.

The HVPDs embedded with chelators were very much appreciated by the conservators of the *Opificio delle pietre Dure* (OPD) because of the gradualness of their action that let to control the level of the cleaning, the efficacy in the thinning of the alteration layers, their good adhesion to the treated vertical surface and their easiness of removal with the spatula in one piece minimizing the residues (XRF and FTIR analyses performed onto the reliquary box revealed, in fact, the total absence of HVPD residues). Finally, even when the thinning of the patina seemed not so good, the degradation layer resulted anyway enough softened and swollen to be easily and completely removed mechanically using the scalpel.

Further tests onto artificial gilded bronze dowels, aged and not, revealed that our HVPDs are suitable also for the treatment of fragile gold surfaces because they don't exercise a tearing action against the gold coating.

Fluorescence studies at confocal microscopy on HVPD samples prepared with 87PVAc labelled with fluorescein revealed that the very few residues left were concentrated along the edge of the treated area probably as a consequence of an "edge effect" due to the greater adhesion forces between the HVPD molecules and the support in the peripheral zone.

The construction of a calibration curve, through fluorescence emission analyses, useful for the future quantification of the residues was also achieved.

## ACKNOWLEDGEMENTS

I would like to thank prof. Richard G. Weiss for his scientific support and dedication and dr. Lora V. Angelova for her help and assistance, during my research period at the chemistry department of the Georgetown University of Washington DC.

Thanks also to Emiliano Fratini for carrying out the SAXS experiments, Rita Traversi and Mirko Severi for the IC and ICP analyses, Costanza Montis for the confocal microscopy measurements.

Marco Ciatti, superintendent of the *Opificio delle Pietre Dure* (OPD), Maria Donata Mazzoni, director of the “*Bronzes and Antique Weapons*” sector of the OPD and Monica Bietti, director of the Ognissanti Museum, are acknowledged for letting me carry out the cleaning tests onto the “*Cassetta-reliquiario con stemma dell’Arte di Calimala*” and for giving me the authorization to use the relative data and the pictures for the present work.

Franco Lucchesi, president of the *Opera del Duomo* Museum, Beatrice Agostini, responsible of the restorations at the *Opera del Duomo* Museum, Marco Ciatti and Dr. Maria Donata Mazzoni are thanked as well, for permitting me to carry out the cleaning tests onto the North Door of the Baptistery of Florence, currently under restoration at the OPD, and to use the relative data and the pictures for my thesis.

I would like to thank also the restorers of the OPD Stefania Agnoletti and Elena della Schiava for assisting me during the experimentations onto the “*Cassetta-reliquiario con stemma dell’Arte di Calimala*” and the North Door of the Baptistery of Florence.

Finally, I’m grateful to my supervisor, prof. Luigi Dei, for his availability and his always appreciable scientific contribute, and to dr. Emiliano Carretti for his constant help, his advices and his support during these three years.

## List of publications


Matarrese C., Angelova L.V., Carretti E., Weiss R.G., Dei L., Baglioni P., *Chelating agents in aqueous, partially-hydrolyzed, poly(vinyl acetate) dispersions cross-linked with borax. A rheological and <sup>11</sup>B NMR study*, forthcoming.

Matarrese C., Carretti E., Traversi R., Severi M., Dei L., Baglioni P., *Chelators confined into 80PVAc-borax Highly Viscous Dispersions for the removal of gypsum degradation layers*, manuscript under review; submitted to Journal of Cultural Heritage on October 2014.

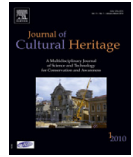
E. Carretti, C. Matarrese, E. Fratini, P. Baglioni, L. Dei, *Physicochemical characterization of partially hydrolyzed poly(vinyl acetate)-borate aqueous dispersions*, *Soft Matter*, 2014, 10, 4443-4450.

E. Carretti, I. Natali, C. Matarrese, P. Bracco, R.G. Weiss, P. Baglioni, A. Salvini, L. Dei, *A new family of high viscosity polymeric dispersions for cleaning easel paintings*, *Journal of Cultural Heritage*, 2010, 11, 373-380.



Available online at  
  
 www.sciencedirect.com

Elsevier Masson France  
  
 www.em-consulte.com



Original article

## A new family of high viscosity polymeric dispersions for cleaning easel paintings

Emiliano Carretti<sup>a</sup>, Irene Natali<sup>a</sup>, Caterina Matarrese<sup>b</sup>, Paola Bracco<sup>c</sup>, Richard G. Weiss<sup>d</sup>,  
 Piero Baglioni<sup>a</sup>, Antonella Salvini<sup>e</sup>, Luigi Dei<sup>a,\*</sup>

<sup>a</sup> Department of Chemistry & CSGI Consortium, University of Florence, via della Lastruccia, 3, 50019 Sesto Fiorentino (Florence), Italy

<sup>b</sup> Faculty of Sciences, University of Florence, Florence, Italy

<sup>c</sup> Fondazione Università Internazionale dell'Arte, Villa Il Ventaglio, via delle Forbici, 24/26, 50133 Florence, Italy

<sup>d</sup> Department of Chemistry, Georgetown University, Washington, D.C. 20057-1227, USA

<sup>e</sup> Department of Chemistry, University of Florence, via della Lastruccia, 13, 50019 Sesto Fiorentino (Florence), Italy

### ARTICLE INFO

#### Article history:

Received 10 September 2009

Accepted 1<sup>st</sup> April 2010

Available online 13 May 2010

#### Keywords:

Easel paintings

Cleaning

Viscous polymeric dispersions

Viscoelasticity

Poly(vinyl alcohol)

Borax

### ABSTRACT

The procedures for making and applying a new family of high viscosity aqueous polymeric dispersions based on poly(vinyl alcohol)-borax (PVA-borax) matrices are presented. A specific system of this type has been used to remove an oxidized varnish coating from the surface of "Coronation of the Virgin with Saints", a 15th century egg tempera painting on wood by Neri di Bicci (Florence, 1418–1492). FTIR spectra showed that the oxidized varnish was constituted of highly aged shellac resin. Good cleaning performance was attained when the liquid portion of the dispersion consisted of a mixture of water and acetone. Rheological investigations indicate that the acetone content does not affect the mechanical properties of the polymeric dispersion. Those mechanical properties permit easy removal of the cleaning agent simply by peeling it from the surface by means of a forceps or spatula once it has carried out its cleaning function. Optical microscopic and FTIR investigations show that the cleaning agent is able to remove the oxidized varnish coating from the surface of the Neri di Bicci painting without leaving detectable residues.

© 2010 Elsevier Masson SAS. All rights reserved.

### 1. Introduction

During the conservation of the surface of a work of art, the cleaning process is, perhaps, the most important and delicate because it is an irreversible operation and, if improperly performed, it can be invasive and potentially lead to undesired effects. The direct application of organic solvents for cleaning canvas and wood paintings is still a widely used technique for the removal of foreign deteriorating coatings. Unfortunately, this approach sometimes causes some damage if the liquids penetrate into the painting layers and swell them. The swelling of natural polymeric organic materials (most of which have a structural function for the painting) in organic solvents can be evaluated (e.g., for oil paintings [1–3]) and discussed in relationship to the implications for the cleaning action.

During the last 15 years, several cleaning procedures for works of art, employing new cleaning agents, have been developed using as a guiding principle that they would be very selective [4]. Most involve the use of highly viscous cleaning agents [5], such as gels, in order to minimize the negative effects related to the penetra-

tion of the liquid phase into the painting matrix. However, it is not always possible to ensure complete removal of the gelling polymer after its application [6,7]. For example, Burnstock and Kieslich demonstrated that residues of a poly(acrylic acid)-based gelator can remain after the application of its gels onto and removal from a painted surface [8]. Thus, new methods that ensure greater efficiency of removal of all of the gel components are needed.

A possible approach that minimizes the deleterious aspects of gel removal from a painted surface might utilize high viscosity polymeric dispersions with mechanical properties characterized by a high elastic modulus (i.e., that make them rigid systems). Such systems could be peeled from the surface onto which they were applied by means of a benign mechanical action and without addition of a second liquid component (Fig. 1). In principle, such a cleaning system and removal procedure would reduce the amount of the polymeric residues from the dispersion on the painting surface to a greater extent [7] than gels that must be removed by more conventional means [9,10].

Solutions of poly(vinyl alcohol) (PVA), in the presence of borax ( $\text{Na}_2\text{B}_4\text{O}_7 \cdot 10\text{H}_2\text{O}$ ) as cross-linker, are known to form aqueous dispersions with high elastic modulus [11–16]. The borate ester cross-links result in very strong interactions between PVA chains [17]. Furthermore, the elasticity and, more generally, all the rheological properties of these systems can be tuned by changing either the ratio of PVA to borax or their total concentration [18]. Another important characteristic of the PVA-based high viscosity systems is

\* Corresponding author. Fax: +39 0554573036.

E-mail addresses: carretti@csgi.unifi.it (E. Carretti), natali@csgi.unifi.it (I. Natali), caterinaciligia@yahoo.it (C. Matarrese), paolabracco1@virgilio.it (P. Bracco), weissr@georgetown.edu (R.G. Weiss), baglioni@csgi.unifi.it (P. Baglioni), antonella.salvini@unifi.it (A. Salvini), dei@csgi.unifi.it (L. Dei).



**Fig. 1.** Removal of a PVA/borax/water-based dispersion after it was in contact with a gilded surface for the minimum time necessary to soften the outermost surface layer. The gel was peeled easily from the surface by forceps.

their chemical versatility: recently, it has been shown that thermodynamically stable aqueous PVA-borax dispersions can be prepared with some organic liquids as cosolvents [19]. This discovery is particularly important to the use of these systems to clean painting surfaces because both the polarity of the continuous phase and the mechanical properties of the dispersions can be modulated; specific polarities of the liquid component enhance the extracting power of the cleaning system [20]. Objectives of this work are to learn how to modulate the behaviour of these PVA/borate/cosolvent systems and to test their efficacy as new cleaning agents for easel paintings as assessed by their ability to clean coatings from painting surfaces and to be removed easily from them while leaving minimal residues.

As a test, PVA-borax based mixtures containing up to 6% (w/w) of acetone as a cosolvent were used to remove a dark coating composed of highly oxidized varnishes from the surface of “*Coronation of the Virgin with Saints*”, a wood panel by Neri di Bicci (1418–1492). The degree of success of those cleaning processes has been assessed visually (i.e., an aesthetic effect) and by comparing the results with those obtained with traditional methods. Results from those tests have been correlated with the viscoelastic properties (i.e., the elastic modulus [ $G'$ ] and the loss modulus [ $G''$ ]) of the PVA-based aqueous systems.

## 2. Materials and methods

PVA (99+ % hydrolyzed, [Mw] 124,000–186,000, Aldrich), sodium tetraborate decahydrate (99.5%, Merck), acetone (99.5%, Merck), ethanol (95.5%, Merck) and KBr (Merck, 99.98%) were used as received. Shellac resin was purchased from Zecchi (Florence, Italy) and its infrared spectrum was used as a standard in subsequent work. Water was purified by a Millipore Organex system ( $R \geq 18 \text{ M}\Omega \text{ cm}$ ).

### 2.1. Preparation and application of the polymeric dispersions

Aqueous dispersions with 2 wt% of PVA and 0.4 wt% of sodium tetraborate decahydrate were prepared by dissolving the salt in water. Then, the PVA was added and dissolved by stirring and heating the mixture at 90 °C for 3 hours in hermetically closed vials (to prevent evaporation of water). Finally, the samples were cooled slowly to room temperature. Unless stated otherwise, all samples contain 2 wt% of PVA and 0.4 wt% of sodium tetraborate decahy-

drate. Once a rigid material was obtained, an amount of cosolvent was added and the mixture was shaken by means of a vortex stirrer for 10 minutes. About 48 hours after their preparation, the cleaning systems were applied directly onto the painting surface by means of a spatula and left there for a maximum of 5 minutes. The cleaning agent was peeled from the painting surface by means of a forceps or a spatula as shown in Fig. 1, without adding any additional liquid component to the remaining polymeric dispersion or on the painting surface after the peeling process. The application of the dispersions on microscope slides was carried out as above. Fluorescence images (under a Wood lamp; emission maximum 364 nm) were collected from the microscope slides after various treatments (*vide infra*).

### 2.2. Accelerated photochemical aging

The FTIR spectra of three KBr pellets were recorded and then a few drops of a solution of shellac resin in ethanol were placed on each. Then the pellets were dried for 48 hours in the atmosphere and for 48 hours in a drier at room temperature to produce very thin films of shellac on one side of the pellets. An FTIR spectrum of one pellet (not aged shellac) was recorded and the other two pellets were irradiated (and “aged”) under a Xe lamp ( $\lambda > 305 \text{ nm}$ ;  $500 \text{ W/m}^2$ ) for 120 and 240 hours, respectively. Thereafter, their FTIR spectra were recorded.

### 2.3. Evaporation measurements of acetone-containing dispersions

A 2 g sample of dispersion was placed on a microscope slide so that it covered ca.  $2 \times 2 \text{ cm}^2$  and left in contact with the atmosphere for 1 hour, during which time the weight decrease was measured on a Sartorius CP225D model analytical balance. The contribution due to the evaporation of water was determined from experiments with PVA systems that did not contain any acetone. To estimate the loss of acetone alone, the weight loss of a totally aqueous dispersion (same amount and same area exposure) was subtracted from the loss noted for the corresponding system containing acetone. Each point is the average of four measurements.

### 2.4. Instrumentation

Mid-infrared spectra were acquired from 4000 to 800  $\text{cm}^{-1}$  with a Nexus 870-FTIR (Thermo-Nicolet) and a FT-IR Continuum microscope in the reflectance mode (beam splitter: KBr; detector: MCT) with a resolution of 4  $\text{cm}^{-1}$  and 512 scans. Rotational and oscillatory shear measurements were carried out at  $25.0 \pm 0.1 \text{ }^\circ\text{C}$  (Peltier temperature control system) on a Paar Physica UDS 200 rheometer using a 2° cone and plate geometry (25 mm diameter) and working at controlled shear stress. After their loading, samples were equilibrated for 1 hour at 25 °C prior to carrying out the experiments. Rotational tests were carried out at constant PVA concentration (2 wt%) and varying the borax amount from 0 to 0.4 wt%; at each composition, a viscosity versus shear stress curve was established. The intrinsic viscosity ( $\eta_0$ ) values plotted versus borax concentration were deduced from the plateau of the curves in the low shear rate regime (low Newtonian region) [20].  $G'$  and  $G''$  were measured over the frequency range 0.005–15 Hz. The values of the stress amplitude were checked by means of amplitude sweep tests in order to ensure that all measurements were performed within the linear viscoelastic region. For all the frequency sweep measurements, the stress amplitude chosen was 2%. Optical micrographs were recorded on a USB Scalar portable microscope (model M2) and a Heerbrugg Wild M5A long focal microscope equipped with 6x, 12x, 25x, and 50x objectives. The USB portable microscope collects images by illuminating the region to be magnified

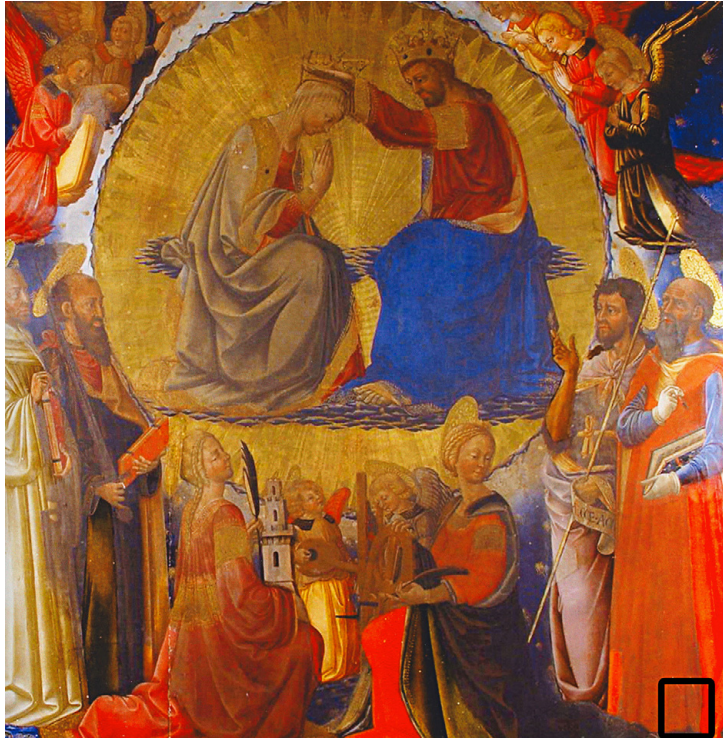


**Fig. 2.** "Coronation of the Virgin with Saints", a 15th century egg tempera wood panel by Neri di Bicci, Galleria degli Uffizi, Florence, Italy. The black box indicates the region where the cleaning tests using PVA-based dispersions were carried out.

with its own light source; the resulting micrographs were in false colours.

### 3. Results and discussion

Fig. 2 shows "Coronation of the Virgin with Saints", an egg tempera wood panel (15th century, 150 × 150 cm) by Neri di Bicci housed at

the Galleria degli Uffizi in Florence, Italy, and presently on loan to the Civic Museum in Pescia (Pistoia), Italy. The original appearance of the work of art was modified by a highly degraded and yellowed brown varnish (Fig. 3). In the regions where the red vermilion pigment is present (N.B., the mantle of Saint-Caterina and Saint-Girolamo in the lower part of the painting), the aging effects were particularly pronounced. As shown in the two images of Fig. 3,

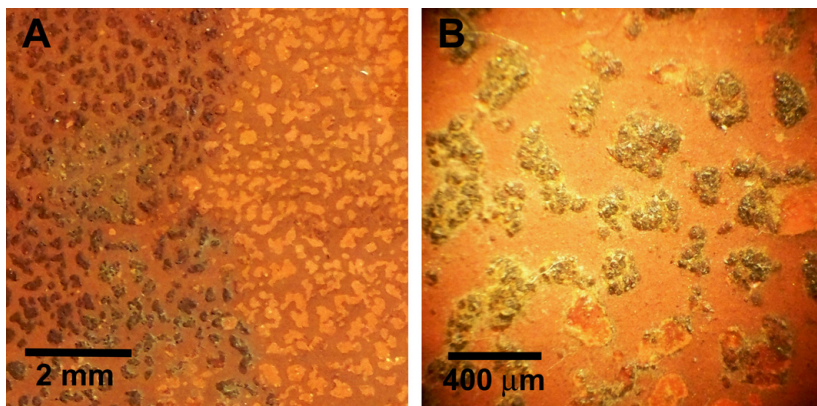


**Fig. 3.** Optical micrographs at two different magnifications of the region of the "Coronation of the Virgin with Saints" showing the morphology of the degraded varnish coatings to be removed. In A, the two features of the coatings are seen as brown clots (on the left) and a dark texture underneath (right). B shows the clots at higher magnification.



**Table 1**Some spectral features associated with changes arising in FTIR spectra as a result of photochemical aging (see the *Materials and methods* section for details) [21].

	Photochemical aging time (h)			Brown coating from painting Natural aging
	0	120	240	
$\nu$ ( $\text{cm}^{-1}$ ) C-O stretch	1251	1249	1246	1245
$A_{-1250}/A_{1141-1171}$	1.63	1.12	1.00	0.95
Resolution of peaks at 1141 and 1171 per centimetre	Yes	No	No	No
Shoulder at $\sim 1245$ per centimetre	Yes	Yes	No	No

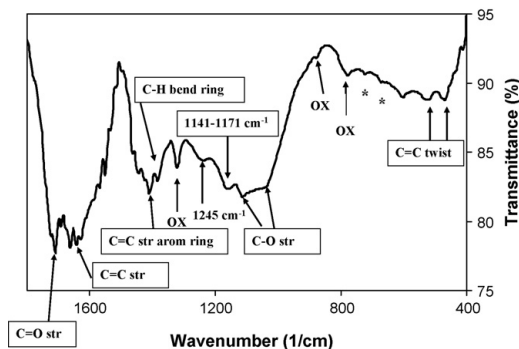


**Fig. 4.** FTIR spectrum in the 1800–400  $\text{cm}^{-1}$  range of the powdered brown surface coating present on the red painting layers of the “Coronation of the Virgin with Saints”. The assignment of the absorptions are based on [22]. The asterisks refer to peaks typical of naturally aged shellac but not assigned; OX means oxalates.

shrinkage induced by the oxidation of the varnish layer as a consequence of its aging was inhomogeneous and it was manifested in two superimposed layers. The first was characterised by the presence of brown, rough clots, while the second one by a dark texture underneath that was bound strongly to the paint layer. Accordingly, the first step in the conservation protocol devised by the conservators was to remove selectively both varnish coatings without damaging the red pigment layer underneath. Insights about the chemical nature of the brown coatings were derived from comparisons between FTIR spectra of the artificially aged (photochemically oxidized) standard shellac varnish and a micro-sample from the surface brown coating of the painting (Table 1). Preliminary investigation by FTIR had shown that the brown coating was not composed of varnishes usually employed in past conservation treatments (i.e. dammar, mastic, copal, or sandarac). Instead, the FTIR spectrum of the brown coating clot sample presented some, but not all, features matching those of shellac. In order to ascertain whether the brown coating was attributable to shellac, and to investigate the discrepancies between the FTIR spectrum of the brown coating and that of the standard shellac resin, FTIR spectra of the two photochemically-aged samples were recorded also and compared with the features of the Neri di Bicci sample. Table 1 summarises the results: the spectrum of the brown coating sample from the Neri di Bicci panel is extremely similar to those of the extremely aged shellac varnish.

Photo-oxidation from natural or artificial aging results in:

- a slight shift of the band associated with the C-O stretching;
- an inversion of the reciprocal absorbance of the peaks at 1250  $\text{cm}^{-1}$  and that in the range 1147–1171  $\text{cm}^{-1}$ ;
- a loss of resolution of the two peaks at 1147 and 1171  $\text{cm}^{-1}$ ;
- disappearance of the shoulder at ca. 1245  $\text{cm}^{-1}$ .

Interestingly, inversion of the reciprocal absorbance of the band at 1250 and that in the range 1147–1171  $\text{cm}^{-1}$  has been recently reported for the shellac varnish coating the canvas painting, “*Virgin of Sorrows*”. [22] The spectrum of the sample of the powdered

brown coating from the red mantle of the Neri di Bicci panel is reported in Fig. 4. Apart from the peaks labelled with the assignment or asterisks (that match those of a naturally aged shellac varnish [22]), we observe three additional peaks typical of oxalates whose presence can be attributed to photo-oxidation. Table 2 reports all the peak wavenumbers with the corresponding – when known – vibrational modes assignment. From the Table 2, it is possible to deduce that the part of the spectrum not reported (in the range 4000–1800  $\text{cm}^{-1}$ ) did not show particular features apart the broad peak centered at 3429  $\text{cm}^{-1}$  and the two absorptions relative to the C-H stretching at 2929 and 2856  $\text{cm}^{-1}$  in perfect agreement with the spectrum of shellac. Despite the comparison of our spectra with those reported in the cited work [22] and with the ones made on artificially aged shellac [21] gave clear indication on the presence of aged shellac, nevertheless, the spectrum of our sample (Fig. 4) evidenced a fine structure in the 1600–1750  $\text{cm}^{-1}$  region not compatible with shellac (see also IRUG database at <http://www.irug.org>). In particular, the two strong and medium absorptions at 1653 and 1540  $\text{cm}^{-1}$  attributable to C=O amide I and II stretching mode (Table 2) associated with the presence of the peaks of oxalates infer that the brown coating could not be constituted only by shellac, but possibly by some other coatings with white egg based varnishes widely diffused in the conservation practice. Finally, because the dark texture of the undercoating (second) layer had the same spectral characteristics as the outer layer, we conclude that the two have one origin (i.e., oxidized shellac) and, therefore, the underlayer is not an older, possibly original glaze.

Some preliminary cleaning tests using Feller mixtures [20] were carried out on the dark coating on the red mantle (see black box of

**Table 2**

Band assignments for the FTIR spectrum.

Wavenumber ( $\text{cm}^{-1}$ )	Intensity	Vibrational modes
3429	s (broad peak)	O-H str, N-H str
2929	s	C-H str
2856	m	C-H str methyl
1740	s (shoulder)	C=O str
1716	s	C=O str
1653 <sup>a</sup>	s	C=O amide I, C=C str aromatic rings
1540 <sup>a</sup>	m	C=O amide II
1457	m	C=C str aromatic rings, C-H bend
1385	w	C-H bend ring
1329	m	Oxalates
1245	w	C-O str
1171	w (broad not resolved)	C-O str, C-N str
1068	w (broad not resolved)	C-O str
781	w	Not assigned
726	w	Not assigned
943	w	Oxalates
875	w	Oxalates
517	w	C=C twist
463	w	C=C twist

s: strong; m: medium intensity; and w: weak.

<sup>a</sup> The two absorptions at 1653 and 1540  $\text{cm}^{-1}$  cannot be attributed to aged shellac (see discussion in the text).

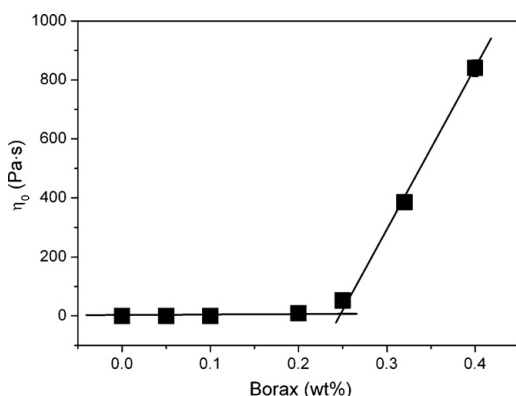


Fig. 5. Intrinsic viscosity  $\eta_0$  of PVA (2 wt%)/borax H<sub>2</sub>O systems as a function of borax concentration (wt%).

Fig. 2) of the painting surface. The results indicated that the best cleaning action was achieved by the mixture with a  $f_d$  value of 47 (i.e., corresponding to neat acetone). Although this solvent did not succeed in solubilising the dark coating, it did soften and swell the clots, making possible their removal by means of a soft mechanical action. Because the softening achieved by neat acetone was not optimal, additional mixtures were prepared by adding small amounts of other solvents in a rather empirical way. Thus, adding 10 wt% benzyl alcohol to neat acetone resulted in better softening of the clots. However, the texture beneath the clots (see right portion of Fig. 3A) was very difficult to remove: a previous attempt to remove this coating by means of cotton swabs impregnated with conventional organic solvents (acetone, benzyl alcohol, or mixtures of them) led to loss of stability of the red pigment layer due to the high sensitivity of vermilion-containing paints to aqueous and polar organic liquids. These results were quite unexpected since it is well known that acetone is not a good solvent for both aged and not aged shellac.

They and the FTIR characterisations of the shellac discussed above led us to examine the cleaning action of acetone incorporated within our aqueous PVA-borax systems. [23]. First, only acetone was added to the PVA/borax dispersion because systems with added acetone/benzyl alcohol mixtures or with pure benzyl alcohol were neither completely transparent nor stable over reasonable periods of time for cleaning purposes. Second, new PVA-based dispersions were made and characterized to be certain that they maintained their elasticity and easy removal from a painted surface (as had been demonstrated for aqueous PVA/borax systems with added 1-propanol [19]). Because the threshold concentration of PVA ( $C^*$ ) is 1.54 wt% at ambient temperatures [13], 2 wt% was chosen to assure that the entanglements of PVA chains (that are requisite for formation of the 3D-networks that immobilize the liquid phase) were possible. High viscosity and 3D-networks reduce the rates of penetration of a liquid in a dispersion into the porous matrix of a painting. As indicated in Fig. 5, a borax content > 0.25 wt% is necessary to obtain highly viscous material at this PVA concentration: the intrinsic viscosity  $\eta_0$  changed from 8.7 Pa.s to 860 Pa.s when the borax concentration was increased from 0.2 to 0.4 wt% (Fig. 5).

Some experiments were conducted on a gilded surface to determine whether perceptible amounts of residues remain on a surface after its treatment with a PVA/borax cleaning system (Fig. 1). The gilded surface was selected to achieve maximum sensitivity with the FTIR micro-reflectance mode. The FTIR spectra of the surface (Fig. 6), collected before (black line, upper spectrum) and

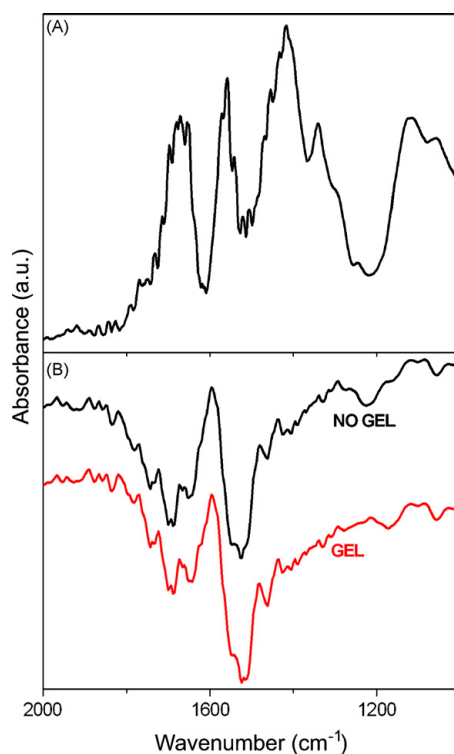
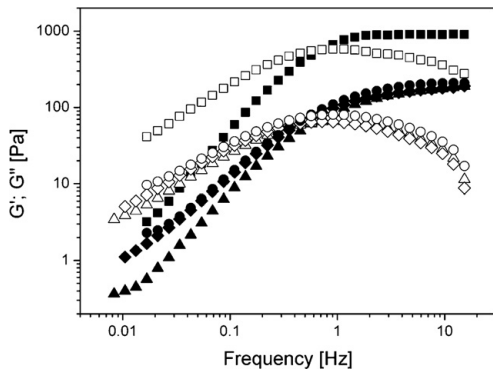


Fig. 6. (A) FTIR spectrum of the dried residue of a thin film of the PVA/borax aqueous dispersion. (B) Microreflectance FTIR spectra collected from the surface of a gilded wood support in a region where the PVA/borax aliquot was applied: before (black line, upper spectrum) and after the application (red line, lower spectrum). The contact time was 10 minutes.

after (red line, lower spectrum, part B) treatment with a PVA/borax dispersion for 10 minutes and removing it by peeling, are nearly identical in the fingerprint region. In particular, the region below 1400  $\text{cm}^{-1}$ , where strong bands from PVA and borax are normally seen (Fig. 6A), was nearly without absorptions and lacked the characteristic pattern of either polymeric dispersion component; more than a very small trace of dispersion residue would have been detected. We note that it is not possible to conclude from these results that this cleaning agent is removed from gilding in the same way as from a painting surface; additional experimentation will be required to make that determination.

Based upon a recent theory concerning the solubilisation of hydrophobic substances by liquid hydrotropes in water [24], some water/cosolvent mixtures embedded into a high viscosity polymeric dispersion should be able to soften and/or swell many water-insoluble materials present in foreign coatings on easel painting surfaces. Thus, the approach taken in this work was to thicken a mixture of water containing some organic liquid that should be able to swell the oxidized varnish. The strength of the cleaning action would be modulated by varying the total amount of the organic cosolvent in the continuous phase of the dispersion. Acetone was chosen as the cosolvent because, as previously noted, it was able to soften the hard, highly degraded coating to be removed from the Neri di Bicci painting. Thus, PVA/borax systems containing from 5 to 15 wt% of acetone were prepared according to the procedure described in the *Materials and methods* section.





**Fig. 7.** Viscoelastic curves of PVA/borate dispersions at various acetone concentrations: elastic (storage) modulus  $G'$  (closed symbols) and loss modulus  $G''$  (open symbols) at 0 (squares), 3 (triangles), 5 (diamonds) and 10 (circles) wt% of acetone.

Because the mechanical properties (especially the elastic modulus of the systems) are very important in determining the ease with which a cleaning system can remove a coating from the surface of a painting (Fig. 1), the viscoelastic natures of the PVA/borax dispersions with acetone were measured. In particular, the ease of removal of these systems from a surface after they have carried out their function is directly related to the density of the entanglements among the polymer chains of the 3D dispersion matrices: the higher is the entanglement density  $\rho$  [25], the higher is the intrinsic elasticity of the dispersion  $G_0$  (measured as the  $G'$  asymptotic value [26]). Fig. 7 shows frequency sweep curves for aqueous PVA/borax systems at different acetone contents. A decrease of  $G_0$  occurred for all of the acetone concentrations examined, and it was not dependent on the acetone concentration. As shown in Fig. 7, the three curves of the acetone systems are almost superimposable in the high frequency regime; the apparent relaxation time [27] of the dispersions, given by the crossover coordinates of the  $G'$  and  $G''$  curves, was almost unchanged as well. Thus, the mechanical properties of the systems with acetone remained typical of viscoelastic polymeric solutions. This behaviour is probably related to the ability of acetone to act as a water-structure breaker [28]. Also, the crossover between the  $G'$  and the  $G''$  values observed in Fig. 7 indicates that the mechanical behaviour of these systems is characteristic of high viscosity polymer solutions rather than true gels.

For purposes of using these dispersions as cleaning agents on works of art, the invariance of the rheological properties and, especially, of the elastic character as a function of acetone concentration, is very important – it allows easy removal of the cleaning agents by the so-called “peeling-off” technique [19]. However, because acetone decreased the elastic modulus of the aqueous dispersion, it was necessary to determine whether the ease of removal of the cleaning systems from a painting surface was also affected. Thus, acetone-containing dispersions were applied to and then removed from gilded surfaces similar to the one reported in Fig. 1. FTIR spectra again gave no evidence for residues on the areas treated with the polymeric dispersions after their removal.

Because acetone is quite volatile, its rate of evaporation from the aqueous dispersions may limit the utility of the aqueous PVA/borax systems in which it is a cosolvent, especially if the cleaning (contact) period is protracted. To determine the importance of this concern, the data in Fig. 8 were collected. They demonstrate that within the first 5 minutes, the maximum time that a cleaning system is expected to be in contact with the painting surface, the acetone weight loss from films of the aqueous dispersions is no more than 8%. On this basis, the cleaning ability of a dispersion, especially one

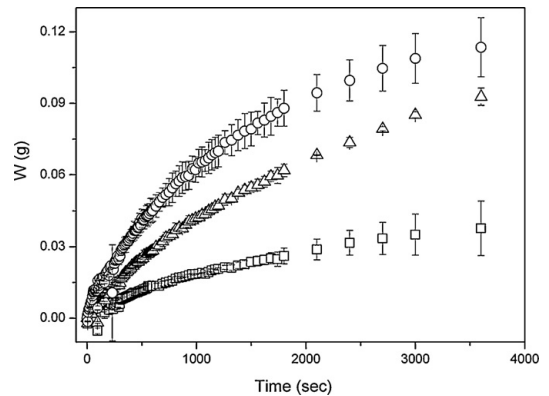


**Fig. 8.** Amount (W/g) of acetone evaporated from 2 g samples of PVA/borax system containing 5 (squares), 10 (triangles), and; 15 wt% acetone (circles) as a function of time. Error bars are the standard deviations.

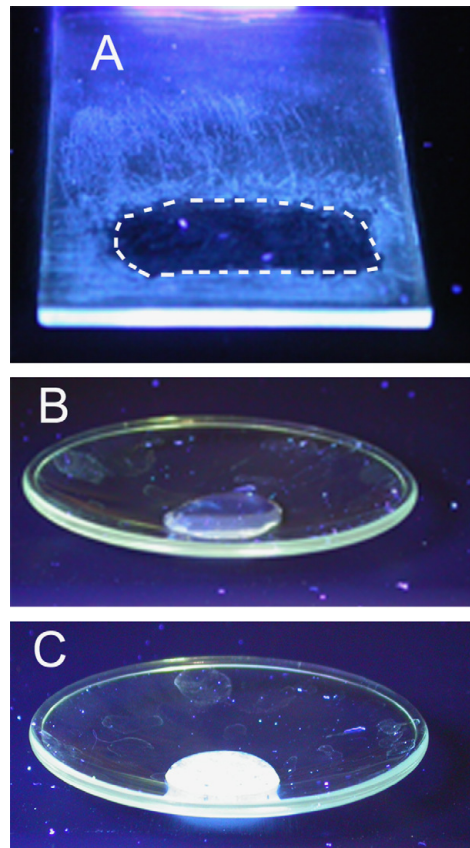


**Fig. 9.** UV-induced fluorescence image under a Wood lamp (emission maximum 364 nm) of A. A microscope glass covered by a thin layer of shellac resin after application and removal of a transparent dispersion of PVA/borax with 15 wt% acetone in a small region delimited by the dotted line. B. A dispersion of PVA/borax with 15 wt% acetone on a clean watch-glass. C. The same sample as in B after its removal from a glass surface covered by a thin layer of shellac resin.

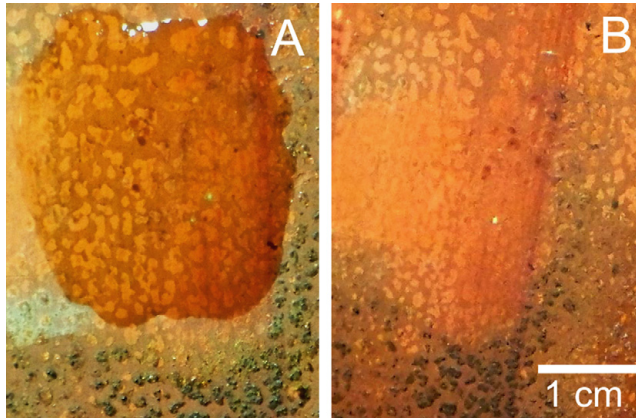


**Fig. 10.** Images of the surface area of the “Coronation of the Virgin with Saints” subjected to a cleaning test (see box in Fig. 2): A. Transparent dispersion of PVA-borax with 15 wt% acetone, applied on the painting surface where the clots had been already removed and only the dark undercoating layer that strongly adhered to the red pigment layer remained. B. The surface after the removal of the dispersion. The distance bar applies to both images.

containing 10 or 15 wt% of acetone, is not expected to decrease significantly during a 5-minute application.

Before applying the cleaning agent based on the PVA/borax system containing 15 wt% of acetone, we carried out several measurements on laboratory specimens coated with various types of not aged and aged shellac resins. The results were quite intriguing: in some cases, softening/swelling or solubilisation did not occur, while in others, it did and allowed complete removal. This, in part, helps to explain the aforementioned unexpected results with acetone as a good solvent for the aged shellac coating on the Neri di Bicci panel. As an example of good performance, Fig. 9 shows the effect of cleaning by the PVA/borax system containing 15 wt% of acetone as followed by fluorescence imaging. The typical fluorescence of shellac is shown in (A), a microscope slide completely covered by a thin layer of this varnish; application of the cleaning agent leads to removal of the varnish layer (as deduced from the region marked with dotted line [A]). Interestingly, the typical fluorescence of shellac “migrated” into the cleaning agent, as shown in (C) where the cleaning system is strongly fluorescent compared to the same system before application in (B).

Fig. 10 shows details of the region of the “Coronation of the Virgin with Saints” (Fig. 2) where the cleaning test was conducted. After a first application of a PVA/borax system containing 15 wt% of acetone for ca. 5 minutes (see *Materials and methods* section for details), the clots were softened (see Fig. 3A left side and 3B) and a weak mechanical action, carried out with a spatula, was sufficient to remove them completely. However, the lower inhomogeneous texture of dark residual resin (see Fig. 3A right side) was not removed

by an aliquot of the same dispersion in some regions of the painting. In these cases, complete cleaning was possible only after application of a second aliquot of the dispersion. Fig. 10A shows a region with the dark texture beneath the clots removed by the first application; the dark coating is visible because the polymeric dispersion is transparent, an attribute that allows the cleaning action to be followed visually by a conservator. The additional cleaning action by the second application is apparent in Fig. 10B – there is a very large reduction in the amount of dark brown coating only in the treated area.

Additional optical microscopy investigations, always in situ, were carried out with a USB microscope interfaced with a computer. Fig. 11B shows false colour micrograph of the same region after the first application. Note that the appearances of the surface with the clots, with the lower undercoating layer, and without any coatings (as collected from other regions of the painting) allow the features noted in Fig. 11B and C to be attributed to the lower undercoating layer and to the completely cleaned painting layer, respectively. No traces of the dark clots constituting the degraded organic surface materials (see Fig. 3B) were present in Fig. 11B; a real colour image of the texture of the surface after the removal of the clots is reported in Fig. 11A. Complete softening of the lower undercoating layer was achieved after an additional application of the dispersion (Fig. 11C). Importantly and unlike the results from cleaning procedures using traditional methods with conventional liquids (i.e., ungelled or unthickened solvents), softening of the coating here was accomplished without any apparent damage to the red pigment layer.

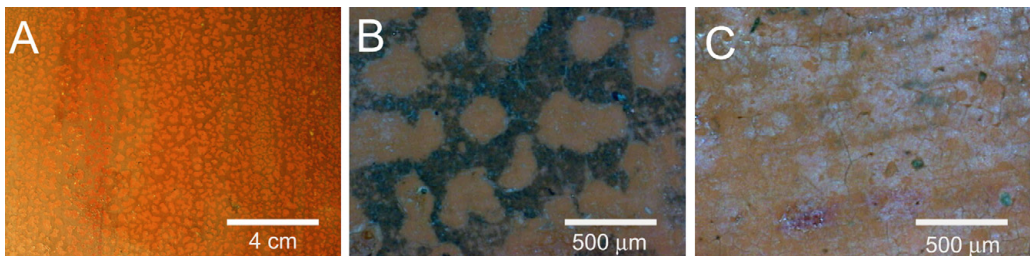


**Fig. 11.** True colour image of the texture of the residual resin after removal of the clots A and USB false colour micrographs before B and after C a second application of the cleaning dispersion.

These results indicate that the aqueous PVA/borax systems containing acetone allow both excellent control of the cleaning action and a gradual loss of difficult to remove materials from a painting surface. These PVA-based dispersions are an important improvement over traditional cleaning methods because they permit removal of a surface coating while minimising the risk of altering or damaging the colour layers underneath, and the cleaning action can be monitored visually or in situ with a microscope.

#### 4. Conclusions

Aqueous PVA/borax polymeric dispersions containing acetone have been developed, characterized, and used as cleaning agents for an easel painting with an aged and oxidized coating. The mechanical properties of the dispersions were found to be dependent on the composition of the continuous phase. The optimal ones could be removed from a painting surface by gentle peeling using a spatula or a forceps. The efficacy of the cleaning process, removal of a surface organic coating from "Coronation of the Virgin with Saints", an egg tempera wood panel by Neri di Bicci, was ascertained both macroscopically and by means of optical microscopy.

The major innovation in the application of these systems for cultural heritage conservation is that the cleaning agent can be easily removed in one step from a surface simply by peeling. This methodology did not lead to measurable amounts of surface residues from the aqueous PVA/borax dispersions. Yet, these systems retain many of the best qualities of gels and other thickened liquids used in conservation and cleaning of objects of art: they are very viscous (so that lateral flow on the surface does not occur and only the area desired to be cleaned is exposed to the cleaning agent), they are transparent and uncoloured (so that the cleaning action can be monitored visually by a conservator), and they slow the rate of penetration of the solvent into the painting matrix. For these reasons, the PVA/borax systems, especially when organic liquids are added to the aqueous continuous phases, appear to be very promising cleaning agents for conservators. Additional studies with other cosolvents and analytical tests are ongoing to determine the range of applications of these high viscosity polymeric dispersions in cultural heritage.

#### Acknowledgments

The authors express their gratitude to Mrs. Daniela Ristori and Mrs. Kioko Nakahara of the Fondazione Università Internazionale dell'Arte di Firenze, to Dr. Maria Sframeli, Soprintendenza Speciale per il Polo Museale della Città di Firenze, and to Dr. Cristina Masdea, Soprintendenza ai Beni Architettonici e del Paesaggio e al Patrimonio Storico, Artistico ed Etnoantropologico per le Province di Firenze, Prato e Pistoia for their cooperation during the tests on the wood panel. We thank Dr. Susanna Bracci, CNR-ICVBC of Florence, and Dr. Alice Fietta for making available some unpublished results on FTIR data on artificially aged shellac. The Italian authors thank the Consorzio interuniversitario per lo sviluppo dei Sistemi a Grande Interfase (CSGI) and the University of Florence (Fondi d'Ateneo ex-60%) and RGW thanks the US National Science Foundation for financial support.

#### References

- [1] A. Phenix, The swelling of artists' paints in organic solvents. Part 1, a simple method for measuring the in-plane swelling of unsupported paint films, *J. Amer. Inst. Conserv.* 41 (2002) 43–60.
- [2] A. Phenix, The swelling of artists' paints in organic solvents. Part 2, comparative swelling powers of selected organic solvents and solvent mixtures, *J. Amer. Inst. Conserv.* 41 (2002) 61–90.
- [3] A. Phenix, K. Sutherland, The cleaning of paintings: effects of organic solvents on oil paint films, *Reviews in Conservation 2 IIC*, London (2001) 47–60.
- [4] R. Wolbers, *Cleaning painted surfaces: aqueous methods*, Archetype, London, UK, 2000.
- [5] S. Bertolucci, E. Bianchini, C. Biave, F. Caliori, P. Cremonesi, S. Gravina, M. Zammataro, B. Zangani, Preparazione e utilizzo di soluzioni acquose addensate, reagenti per la pulitura di opere policrome, *Progetto Restauro 8* (2001) 11–21.
- [6] D. Stulik, H. Khanjian, V. Dorge, A. de Tagle, J. Maish, B. Considine, D. Miller, N. Khandekar, Scientific investigation of surface cleaning processes: quantitative study of gel residue on porous and topographically complex surfaces, in: *ICOM Committee for Conservation, ICOM-CC: 13th Triennial Meeting, Rio de Janeiro, 22–27 September 2002*; James & James, London, 2002, pp. 245–251.
- [7] V. Dorge (Ed.), *Solvent gels for the cleaning of works of art: the residue question*, Getty Publications, Los Angeles, USA, 2004.
- [8] A. Burnstock, T. Kieslich, A study of the clearance of solvent gels used for varnish removal from paintings, in: *ICOM Committee for Conservation, 11th Triennial Meeting in Edinburgh*, James & James, London, 1996, pp. 253–262.
- [9] E. Carretti, L. Dei, P. Baglioni, R.G. Weiss, Synthesis and characterization of gels from polyallylamine and carbon dioxide as gellant, *J. Amer. Chem. Soc.* 125 (2003) 5121–5129.
- [10] E. Carretti, A. Macherelli, L. Dei, R.G. Weiss, Rheoreversible polymeric organogels: the art of science for art conservation, *Langmuir* 20 (2004) 8414–8418.
- [11] K. Juntanon, S. Niamlang, R. Rujiravanit, A. Sirivat, Electrically controlled release of sulfosalicylic acid from crosslinked poly(vinyl alcohol) hydrogel, *Int. J. Pharm.* 356 (2008) 1–11.
- [12] L. Wu, C. Brazel, Modifying the release of proxiphylline from PVA hydrogels using surface crosslinking, *Int. J. Pharm.* 349 (2008) 144–151.
- [13] C.Y. Chen, T.L. Yu, Dynamic light scattering of poly(vinyl alcohol)-borax aqueous solution near overlap concentration, *Polymer* 38 (1997) 2019–2025.
- [14] A. Koike, N. Nemoto, T. Inoue, K. Osaki, Dynamic light scattering and dynamic viscoelasticity of poly(vinyl alcohol) in aqueous borax solutions. 1. Concentration effect, *Macromolecules* 28 (1995) 2339–2344.
- [15] W. Wu, M. Shibayama, S. Roy, H. Kurokawa, L.D. Coyne, S. Nomura, R.S. Stein, Physical gels of aqueous poly(vinyl alcohol) solutions: a small-angle neutron-scattering study, *Macromolecules* 23 (1990) 2245–2251.
- [16] G. Keita, A. Ricard, R. Audebert, E. Pezron, L. Leibler, The poly(vinyl alcohol)-borate system: influence of polyelectrolyte effects on phase diagrams, *Polymer* 36 (1995) 49–54.
- [17] H.L. Lin, Y.F. Liu, T.L. Yu, W.H. Liu, S.P. Rwei, Light scattering and viscoelasticity study of poly(vinyl alcohol)-borax aqueous solutions and gels, *Polymer* 46 (2005) 5541–5549.
- [18] H.A. Barnes, J.F. Hutton, K. Walters, *An introduction to rheology*, Elsevier, Amsterdam, ND, 1989.
- [19] E. Carretti, S. Grassi, M. Cossalter, I. Natali, G. Caminati, R.G. Weiss, P. Baglioni, L. Dei, Poly(vinyl alcohol)-borate hydro/cosolvent gels. Viscoelastic properties, solubilizing power and application in art conservation, *Langmuir* 25 (2009) 8656–8662.
- [20] P. Cremonesi, Un approccio più scientifico alla pulitura dei dipinti: il test di solubilità di Feller, *Progetto Restauro 8* (1998) 38–42.
- [21] S. Bracci, A. Fietta, A. Salvini, unpublished results in "Spectroscopic characterization of varnishes for musical instruments: artificial aging", First level degree thesis in technology for cultural heritage conservation, Library of Sciences, University of Florence, Italy, 2008.
- [22] M. Ortega-Avilés, P. Vandenabeele, D. Tenorio, G. Murillo, M. Jiménez-Reyes, N. Gutiérrez, *Anal. Chim. Acta* 550 (2005) 164–172.
- [23] M. Shibayama, T. Takeuchi, S. Nomura, Swelling/shrinking and dynamic light scattering studies on chemically cross-linked poly(vinyl alcohol) gels in the presence of borate ions, *Macromolecules* 27 (1994) 5350–5358.
- [24] P. Bauduin, A. Renoncourt, A. Kopf, D. Touraud, W. Kunz, Unified concept of solubilization in water by hydrotropes and cosolvents, *Langmuir* 21 (2005) 6769–6775.
- [25] B.A. Schubert, E.W. Kaler, N.J. Wagner, The microstructure and rheology of mixed cationic/anionic wormlike micelles, *Langmuir* 19 (2003) 4079–4089.
- [26] J.W. Goodwin, R.W. Hughes, *Rheology for chemists, an introduction*, Royal Society of Chemistry, London, UK, 2000.
- [27] L. Piculell, M. Egermayer, J. Sjostrom, Rheology of mixed solutions of an associating polymer with a surfactant. Why are different surfactants different? *Langmuir* 19 (2003) 3643–3649.
- [28] A. Idrissi, S. Longelin, F. Sokolic, Study of aqueous acetone solution at various concentrations: low-frequency Raman and molecular dynamics simulations, *J. Phys. Chem. B* 105 (2001) 6004–6009.

## Physicochemical characterization of partially hydrolyzed poly(vinyl acetate)–borate aqueous dispersions<sup>†</sup>

Cite this: DOI: 10.1039/c4sm00355a

E. Carretti, C. Matarrese, E. Fratini, P. Baglioni and L. Dei\*

The dynamic and structural properties of Highly Viscous Polymeric Dispersions (HVPDs), constituted of polyvinyl alcohol obtained from the 75% hydrolysis (75PVA) of polyvinyl acetate (PVAc) cross-linked with borate ions, were studied as a function of the 75PVA concentration at a constant ratio between the OH groups and the borate ions (OH/B(OH)<sub>4</sub><sup>-</sup>). The threshold 75PVA concentration C\* necessary for the formation of the three-dimensional network was determined by flow rheology. The oscillating rheology measurements were performed in the linear viscoelastic region; the relaxation spectra calculated from the frequency sweep curves showed only one peak whose width increased upon increasing the 75PVA concentration due to the broadening of the relaxation modes. The dependence of the mean relaxation time  $\tau_H$  upon the concentration of 75PVA followed a power law expression ( $\tau_H \sim C^x$  with  $x = 1.9$ ) indicating that  $\tau_H$  referred to a sticky reptation mechanism and that water was a good solvent for 75PVA as confirmed also by small angle X-rays scattering (SAXS) investigation. The HVPDs were used for the removal of grime layers from the surface of Carlo Carrà (1881–1966) paints decorating the walls of the Palazzo di Giustizia in Milan, Italy.

Received 14th February 2014  
Accepted 31st March 2014

DOI: 10.1039/c4sm00355a

www.rsc.org/softmatter

### Introduction

Poly(vinyl alcohol) (PVA), synthesized for the first time by Herrmann and Haehnel in 1924 through the hydrolysis of poly(vinyl acetate) (PVAc), due to its low price, biodegradability, biocompatibility, and solubility in water, is largely used in cosmetics, fibers, packaging, adhesives, textile industries and for the set up of innovative pharmaceutical and biomedical materials.<sup>1–9</sup>

Polyvinyl alcohols are commercially available in a broad range of hydrolysis degrees and molecular weights making it possible to significantly modulate their properties to optimize their performances for specific applications. This versatility has sparked interest on the study of the physico-chemical properties of aqueous solutions of xPVA,<sup>10</sup> mainly on the study of the properties related to the polymer concentration,<sup>11,12</sup> on the rheological properties,<sup>13</sup> and on the effect of different cross-linking agents that allow the formation of chemical (*i.e.* using glutaraldehyde as a cross-linker) or physical gels (from hydrogen bonds involving the hydroxyl groups).<sup>14</sup> An interesting property of xPVA aqueous solution is the formation of gel-like systems as a consequence of complexation or reaction with ions

such as borate, vanadate or antimonite with the side-chain hydroxyl groups.<sup>15,16</sup> In particular, aqueous solutions of PVA are known to form thermally-reversible high-viscous polymeric dispersions (HVPDs) in the presence of borate ions. The cross-links, made through interchain esterification reactions between pairs of vicinal diols,<sup>17</sup> are dynamic because ester formation is reversible and a steady-state concentration of them is established under isothermal conditions.<sup>16</sup> The conformations of the polymer chains in these HVPDs depend on a balance among electrostatic repulsions, polymer-chain excluded volume, intra- and inter-molecular cross-linking reactions between PVA chains and borate ions, and charge-shielding effects.<sup>18–22</sup>

The PVA–borate HVPDs have been extensively studied in the last decades by dynamic and static light scattering,<sup>21</sup> dynamic viscoelastic measurements,<sup>23</sup> X-ray analysis,<sup>24</sup> and differential scanning calorimetry,<sup>25</sup> as well as by SANS and NMR.<sup>16</sup> From these studies the structure and properties of the PVA–borate HVPDs have been found to depend on the PVA and borate concentrations, temperature, length (average molecular weight) of the PVA chains, and the pH of the aqueous region; depending upon these factors, the HVPDs can be very sticky or quite fluid.<sup>26</sup> In spite of several papers about the structural and mechanical properties of aqueous PVA–borate HVPDs, only a few studies were devoted to the study of the properties of PVAc with lower hydrolysis degrees cross-linked with borate. The possible modulation of their mechanical behavior induced the exploration of their use in the removal of extraneous materials from surfaces of works of art.<sup>27</sup> In the past few years, some studies

Department of Chemistry & CSGI Consortium, University of Florence, via della Lastruccia, 3 – 50019 Sesto Fiorentino, Florence, Italy. E-mail: carretti@csgi.unifi.it; matarrese@csgi.unifi.it; fratini@csgi.unifi.it; baglioni@csgi.unifi.it; dei@csgi.unifi.it  
† Electronic supplementary information (ESI) available: Additional rheological data. See DOI: 10.1039/c4sm00355a

dealt with the use of peelable aqueous highly viscous systems<sup>24,28</sup> as innovative tools for cleaning painted and decorative surfaces. For cleaning purposes<sup>29</sup> HVPD should be sufficiently soft to have a good contact with the surface to be treated and its elasticity and viscosity should be sufficiently high to maintain its ability to be easily removed from the surface after cleaning.

In the present paper the structural, mechanical and calorimetric properties of these aqueous viscoelastic dispersions of 75PVA and borate as the cross-linker are presented while maintaining a constant molar ratio between the OH groups and borax. The systems were analyzed by a detailed rheology investigation (in particular, trends between the viscoelastic parameters like the storage modulus ( $G'$ ) and loss modulus ( $G''$ ) and HVPD compositions). The free water indices (FWI) were determined from differential scanning calorimetry (DSC) measurements and their structural properties were established through small angle X-ray scattering (SAXS) measurements. Some application tests on wall paintings were also reported to assess their possible use in the field of works of art conservation.

## Experimental section

75% hydrolyzed poly(vinyl acetate)s (75PVAs), as the random copolymer, was supplied by Kuraray Co., Ltd. It was copiously washed with ice-cold water and dried under vacuum in order to eliminate by-products and residual free acetate. Sodium tetraborate decahydrate (>99.5%, Fluka) was used as received. Water was purified by a Millipore Elix3 apparatus ( $R \geq 15 \text{ M}\Omega \text{ cm}$ ).

The molecular weight ( $M$ ) distribution of 75PVA was obtained by means of a Size-Exclusion Chromatography (SEC) apparatus equipped with a column calibration based on dextran standards. The mobile phase was aqueous phosphate-buffered saline (PBS). The molecular weight distribution was obtained by linearly fitting the  $\log M$  vs. elution volume and then generating the  $M$ -value using the Empower software from Waters. Analyses were performed using 2 TSKGM PWXL columns (in series) from Tosoh Biosciences and a Waters SEC-LS chromatograph consisting of a Waters Alliance 2690 (solvent delivery and auto-injector) component, a temperature-controlled column compartment, and a Waters 410 differential refractive index detector. The  $M_w$ -value determined in this way of 75PVA was 7300.

For the preparation of the HVPDs the polymer was placed in a vial and was dissolved in water by heating under stirring at 85 °C for 2 h. Then, an aliquot of an aqueous 4 wt% borax solution was added drop-wise by stirring (vortex apparatus). The sample became rigid after a few minutes. Mechanical equilibration of all the investigated samples was monitored by means of rheology. Frequency sweeps (*vide infra* for the measurement set up) were carried out 1, 2, 5 and 10 hours after the sample preparation. It was observed that after 2 hours the trend of both the elastic ( $G'$ ) and the loss ( $G''$ ) moduli remained constant. On the other hand, the chemical equilibrium detected by the invariance of pH was anticipated, since pH remained equal to

$7.30 \pm 0.20$  1 hour after the sample preparation. pH measurements were performed with a digital pH-meter CrisonBasic 20.

All the characterization studies were carried out 24 h after sample preparation to ensure the reaching of equilibrium of the HVPDs. The ratio between the amount of polymer hydroxyl groups and the borate ions ( $\text{OH}/\text{B}(\text{OH})_4^-$ ) was kept equal to 20.4 : 1 throughout.

For the falling drop studies,<sup>30</sup> a 0.5 g portion of each HVPD, prepared as described above, was sealed in a glass tube and cooled to 5 °C. Then, the tube was inverted and placed in a water bath at 0 °C; the temperature of the bath was raised by 2 °C  $\text{min}^{-1}$ . The temperature ranges over which each HVPD first showed signs of flow and fell completely were recorded. The falling drop tests normally give the sol-gel transition, whereas in the case of HVPDs the method was used to establish the temperature at which the HVPD's network starts to loose strength ( $T_{lg}$ ). Before the tests, all the glass tubes were washed with piranha solution and demineralised water.

SAXS measurements were carried out with a HECUS S3-MICRO camera (Kratky-type) equipped with a position-sensitive detector (OED 50M) containing 1024 channels of width 54  $\mu\text{m}$ . Cu K $\alpha$  radiation ( $\lambda = 1.542 \text{ \AA}$ ) was provided by an ultra-brilliant point micro-focus X-ray source (GENIX-Fox 3D, Xenocs, Grenoble), operating at a maximum power of 50 W (50 kV and 1 mA). The sample-to-detector distance was 269 mm. The space between the sample and the detector was kept under vacuum during the measurements to minimize scattering from the air. The Kratky camera was calibrated in the small angle region using silver behenate ( $d = 58.34 \text{ \AA}$ ).<sup>31</sup> Scattering curves were obtained in the  $q$ -range between 0.01 and  $0.54 \text{ \AA}^{-1}$ , assuming that  $q = 4\pi/\lambda \sin \theta$ , where  $2\theta$  is the scattering angle. Gel samples were placed into 1 mm demountable cells having Mylar films as windows. Liquid samples were filled into a 1 mm borosilicate Mark-tube (Hilgenberg GmbH, Germany) using a syringe. The borosilicate capillaries were sealed to avoid solvent evaporation. The temperature was maintained at  $25 \pm 0.1 \text{ }^\circ\text{C}$  by a Peltier controller. All scattering curves were corrected for the empty cell contribution considering the relative transmission factor.

Oscillatory shear measurements were carried out on a Paar Physica UDS200 rheometer at  $25 \pm 0.1 \text{ }^\circ\text{C}$  (Peltier temperature control system) using a cone-plate geometry (25 mm diameter and 1° cone angle). The minimum gap between the plates at the zero radial position was 0.5 mm. The cone was lowered up to the measuring position in the  $z$  axis force controlled mode; the maximum squeezing force was 3.0 N. After being loaded, the samples were allowed to equilibrate for 30 min at 25 °C prior to start of the experiments. Frequency sweep measurements were carried out within the linear viscoelastic range (4% strain), determined by means of an amplitude sweep test. The storage and loss moduli ( $G'$  and  $G''$ , respectively) were measured over the frequency range of 0.01 to 100 Hz. The intrinsic viscosity,  $\eta_0$ , values were deduced from the plateau of the flow curves in the low Newtonian region (low-shear-rate regime). This value was plotted as a function of the polymer concentration in order to determine the threshold 75PVA concentrations  $C^*$  above which the drastic increase of the  $\eta_0$  value indicates the formation of



the extended 3D polymer networks at different  $(\text{OH}/\text{B}(\text{OH})_4^-)$  ratios (see Fig. S1†). In order to minimise the handling of the HVPDs, immediately after the addition of the borax solution, the vials were turned upside down to favour the accumulation of the sample on the cap side. Then, all the HVPDs were easily directly transferred onto the measurement plate.

DSC measurements were performed with a Q1000TA Instruments apparatus. The samples, sealed in aluminum pans, were equilibrated at 25 °C, cooled to −90 °C at a cooling rate of 5 °C min<sup>−1</sup>, kept at −90 °C for 8 min, and then heated to 30 °C at 5 °C min<sup>−1</sup>, under a 50 mL min<sup>−1</sup> stream of nitrogen. An empty sealed aluminum pan was used as the reference. For each system, three different samples were prepared and scanned. The enthalpy of fusion of the water was calculated by integrating the heat flow curves. The Free Water Index (FWI), a parameter that represents the percent of free and freezing bound water contained in the samples, was calculated using the following formula:<sup>32</sup>

$$\text{FWI} = \Delta H_{\text{sample}} / \Delta H_{\text{purewater}} \times 100 \quad (1)$$

where  $\Delta H_{\text{sample}}$  is the enthalpy change due to the fusion of the ice contained in the HVPD sample ( $\text{J g}_{\text{water}}^{-1}$ ), experimentally determined from the DSC curve;  $\Delta H_{\text{freewater}}$  ( $=333.6 \text{ J g}^{-1}$ ) is the theoretical value of the specific fusion enthalpy of pure ice at 0 °C.

The HVPD was applied onto the surface of a wall painting by Carlo Carrà 48 hours after its preparation. It was applied directly onto the wall painting surface by means of a spatula and left there for about 5 minutes. The HVPD was peeled from the surface by means of a pincer, without adding any additional liquid component to the remaining polymeric dispersion or on the painting surface after the peeling process. The procedure was repeated twice.

## Results and discussion

The falling drop test<sup>33,34</sup> indicated that the  $T_{\text{is}}$  of the investigated HVPDs significantly increases upon increasing the 75PVA concentration (Fig. 1A), while the effect of the cross-linker concentration was much less pronounced. The data indicated that the  $T_{\text{is}}$  was mainly determined by the number of the hydroxyl groups that are the only ones able to form cross-linking. As indicated by Kanaya *et al.*<sup>35</sup> and by Kjoniksen *et al.*,<sup>36</sup> this behaviour can be interpreted considering that the driving factor for the HVPD formation is the entanglement between polymer chains rather than the borax-modulated cross-linking (Fig. 1B).

The threshold 75PVA concentrations (indicated as  $C^*$ ) necessary for the formation of an extended three-dimensional network were determined rheologically from the trends of the changes in the zero shear viscosity  $\eta_0$  as a function of the polymer concentrations: the amounts of both 75PVA and borax were varied incrementally while keeping the  $(\text{OH}/\text{B}(\text{OH})_4^-)$  ratio constantly equal to 20.4. The obtained  $C^*$  value is 3.0. Furthermore, Fig. S1† indicated that upon increasing the  $(\text{OH}/\text{B}(\text{OH})_4^-)$  ratio an increase of the  $C^*$  value is observed.

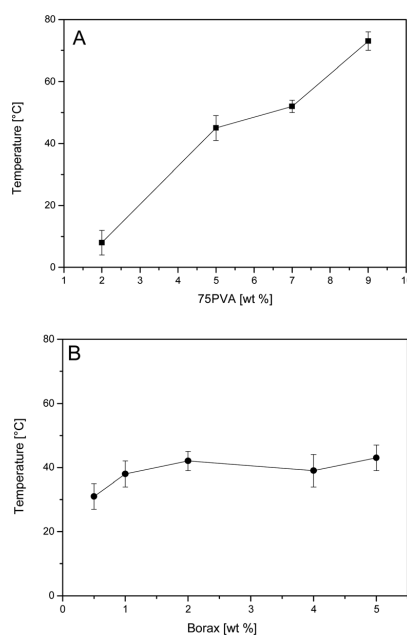


Fig. 1 (A) Variation of the  $T_{\text{is}}$  for HVPDs maintaining constant the molar ratio between the  $-\text{OH}$  groups and  $\text{B}(\text{OH})_4^-$  ions equal to 20.4; (B)  $T_{\text{is}}$  of HVPDs containing 5 wt% of 75PVA. Bars indicate the melting ranges.

Small angle X-ray scattering (SAXS) experiments were conducted to investigate the polymer structure at the nanometer level and to visualize the changes imposed by the presence of borax. Fig. 2 shows the SAXS intensity distribution in the case of 75PVA (see panel A) and 75PVA-borax (panel B) systems from 5 to 12 wt% polymer. All the SAXS curves were modeled according to a functional form<sup>37</sup> that can be interpreted as a generalized version of the Debye-Bueche (DB) approach.<sup>28</sup> The generalized DB model in its original form presents a low- $q$  clustering and high- $q$  solvation contribution plus a flat background, and it has been used to fit small angle neutron scattering curves obtained in the case of both neutral and charged polymeric solutions consisting of synthetic and biological macromolecules.<sup>37</sup> In our case, the low- $q$  clustering term is omitted because no intensity increase was evidenced in the low- $q$  region of the SAXS curves (see both panels of Fig. 2). A previous SANS investigation confirms that the clusters in similar systems are evident only below  $0.01 \text{ \AA}^{-1}$ .<sup>16</sup> For this reason, the SAXS curves were modeled according to a solvation term plus a flat background (eqn (2)):

$$I(q) = \frac{I_0}{[1 + (q - q_0)\xi]^m} + \text{bkg} \quad (2)$$

where  $I_0$  is the scattering intensity at  $q = 0$ ,  $q_0$  is the peak position,  $\xi$  is the correlation length which corresponds in a semi-diluted solution to the average distance between neighboring entanglement points,<sup>38</sup>  $m$  is the Porod exponent

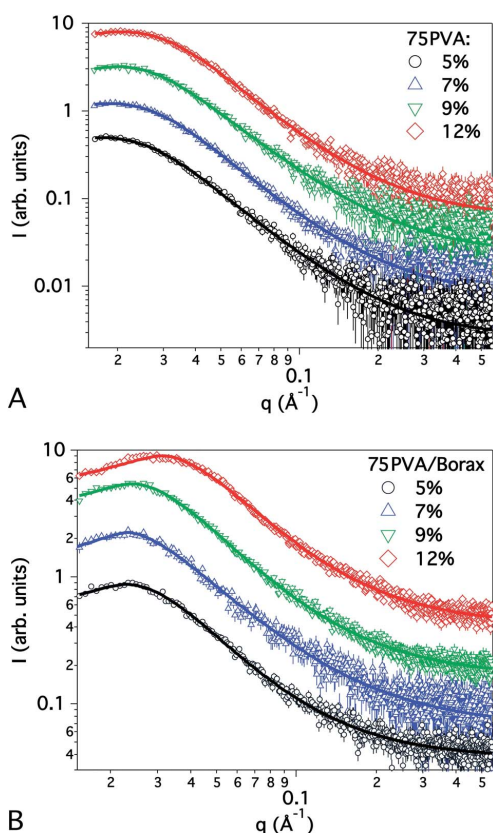


Fig. 2 Double-logarithmic representation of the SAXS intensity distribution for: (A) 75PVA and (B) 75PVA–borax dispersions. The solid lines are the best fits to the scattering points according to eqn (2). The curves are offset vertically by an arbitrary factor to avoid overlap.

associated with the solvation term and  $bkg$  is a  $q$ -independent instrumental background term. All these parameters were allowed to vary during the least-square fitting procedure.

Table 1 lists the parameters according to the best fits of the SAXS curves in Fig. 2. While for 75PVA concentrations between 5 wt% and 7 wt%  $\xi$  remains constant, a further increase of the amount of the polymer in its dispersions decreased the correlation length from 55.1 to 49.3 nm. The presence of a finite  $q_0$  can be questionable in this 75PVA series because this polymer is expected to be uncharged. However, it must be noted that the  $q_0$  values are very close to the lowest  $q$  accessed by the SAXS experiment and, moreover, the curves could also be fitted by constraining  $q_0$  to zero with only a very small increase of the overall  $\chi^2$ . This result clearly indicated that the charge present on the 75PVA polymer (perhaps as a result of its partial hydrolysis during sample preparation or storage) is almost negligible.  $q_0$  shifted slightly towards high- $q$  as a consequence of increase in the concentration. The average distance between the charges,

Table 1 Parameters associated with the best fits to the SAXS curves of the 75PVA (column A) and 75PVA–borax systems (column B). The  $(OH/B(OH)_4^-)$  ratio was kept equal to 20.4 : 1 for all the investigated samples

75PVA				
A	5%	7%	9%	12%
$I_0$	$4.96 \pm 0.05$	$6.02 \pm 0.04$	$5.25 \pm 0.07$	$7.19 \pm 0.06$
$\xi$ (Å)	$55.1 \pm 0.04$	$55.0 \pm 0.05$	$50.7 \pm 0.04$	$49.3 \pm 0.04$
$q_0$ (Å <sup>-1</sup> )	$0.0168 \pm 0.07$	$0.0188 \pm 0.07$	$0.0189 \pm 0.06$	$0.0208 \pm 0.04$
$M$	$2.02 \pm 0.08$	$1.98 \pm 0.07$	$1.97 \pm 0.08$	$1.96 \pm 0.06$
Bkg	$0.0268 \pm 0.02$	$0.0396 \pm 0.02$	$0.0487 \pm 0.03$	$0.0572 \pm 0.03$
75PVA–borax				
B	5%	7%	9%	12%
$I_0$	$3.34 \pm 0.08$	$5.53 \pm 0.02$	$6.56 \pm 0.03$	$6.14 \pm 0.06$
$\xi$ (Å)	$51.8 \pm 0.03$	$51.1 \pm 0.07$	$50.5 \pm 0.06$	$39.0 \pm 0.05$
$q_0$ (Å <sup>-1</sup> )	$0.0231 \pm 0.08$	$0.0227 \pm 0.09$	$0.0241 \pm 0.04$	$0.0312 \pm 0.03$
$M$	$1.69 \pm 0.06$	$1.67 \pm 0.06$	$1.67 \pm 0.05$	$1.64 \pm 0.03$
Bkg	$0.150 \pm 0.02$	$0.157 \pm 0.03$	$0.210 \pm 0.05$	$0.300 \pm 0.04$

estimated as  $2\pi/q_0$ , varied from 37 to 30 nm as the concentration was raised from 5 to 12 wt%. The parameter  $m$  has a constant value of 2, corresponding to a Gaussian coil conformation arising from monomer–solvent and monomer–monomer interactions being equal in strength. In the systems in which borax was present, similar considerations hold. However, the correlation lengths decreased by 0.5–1 nm in all cases as a consequence of the cross-links made by the borate ions. The inclusion of these ions in the polymeric network rendered the chains negatively charged, and the interaction peak became more evident and shifted to higher  $q$ -values. The associated average distances  $2\pi/q_0$  decrease to 27.5–20.1 nm (following the shifts to higher  $q$  values imposed on the more concentrated dispersions). In the 75PVA–borax series, the Porod exponent  $m$  passed from 2 to about 1.67 as a consequence of the borax addition, which changed the complexity of the network topology and, more importantly, increased the solvent–polymer compatibility. A value of 5/3 (=1.67) describes the behavior of a polymer coil in a ‘good’ solvent (*i.e.*, when the monomer–solvent interaction is more favorable than monomer–monomer interaction).<sup>36</sup>

In order to understand the effect of the polymer concentration on the mechanical properties of the 75PVA HVPDs and to obtain information about their relaxation dynamics, oscillatory frequency sweep tests were carried out in the linear viscoelastic regime in order to obtain the dependence of the complex moduli  $G'$  and  $G''$  on the frequency of the applied shear perturbation. As the 75PVA concentration was increased, the decrease of  $\tan \delta$  indicated enhanced elasticity (see Fig. S2†) due to the increased number of interchain interactions and entanglements between the 75PVA molecules resulting from the decreased chain flexibility and increased molecular size.

As shown in Fig. 3, the 75PVA–borax systems showed a behavior typical of viscoelastic polymeric dispersions; two different regimes can be individuated: for  $\omega > \omega_c$  ( $\omega_c$  is the

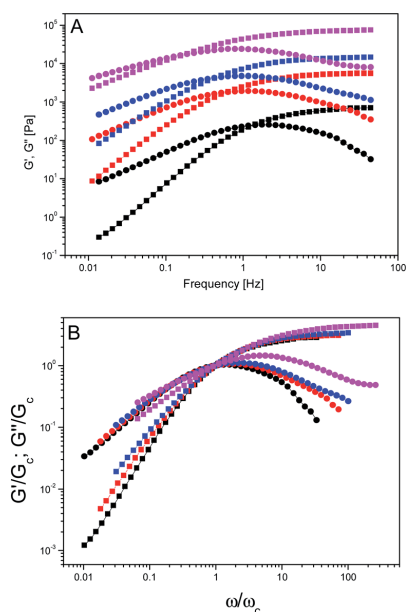


Fig. 3 (A) Frequency sweep curves at 5 (black), 7 (red), 9 (blue) and 12 (purple) wt% 75PVA concentration. Squared symbols indicate the elastic modulus  $G'$ , circles indicate the loss modulus  $G''$ . (B) Normalized mechanical spectra at 2 (black), 5 (red), 7 (blue) and 9 (purple) wt% 75PVA concentrations. Closed symbols indicate the  $G'/G_c$  ratio and open symbols indicate the  $G''/G_c$  ratio.  $G_c$  and  $\omega_c$  are the crossover modulus and the crossover frequency respectively.

crossover frequency between the  $G'$  and  $G''$  curves)  $G' > G''$ , indicating a predominantly elastic behavior; for  $\omega < \omega_c$  the viscous character prevails ( $G' < G''$ ).

The value of the intrinsic elastic modulus  $G^0$ , given by the asymptote of  $G'$  curves of the HVPDs, is correlated with the density of the borate-modulated cross-linking ( $\rho_e$ ) between the 75PVA chains (eqn (3)):

$$G^0 = \rho_e k_B T \quad (3)$$

where  $k_B$  is the Boltzmann constant and  $T$  is the temperature (K).<sup>39</sup> The increased  $\rho_e$ , upon increasing the 75PVA content (Fig. 4), indicated an increase of the complexity of the HVPD structures and an increase of the strength of the 3D network confirming that the driving factor for the formation of the 3D network is the number of OH groups available for the formation of covalent cross-links.

Normalized frequency sweeps are reported in Fig. 3B and indicate that increasing 75PVA and borax concentrations had little effect on the rheological behavior of the HVPDs: the normalized curves overlapped, indicating that, even if the global time scale of the relaxation phenomena slightly changes, the mechanism was almost the same at all concentrations.

Since the dynamic of the 75PVA based HVPDs cannot be described by a single-element Maxwell model (see Fig. S3†),

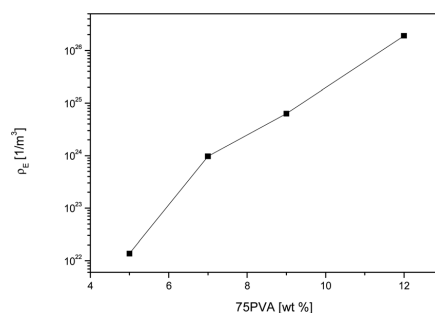


Fig. 4 Effect of the 75PVA concentration on the density of the borate-modulated cross-linking  $\rho_e$  on the HVPDs.

both  $G'$  and  $G''$  were used to calculate the time-weighted relaxation spectrum  $H(\tau)$ .<sup>40</sup> In Fig. 5 the  $H(\tau)$  spectra are normalized with respect to the zero shear viscosity in order to compare them on similar scales. All the spectra showed only one peak, confirming that the main relaxation mechanism was unchanged upon increasing the 75PVA concentration. However, the observed increase in the width of the spectra indicated that additional modes of relaxation, resulting from increasing entanglements among the polymer chains (*i.e.*, enhancement of polymer-polymer interactions), were operating.

Fig. 6 shows a nearly quadratic dependence of the mean relaxation time  $\tau_H$ , given by the peak of the relaxation spectra, on the 75PVA concentrations (*i.e.*,  $\tau_H \sim C^a$ , in the linearised form  $\log(\tau_H) = a \log C + b$ ). The slope  $a$  of the plot  $\log(\tau_H)$  vs.  $\log C$  is equal to 1.9). In order to identify the main relaxation mechanism  $G(t)$ , the trend of the stress relaxation modulus has been investigated. The Doi-Edwards model (eqn (4))<sup>41</sup> for a pure reptation process indicates that  $G(t)$  is given by:

$$G(t) = \frac{8}{\pi^2} G^0 \sum_{\text{odd } k} \frac{1}{k^2} \exp\left(-\frac{k^2}{\tau_{\text{rep}}}\right) \quad (4)$$

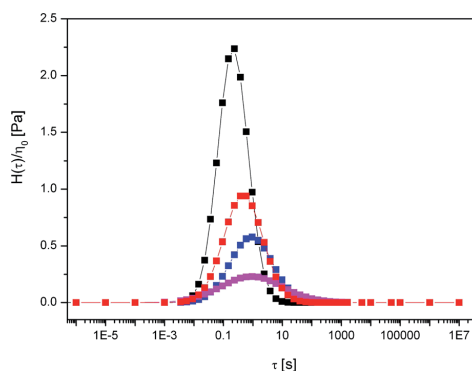


Fig. 5  $\eta_0$  normalised stress relaxation spectra ( $H(\tau)$ ) at 5 (black), 7 (red), 9 (blue) and 12 (purple) wt% 75PVA concentration.



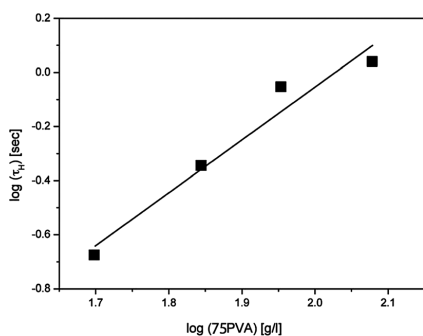


Fig. 6 Effect of the concentration of 75PVA on the mean relaxation times ( $\tau_H$ ) of their HVPDs.

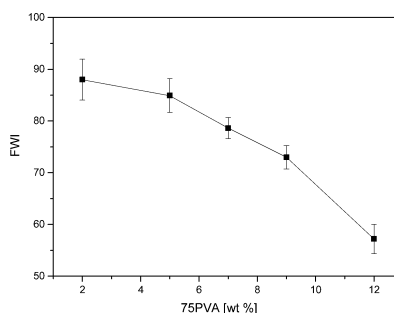


Fig. 7 FWI values of the HVPDs as a function of the 75PVA concentration. The  $(\text{OH}/\text{B}(\text{OH})_4^-)$  ratio was kept equal to 20 : 1 for all the investigated samples.

where  $G^0$  is the asymptote of the  $G'$  curve and  $\tau_{\text{rep}}$  was taken as the mean relaxation time  $\tau_H$  of Fig. 5. The comparison between the experimental trend of the stress relaxation modulus and the Doi-Edwards equation indicated that the 75PVA based HVPDs did not relax following a pure reptation mechanism (Fig. S4†). This was probably due to the interchain interactions that slowdown the relaxation process. Rubinstein and Semenov<sup>42</sup> studied the dynamic of entangled solution of associating polymers and demonstrated that their dynamic in good solvents is controlled by the associating groups (stickers). They explained this behaviour in terms of sticky reptation. The corresponding reptation time strongly depends upon the concentration as follows:  $\tau_{\text{rep}} \sim C_{\text{a}}$ , ranging from 1.44 to 4.5 as a function of the length of the strands between 'sticking points'. Our data supported all the HVPDs investigated:

- water is a good solvent as demonstrated also by SAXS data;
- the mean relaxation process is controlled by a sticky reptation mechanism.

In order to estimate the level of interaction of water with the 75PVA-borax network, and relate it to the elastic properties of the polymeric dispersions, the Free Water Index (FWI) was determined from DSC measurements.<sup>18,43</sup>

As seen in Fig. 7, for 75PVA concentrations between 2 wt% and 5 wt%, the FWI value is almost constant. By further increasing the polymer concentration, the percent of non-frozen, bound water at temperatures below 0 °C (*i.e.*, water that interacts strongly with the polymer chains and borate ions) strongly increases up to the 45% for a concentration equal to 12 wt%.

Previous tests carried out on different surfaces<sup>26,44</sup> demonstrated that PVA-borate hydro HVPDs are effective low impact cleaning agents for delicate surfaces of artistic and historical interest. From the applicative point of view, their peculiarities are mainly the gradualness of the cleaning action (that makes these HVPDs suitable for delicate and precious surfaces) and their ease of removal that can be achieved simply by a peeling action, without leaving onto the treated surface any detectable residue. Both these features are strictly related to the rheological properties of the HVPDs. In a previous paper,<sup>29</sup> we

proposed a direct correlation between these parameters and the efficacy of the HVPDs in terms of cleaning ability and ease of removal. In particular, we showed that a value of  $G^0 > 400$  Pa ( $G^0$  corresponds to the intrinsic elastic modulus given by the asymptotic value of the  $G'$  curve, see Fig. 3A) allows the peeling of the cleaning system from the treated surface by a onestep not invasive mechanical action realized by tweezers; all the investigated systems satisfy this condition. Then, on the basis of both the rheological results obtained with the PVA-borate HVPDs and the test already carried out, the efficacy of these aqueous systems as cleaning tools was tested on a surface of a wall painting. The experimentation was made in cooperation with the restorer Barbara Ferriani on a portion of the *Giudizio Universale* (Fig. 8A), a fresco by Carlo Carrà (1881-1966) in the *Palazzo di Giustizia* in Milan. The painted surface had been altered by a uniform thin dark grey layer present all over the surface and constituted by carbonaceous particles mainly derived from atmospheric pollution (Fig. 8B). For the realisation of the paint Carrà used substances highly sensitive to aqueous media like gypsum and white egg as the binding medium, in order to obtain the effect of different colour saturations. The first attempt for the removal of the surface dirt layer showed that deionised water was able to solubilise the surface dark layer but its penetration into the mortar's porous structure caused the swelling of the binder with consequent local surface whitening. In order to avoid all these drawbacks, the cleaning was carried out by means of the 75PVA-borax-H<sub>2</sub>O based HVPDs (cleaning tests were performed by means of the systems containing the 7 wt% of 75PVA): according to the Washburn equation, due to their high viscosity, the penetration of the water into the porous support was minimised. The system was applied with a spatula and maintained in contact with the surface for 4 min; thanks to its elasticity, the gel was completely removed in one step without residues left on the painting surface. After the gel application some dark layers were still present on the surface and were completely removed with a second application of the gel (Fig. 8C). It is worth noting that an important advantage in using these gel-like systems, beside the lack of residues, is

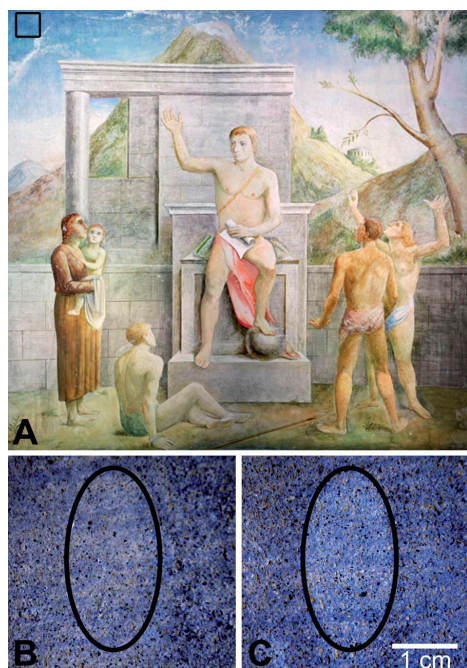


Fig. 8 (A) "Giudizio Universale" a XX century wall painting by Carlo Carrà (1881–1966), Palazzo di Giustizia, Milano, Italy. The black box indicates the region where the cleaning test was carried out by means of the 75PVA–borax based HVPD. Magnification of the area interested by the cleaning test before (B) and after (C) the application of the HVPD. The application procedure is described in the Materials and methods section.

related to the selective, controllable and progressive cleaning of the surface.

## Conclusions

In this paper 75PVA–borax cross-linked based HVPDs were studied in order to obtain information about the role of the hydrolysis degree, the molecular weight and the concentration in the structural and dynamic properties of the polymer systems; the ratio between the borax and the OH groups of the 75PVA molecules ( $\text{OH}/\text{B}(\text{OH})_4^-$ ) was maintained equal to 20.4.

Dynamic rheological measurements were also performed in the linear viscoelastic regime for 75PVA concentrations above the entanglement threshold  $C^*$ . The frequency sweep indicates that at low 75PVA concentrations, the HVPDs show a behaviour typical of the viscoelastic solutions: in the low frequency regime  $G' \sim \omega^2$  and  $G'' \sim \omega$ . The fitting, carried out by means of a single-mode Maxwell element model, indicated a deviation from this behaviour. The increase of the  $R^2$  value with the 75PVA concentration suggested a multimodal relaxation process. The relaxation spectra calculated from the frequency sweep curves were all characterised by the presence of a single peak whose

shape resulted unvaried by increasing the polymer concentration. This indicates that the main relaxation mechanism is independent of the above mentioned parameters. Nevertheless, the increase of the width of the peak observed by increasing the 75PVA concentration could be related to extra relaxation modes, mainly attributable to the enhancement of the entanglement density. Furthermore, it was found that the mean relaxation time  $\tau_H$  was related to the 75PVA concentration by a power law  $\tau_H \sim C^a$  with  $1.7 < a < 2.3$ . As described by Rubinstein *et al.*,<sup>42</sup> this behaviour indicates that the relaxation is characterised by a sticky reptation mechanism and that the polymer coil is in a 'good' solvent ( $\text{H}_2\text{O}$ ) for the 75PVA–borax network, as determined by SAXS analysis. Finally, this paper, together with a recent research<sup>28,45</sup> confirms that, even in the field of the material chemistry applied to the conservation of artefacts, a perfect control of the physico-chemical properties allows an optimisation of the applicative performances.

## Acknowledgements

Financial support from the University of Florence Fondi d'Ateneo ex-60% and from the Consorzio interuniversitario per lo sviluppo dei Sistemi a Grande Interfase (CSGI), Florence, Italy, is gratefully acknowledged. Financial support from the Tuscany Region, Italy, SICAMOR Project PAR-FAS is also acknowledged. This work was also partly supported by the European Union, Project NANOFORART (FP7-ENV-NMP-2011/282816).

## Notes and references

- B. Ding, H. Kim, S. Lee, C. Shao, D. Lee, S. Park, G. Kwag and K. Choi, *J. Polym. Sci., Part B: Polym. Phys.*, 2002, **40**, 1261.
- S. H. Imam, L. Mao, L. Chen and R. V. Greene, *Starch*, 1999, **51**, 225.
- J. Zeng, A. Aigner, F. Czubyko, T. Kissel, J. H. Wendorff and A. Greiner, *Biomacromolecules*, 2005, **6**, 1484.
- T. H. Young, N. K. Yao, R. F. Chang and L. W. Chen, *Biomaterials*, 1996, **17**, 2139.
- T. H. Young, W. Y. Chuang, N. K. Yao and L. W. Chen, *J. Biomed. Mater. Res.*, 1998, **40**, 385.
- K. Inoue, T. Fujisato, Y. J. Gu, K. Burczak, S. Sumi, M. Kogire, T. Tobe, K. Uchida, I. Nakai, S. Maetani and Y. Ikada, *Pancreas*, 1992, **7**, 562.
- W. Paul and C. P. Sharma, *J. Biomater. Sci., Polym. Ed.*, 1997, **8**, 755.
- Y. Hara, S. Kamiya, K. Nishioka, M. Saishin, S. Nakao and A. Yamauchi, *Acta Soc. Ophthalmol. Jpn.*, 1979, **83**, 1478.
- K. Burczak, E. Gamian and A. Kochman, *Biomaterials*, 1996, **17**, 2351.
- H. Gao, R. Yang, J. He and L. Yang, *J. Appl. Polym. Sci.*, 2010, **116**, 1459.
- W. S. Lyoo, S. J. Lee and J. H. Kim, *J. Appl. Polym. Sci.*, 2004, **93**, 1638.
- J. H. Choi, S. W. Ko, B. C. Kim, J. Blackwell and W. S. Lyoo, *Macromolecules*, 2001, **34**, 2964.
- R. K. Schultz and R. R. Myers, *Macromolecules*, 1969, **2**, 281.

- 14 E. V. Basiuk, A. Anis, S. Bandyopadhyay, E. Alvarez-Zauco, S. L. I. Chan and V. A. Basiuk, *Superlattices Microstruct.*, 2009, **46**, 937.
- 15 A. L. Kjøniksen and B. Nyström, *Macromolecules*, 1996, **29**, 5215.
- 16 L. V. Angelova, P. Terech, I. Natali, L. Dei, E. Carretti and R. G. Weiss, *Langmuir*, 2011, **27**, 11671.
- 17 C. Y. Chen, J. Y. Guo, T. L. Yu and S. C. Wu, *J. Polym. Res.*, 1998, **5**, 67.
- 18 S. J. Kim, C. K. Lee and S. I. Kim, *J. Appl. Polym. Sci.*, 2004, **92**, 1467.
- 19 K. Nakamura, T. Hatakeyama and H. Hatakeyama, *Polymer*, 1983, **24**, 871.
- 20 Y. Sakai, S. Kuroki and M. Satoh, *Langmuir*, 2008, **24**, 6981.
- 21 W. Goodwin and R. W. Hughes, *Rheology for Chemists: an introduction*, Royal Society of Chemistry, Cambridge, 2000.
- 22 H. A. Barnes, J. F. Hutton and K. Walters, *An Introduction to Rheology*, Elsevier, Amsterdam, 1989.
- 23 N. Nemoto, *Macromolecules*, 1999, **32**, 8872.
- 24 P. D. Hong, C. M. Chou and H. T. Huang, *Eur. Polym. J.*, 2000, **36**, 2193.
- 25 E. Carretti, S. Grassi, M. Cossalter, I. Natali, G. Caminati, R. G. Weiss, P. Baglioni and L. Dei, *Langmuir*, 2009, **25**, 8656.
- 26 E. Carretti, I. Natali, C. Matarrese, P. Bracco, R. G. Weiss, P. Baglioni and L. Dei, *J. Cult. Herit.*, 2010, **11**, 373.
- 27 E. Carretti, M. Bonini, L. Dei, B. H. Berrie, L. V. Angelova, P. Baglioni and R. G. Weiss, *Acc. Chem. Res.*, 2010, **43**, 751.
- 28 J. Domingues, N. Bonelli, R. Giorgi, E. Fratini, F. Gorel and P. Baglioni, *Langmuir*, 2013, **29**, 2746.
- 29 I. Natali, E. Carretti, L. Angelova, P. Baglioni, R. G. Weiss and L. Dei, *Langmuir*, 2011, **27**, 13226.
- 30 A. A. Sobczuk, S. Tamaru and S. Shinkai, *Chem. Commun.*, 2011, **47**, 3093.
- 31 T. N. Blanton, M. Rajeswaran, P. W. Stephens, D. R. Whitcomb, S. T. Misture and J. A. Kaduk, *Powder Diffr.*, 2011, **26**, 313.
- 32 M. Shibukawa, K. Aoyagi, R. Sakamoto and K. Oguma, *J. Chromatogr., A*, 1999, **832**, 17.
- 33 D. J. Abdallah, L. Lu and R. G. Weiss, *Chem. Mater.*, 1999, **11**, 2907.
- 34 T. Seo, S. Take, K. Miwa, J. K. Hamada and T. Iijimar, *Macromolecules*, 1991, **24**, 4255.
- 35 T. Kanaya, N. Takahashi, K. Nishida, H. Seto, M. Nagao and Y. Takeba, *Phys. B*, 2006, **385–386**, 676.
- 36 A. L. Kjøniksen and B. Nyström, *Macromolecules*, 1996, **29**, 5215.
- 37 F. Horkay and B. Hammouda, *Colloid Polym. Sci.*, 2008, **286**, 611.
- 38 P. G. De Gennes, *Scaling concepts in polymer physics*, Cornell University Press, Ithaca, New York, 1979.
- 39 B. A. Schubert, E. W. Kaler and N. J. Wagner, *Langmuir*, 2003, **19**, 4079.
- 40 J. Honerkamp and J. Weese, *Rheol. Acta*, 1993, **32**, 65.
- 41 M. Doi and S. F. Edwards, *J. Chem. Soc., Faraday Trans.*, 1978, **74**, 1818.
- 42 M. Rubinstein and A. N. Semenov, *Macromolecules*, 2001, **34**, 1058.
- 43 H. Hatakeyama and T. Hatakeyama, *Thermochim. Acta*, 1998, **308**, 3.
- 44 P. Baglioni, D. Berti, M. Bonini, E. Carretti, L. Dei, E. Fratini and R. Giorgi, *Adv. Colloid Interface Sci.*, 2014, **205**, 361.
- 45 I. Natali, P. Tempesti, E. Carretti, M. Potenza, S. Sansoni, P. Baglioni and L. Dei, *Langmuir*, 2014, **30**, 660.